Mineral Resource Report 85

1984

# PETROLOGY AND RESERVOIR CHARACTERISTICS OF THE LOWER SILURIAN MEDINA GROUP SANDSTONES, ATHENS AND GENEVA FIELDS, CRAWFORD COUNTY, PENNSYLVANIA

Christopher D. Laughrey

COMMONWEALTH OF PENNSYLVANIA
DEPARTMENT OF ENVIRONMENTAL RESOURCES
OFFICE OF RESOURCES MANAGEMENT
BUREAU OF
TOPOGRAPHIC AND GEOLOGIC SURVEY
Arthur A. Socolow, State Geologist

Mineral Resource Report 85

# PETROLOGY AND RESERVOIR CHARACTERISTICS OF THE LOWER SILURIAN MEDINA GROUP SANDSTONES, ATHENS AND GENEVA FIELDS, CRAWFORD COUNTY, PENNSYLVANIA

by Christopher D. Laughrey
Pennsylvania Geological Survey

PENNSYLVANIA GEOLOGICAL SURVEY

FOURTH SERIES

HARRISBURG

1984

ISBN: 0-8182-0054-5

ADDITIONAL COPIES
OF THIS PUBLICATION MAY BE PURCHASED FROM
STATE BOOK STORE, P.O. BOX 1365
HARRISBURG, PENNSYLVANIA 17105

# PREFACE

This report concerns the petrology and associated reservoir characteristics of the Lower Silurian Medina Group sandstones in the Athens and Geneva gas fields of Crawford County. The investigation was made to document the composition, texture, and diagenetic fabric of these clastic hydrocarbon reservoirs in northwestern Pennsylvania and to provide a more detailed model of depositional and lithologic patterns to aid exploration, pay recognition and evaluation, and well completion and stimulation design.

The Athens and Geneva gas fields are examples of heterogeneous Medina sandstone reservoirs that posed several problems during development. The reservoir intervals are of variable thickness, and porous, gas-bearing zones capable of commercial production are erratic in occurrence. The distribution of hydrocarbons does not conform to existing structural closure. The calculation and significance of water saturation in the low-porosity, shaly pay intervals is problematic, and the pay zones are both water and acid sensitive. The petrologic study and interpretation of cores from the Athens and Geneva fields help to explain the nature of the reservoirs and the local accumulations of natural gas. A comparison of the Athens and Geneva fields with other productive Medina fields and pools is useful for making some generalizations concerning the regional petrophysical character of the reservoirs in northwestern Pennsylvania.

This report will be of particular interest to oil and gas producers, petroleum geologists, petroleum engineers, and exploration geophysicists. The methods of study employed in this investigation should be applicable to other Silurian and Devonian clastic reservoirs in Pennsylvania and adjacent areas of the central Appalachian basin.

Scanning-electron-microscope (SEM) photomicrographs of the Lower Silurian Medina Group reservoir sandstones from the Athens field, Crawford County, Pennsylvania.

The upper SEM photomicrograph shows a portion of the void space and pore wall in the Grimsby Sandstone at a depth of 4,667 feet (1,423 m). A syntaxial quartz overgrowth (O) extends into the pore. Quartz overgrowths are responsible for the largely reduced primary intergranular porosity in the sandstones. Authigenic iron-rich chlorite rosettes (c) line the crystal face of one of the rhombohedrons that terminate the quartz overgrowth. This iron-rich chlorite is partly responsible for the formation's sensitivity to acid-breakdown fluids. Wispy laths of authigenic illite (I) extend into the pore from a partially dissolved and illitized detrital feldspar grain. Illite renders the formation water sensitive and introduces a production problem with migrating fines. (SEM photomicrograph by Gary Cooke and Feng-Chih Lin, Gulf Research and Development Company.)

The lower photomicrograph is a low-angle backscatter SEM image of the Grimsby Sandstone from a depth of 4,710 feet (1,436 m). The photomicrograph shows a moldic secondary pore which formed through the direct dissolution of a detrital feldspar grain, its authigenic feldspar overgrowth, and calcite (cal) which had partially replaced the feldspar (F). Notice the surface roughness of the pore walls and the extremely restricted pore throats (PT). Such reservoir sandstones, which have very high pore-to-pore-throat ratios and low pore-throat-to-pore coordination, are characterized by low recovery efficiencies and require massive hydraulically induced fractures to produce commercially. Moldic secondary pores are one of the most common porosity types in the Medina Group sandstones. (SEM photomicrograph by Dr. David Krinsley, Arizona State University.)

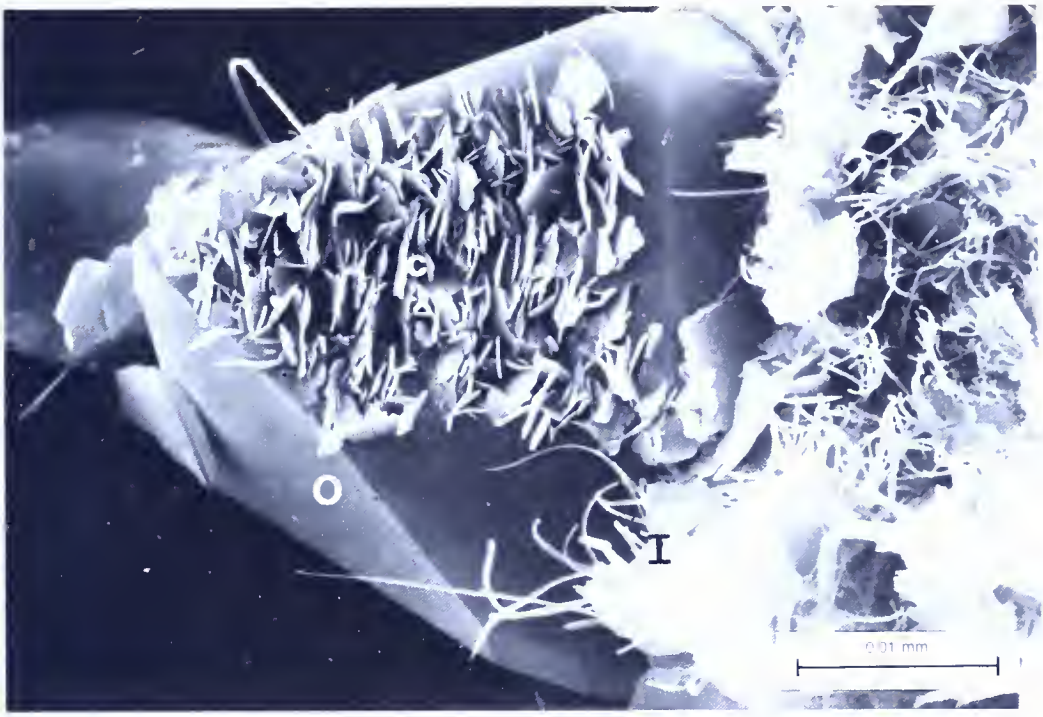
O
I
0.01 mm

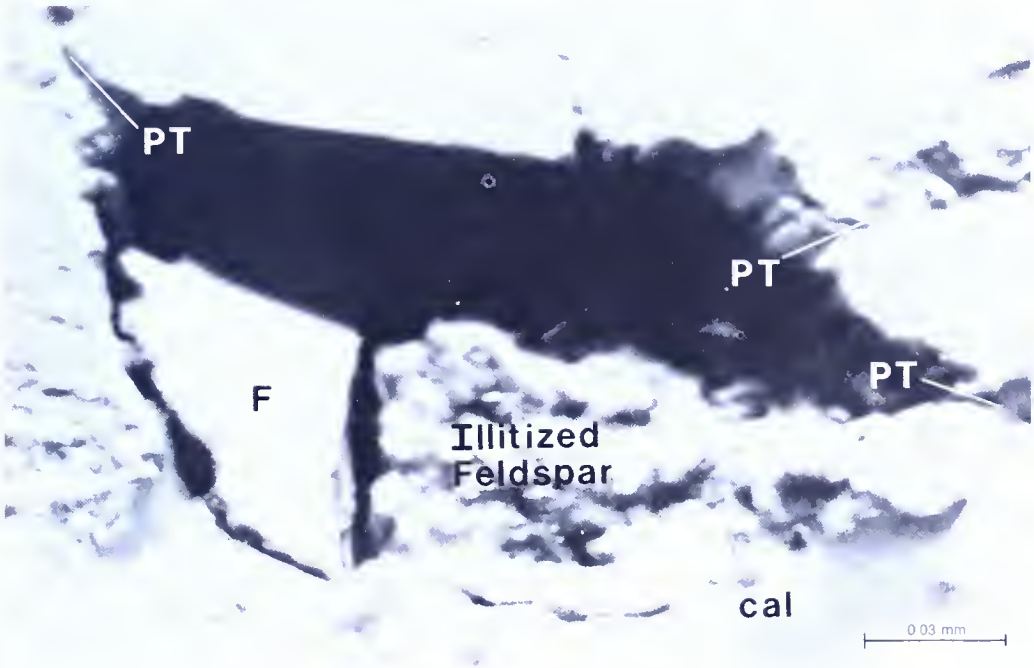
PT
PT
PT
F
Illitized
Feldspar
cal
0.03 mm

# CONTENTS

## FIGURES

## TABLES

# PETROLOGY AND RESERVOIR CHARACTERISTICS OF THE LOWER SILURIAN MEDINA GROUP SANDSTONES, ATHENS AND GENEVA FIELDS, CRAWFORD COUNTY, PENNSYLVANIA

by
Christopher D. Laughrey

## ABSTRACT

The Lower Silurian Medina Group in the Athens and Geneva fields of Crawford County, Pennsylvania, is productive from low-porosity (4 to 9 percent), low-permeability (<0.1 to 0.2 mD) sandstones at depths of 4,650 to 5,500 feet (1,417 to 1,676 m). Petrographic analyses of whole-diameter cores from each field show that the Medina Group consists of texturally immature to supermature, very fine to medium-grained sandstones and interbedded mudrocks. Productive sandstones are composed of siliceous to dolomitic subarkoses, sublitharenites, and quartz arenites. Geologic setting and facies analyses indicate that the Medina Group was deposited in tide-dominated paralic, deltaic, and shelf environments.

Detailed petrographic and scanning-electron-microscope (secondary and backscattered-electron modes) analyses of core samples show that the Athens and Geneva reservoir sandstones underwent a highly complex diagenetic history involving many stages of mineral precipitation and replacement. The overall diagenetic sequence included eight events: (1) precipitation of feldspar overgrowths; (2) nodular anhydrite, calcite, and siderite cementation; (3) clay-mineral authigenesis; (4) silica cementation; (5) titanium-mineral authigenesis; (6) compaction and pressure solution; (7) dolomitization; and (8) hematite cementation. Broadly defined early and late diagenetic stages are discernible, and both stages are characterized by specific diagenetic facies that have their own particular patterns of alteration. Early diagenesis began shortly after deposition and continued through shallow burial at depths of less than 1,000 feet (305 m). Early diagenetic reactions were controlled by detrital-mineral composition, depositional facies, and meteoric and connate pore-water composition. Late diagenesis coincided with progressively deeper burial beneath younger Paleozoic sediments and subsequent uplift during Mesozoic time. Late stage diagenetic reactions were controlled by increasing burial temperatures and pressures and by the compositions of both vertically migrating meteoric waters, which traveled along tectonically induced fractures, and connate pore waters.

Reservoir porosity in the Medina sandstones in the Athens and Geneva fields is largely secondary. Seven porosity types are recognized: (1) relict primary; (2) secondary intergranular; (3) moldic; (4) fabric-selective interlaminar; (5) intraconstituent; (6) microporosity; and (7) fracture. The distribution of porosity types in the sandstones is extremely heterogeneous and is controlled by compaction and cementation. Secondary porosity developed during the late diagenetic stage and was closely related to the major phase of hydrocarbon generation in the basin. Dry gas accumulated in combination traps, and the presence of hydrocarbons in the pores retarded any further diagenetic reactions. Precipitation and replacement of diagenetic minerals did continue, however, below the gas/water contact within the water-saturated portions of the reservoirs. These late diagenetic cements provided an effective seal against gas escape by tertiary migration during uplift and development of the regional southeasterly dip. The traps, as they are now produced, are diagenetic and represent cemented-in hydrocarbon accumulations.

Reservoir characteristics (i.e., porosity, water saturation, fluid sensitivity, and geophysical-log response) of the Medina reservoirs vary considerably, both vertically and laterally. A comparison of petrographic characteristics reveals that good correlation exists between increasing porosity and increasing grain size, and between decreasing sorting and decreasing mineralogic maturity. Irreducible water saturation is proportional to the amount of microporosity developed in the authigenic clays and cements. The sandstones are acid and water sensitive. Acid-sensitive minerals include calcite, dolomite, pyrite, chlorite, and hematite. The chlorite, dolomite, and hematite are particularly troublesome. Commonly utilized "acid breakdown" fluids should include an iron-chelating agent and an oxygen scavenger to avoid iron precipitation complications. Illite is mainly responsible for formation damage due to migrating fines. Mixed-layer clays account for the water sensitivity of the formation. Operators should consider that an oil-based stimulation fluid or a hydrofracture fluid composed of potassium chloride water, clay-control additives, and surface-tension reducers is necessary to minimize formation damage. The effect of variable mineralogy and the high degree of cementation on geophysical-log measurements and calculations must also be considered.

Optimum development and recovery of gas reserves from the tight Medina sandstones of northwestern Pennsylvania depends upon integrated geological and reservoir engineering studies. Petrographic analysis should be combined with petrophysical considerations as the basis for development planning in the reservoir management program. Interpretations of the origin, diagenetic history, and petrophysical character of the Medina sandstones may be applicable to other Paleozoic sandstone reservoirs in the central Appalachians.

# INTRODUCTION

Sandstones of the Lower Silurian Medina Group have produced a number of significant hydrocarbon reservoirs in northwestern Pennsylvania. During the past few years, the Medina Group has rapidly replaced the Lower Devonian Oriskany Sandstone as the principal objective of deep (Middle Devonian or older) drilling in the state. Consequently, the Medina Group now contributes a significant and increasing amount to the production of natural gas in Pennsylvania. For example, Medina reservoirs provided almost 60 percent of the deep gas produced in 1981 and 64 percent of the deep gas produced in 1982 (Harper, 1981, 1982). The prospects for continued exploration, development, and production from these Lower Silurian clastics appear good (Harper, 1981; Pees, 1983a).

From an exploration point of view, the Medina Group largely has been a statistical play (completion based upon anticipated success). The reported success rate for Medina drilling activity in Pennsylvania has exceeded 95 percent during the past three years (Harper, 1982, 1983). Copley (1980, p. 97) points out, however, that the reported high success ratios for Medina wells drilled in the central Appalachian basin more accurately reflect the number of wells completed and that these "run the gamut from totally noneconomic to prolific producers strictly as a function of reservoir characteristics." Indeed, Medina exploitation and development should not be based upon anticipated success, but rather should be carefully planned through a detailed understanding of depositional environments and diagenetic history of the reservoir sandstones. Depositional environment is an important control on orientation and morphology of the reservoirs and those aspects of reservoir quality that are related to sandstone grain size, sorting, and composition. Diagenesis controls the type and amount of porosity and the variety of minerals precipitated in the pores and pore throats. Diagenesis can also affect the geophysical-log response (see section on "Reservoir Evaluation") and can render a formation sensitive to acids or fresh water. Considerable formation damage can result from failing to tailor drilling and stimulation fluids to the composition of diagenetic minerals present in the pore systems of individual reservoir sandstones (Davies, 1979).

The regional and local subsurface stratigraphy of the Medina Group in northwestern Pennsylvania has been studied extensively as a result of the hydrocarbon discoveries and increased drilling activities in these Lower Silurian reservoirs (Cate, 1961; Kelley, 1966; Kelley and McGlade, 1969; Piotrowski, 1981). Few of the investigators, however, attempted to explain the mechanisms that account for adequate reservoir porosities in some Medina lithologies and very low values in other potential reservoir lithologies. None of the investigators provided data concerning the types of diagenetic minerals present in the sandstones, and there are no detailed subsur-

face interpretations of Medina sedimentary depositional environments in Pennsylvania in the literature. The need for such studies of the Medina reservoirs in Pennsylvania was stated by Kelley (1966, p. 36–37): "Detailed petrography of the sandstones has not been made. Such a study is warranted and would produce important results, particularly with regard to the effect the clay and dolomitic cements have in well stimulation and subsequent secondary recovery methods that could be applied." Nevertheless, such studies of the Medina sandstone reservoirs have not been made, despite their economic significance. As a result, wireline logs are often misinterpreted and potential reservoirs are sometimes damaged during drilling, completion, and stimulation activities.

This investigation of the Medina Group reservoir sandstones in the Athens and Geneva gas fields of Crawford County (Figure 1) was conducted for four specific purposes. The first was to describe the vertical and lateral distribution of depositional environments in the subsurface and define the relationship between these environments and the porosity and permeability of the sandstones. The second was to outline the diagenetic history of the sandstones with an emphasis on the postdepositional occlusion and enhancement of porosity. The third was to determine the various effects that detrital and diagenetic minerals have on reservoir quality and geophysical-log response, and the fourth was to describe the sensitivity of the Medina Group sandstones to drilling, completion, and stimulation fluids of different compositions.

The Athens and Geneva gas fields were chosen for this subsurface petrologic study for the following reasons. First, the need for adequate reservoir data in the Athens and Geneva fields prompted operators to drill representative whole-diameter cores in each of the development areas. In addition to these cores, wireline logs, sample logs, and geochemical gas logs (mud logs) provided a wealth of stratigraphic, lithologic, and reservoir engineering data for detailed studies of the sandstone reservoirs. Second, the Athens and Geneva gas fields are among the most southeasterly of the important Medina fields developed along the northwest flank of the central Appalachian basin. Published studies of the Medina Group reservoirs in Pennsylvania and adjacent states (Multer, 1963; Kelley, 1966; Kelley and McGlade, 1969; Knight, 1969; Overbey and Henniger, 1971) were all conducted in the shallower portions of the basin to the northwest and west of the present study areas. The amount of subsurface data now available from the Athens and Geneva fields provides an opportunity to document the nature of the deeper regions of the Medina play. Subsurface data from the Athens and Geneva fields will be more relevant to future drilling activities to the southeast in Venango, Mercer, Forest, and Warren Counties than data obtained from previous investigations.

## ACKNOWLEDGEMENTS

The completion of this report is the result of the cooperation of many individuals and companies who allowed extensive use of their materials and

information. Many of these individuals participated in helpful discussions and provided encouragement during the course of the investigation. Particular thanks are due to Robert Chapman and Anthony Lieonado, formerly with Wainoco Oil and Gas Company; Michael Price, Michael Canich, and Patrick Imbrogno, Cabot Oil and Gas Corporation; and Thomas Schmid, Wainoco Oil and Gas Company. Charles Grapes, Mitchell Energy Corporation, and John Flower of Gearhart Wireline Services, provided data on some of the logging parameters. Whole-diameter cores and cutting samples, on file with the Pennsylvania Geological Survey, were provided by the Wainoco Oil and Gas Company and by the Cabot Oil and Gas Corporation. Special thanks are also due to Jack Donahue, University of Pittsburgh, and David H. Krinsley, Arizona State University, for sharing their important work on the application of low-angle backscatter scanning electron microscopy to applied sedimentology. Gary Cooke and Feng-Chih Lin of the Gulf Research and Development Company provided all of the standard SEM (scanning electron microscope) photographs utilized in this report. Edward Cotter, Bucknell University, shared several of his ideas concerning the sedimentology of Early Silurian clastics. William A. Wescott of the Amoco Production Company kindly supplied the author with his own classification scheme of secondary porosity in sandstones. Jessie Donahue of GeoQuest Associates, and Thomas M. Berg, Pennsylvania Geological Survey, helped the author find methods for the construction of burial curves and sedimentation diagrams. John A. Harper, Pennsylvania Geological Survey, discussed each phase of the investigation with the author and offered considerable guidance throughout the course of the study. Paul Kucsma, Bureau of Oil and Gas Management, assisted in the compilation and calculation of geophysical-log data. Robert Fenton and Helen L. Delano, Pennsylvania Geological Survey, assisted the author in the laboratory and in sample photography.

Arthur A. Socolow, State Geologist, Dana R. Kelley of the Ashtola Production Company, Thomas M. Berg, John A. Harper, and Jack Donahue all read an earlier draft of the manuscript. Their criticisms and comments were very constructive, and the author incorporated many of their suggestions into the final draft.

## LOCATION AND DEVELOPMENT HISTORY OF THE ATHENS AND GENEVA FIELDS

The Athens and Geneva gas fields are located in the eastern and southern portions of Crawford County, Pennsylvania. The Athens field is developed mainly in Athens and Bloomfield Townships, but portions of the field extend into Rome Township. The Geneva field is located in Greenwood Township. Figure 1 shows the 7-1/2-minute quadrangles that encompass the areas occupied by the Athens and Geneva fields.

Hydrocarbons have been produced in the vicinities of the Athens and Geneva fields for many years. Sisler and others (1933) reported that oil pro-

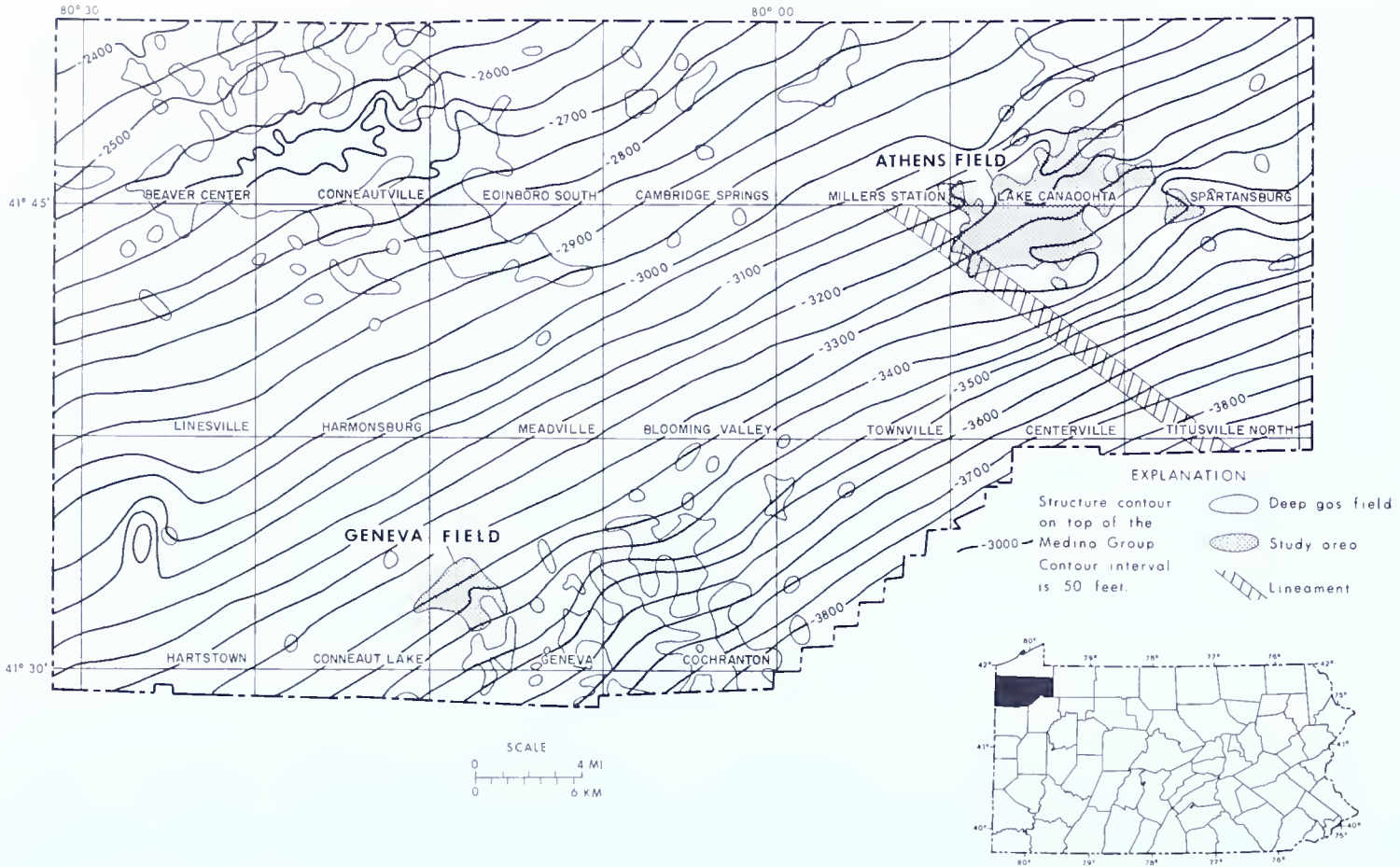


Figure 1. Map of the study area showing the locations of the Athens and Geneva gas fields, structures, and the distribution of deep gas fields in Crawford County. Structure contours are on top of the Medina Group. The trend of the Tyrone-Mount Union lineament is also shown.

duction began in the vicinity of the Athens field in 1861. Production was from the Upper Devonian Venango Group at an average depth of 500 feet (150 m). Ashley and Robinson (1922) noted that both oil and gas were produced in the Geneva area as early as 1900. This production was from the near-surface Mississippian Pocono Formation. Gas shows have been encountered in the Devonian shales and in the Oriskany Sandstone at both the Athens and Geneva fields. Gas shows in the Devonian shales occur at depths of approximately 1,000 feet (300 m). The average depth to the Oriskany in this area is between 3,500 and 4,000 feet (1,050 and 1,200 m).

Initial production from the Medina Group at the Athens field was begun in September 1974 when the Columbia Gas Transmission Company No. 1 A. and R. Post well was completed in the Grimsby and Whirlpool Sandstones (Figure 2A) between 4,961 and 5,061 feet (1,512 and 1,543 m). The total depth was 5,146 feet (1,569 m) in the Upper Ordovician Queenston Shale. The well was stimulated by hydrofracture treatment, and the initial open flow was 726 Mcf (thousand cubic feet) per day with a rock pressure of 1,220 (pounds per square inch) measured after 72 hours. The discovery well was shut-in from 1974 until 1980, when field production began. Thirty-six wells were drilled in the Athens field in 1979, 44 wells were drilled in 1980, 34 wells were drilled in 1981, and 12 wells were drilled in 1982 (Appendix 1). The field is still under infill drilling on 40-acre spacing. All wells have been hydrofractured. Cumulative production from the Athens field was 3,290,452 Mcf at the end of 1982 (Harper, 1982). Table 1 summarizes the Athens field reservoir characteristics and production data.

The Kebert Developers No. 1 well was drilled by the N-Ren Corporation in 1976 and found gas in the Medina Group between 4,798 and 4,953 feet (1,462 and 1,510 m). This discovery, in Greenwood Township, established the Greenwood pool of the Geneva field. The initial after-treatment open flow was 1,229 Mcf per day, and the initial rock pressure was 1,297 psi after 48 hours. The total depth was 4,990 feet (1,521 m) in the Queenston Shale. Eight productive wells were completed in the Greenwood pool by the end of 1976. The ninth well was plugged and abandoned due to casing collapse. The nine wells in the Greenwood pool were drilled on 100-acre spacing. The pool was shut-in from the end of 1976 through 1980. In 1981, a total of 99,490 Mcf of gas was produced from the Greenwood pool. Cumulative production at the end of 1982 was 186,607 Mcf.

Extension drilling in the Geneva field established the Rock Creek pool southeast of the Greenwood development. Gas production was obtained from the N-Ren Corporation No. 1 Bitnec well in June 1977. Gas was encountered in the Medina between 4,892 and 4,990 feet (1,491 and 1,521 m). The after-treatment open flow was reported as 1,100 Mcf per day and the rock pressure was 1,100 psi after 48 hours. The total depth was 5,147 feet (1,569 m). Nine additional wells were completed in the Rock Creek pool by the end of 1981. The development program is now managed by the Cabot Oil and Gas Company. Cumulative production from the Rock Creek pool

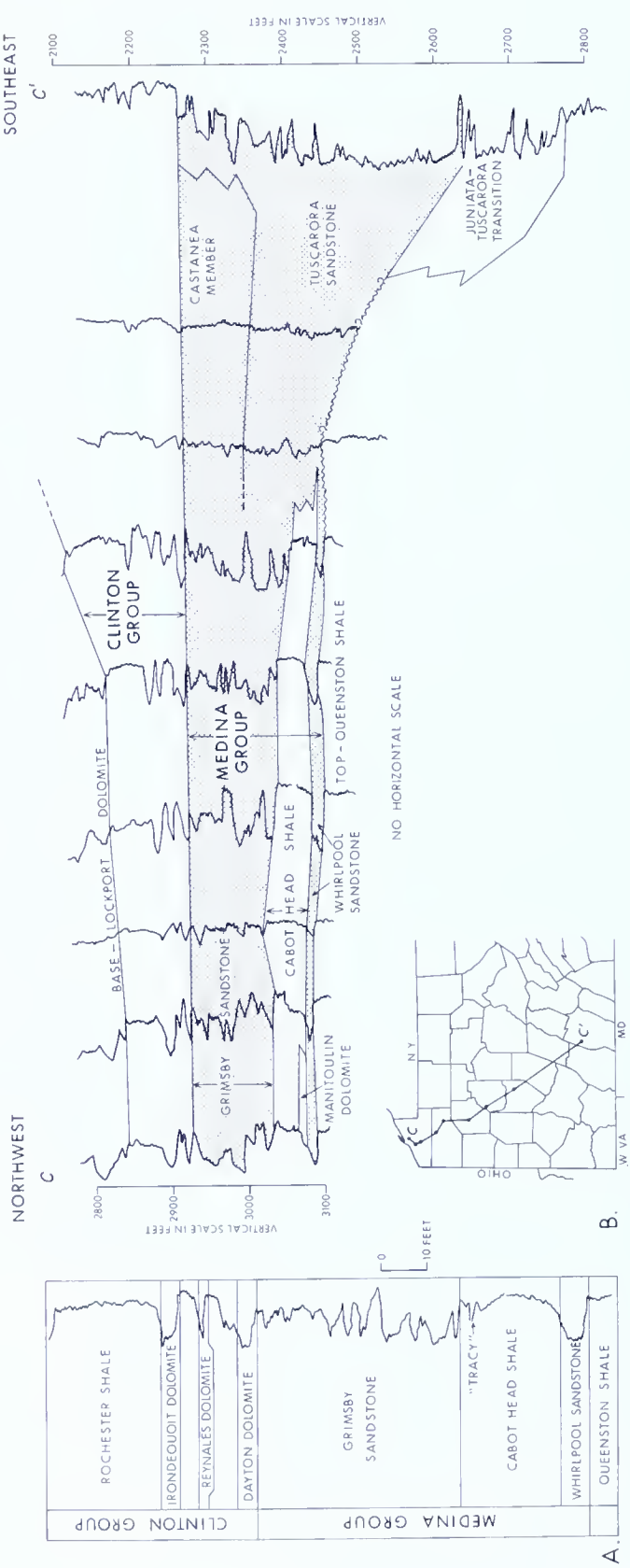


Figure 2A. Stratigraphic column of part of the Lower Silurian Series in northwestern Pennsylvania and geophysical log from the No. 1 A. and R. Post discovery well in the Athens field showing typical geophysical-log response and format. The Medina is approximately 180 feet (55 m) thick in this area.

B. Regional subsurface cross section of the Medina Group and Tuscarora Formation in the subsurface of western Pennsylvania (modified from Piotrowski, 1981).

Table 1. *Reservoir Characteristics and Production Data for the Athens Field*

| | |
|---|---|
| | DISCOVERY WELL |
| Name: | Columbia Gas Transmission Company, #1 Alden & Roberta Post |
| Date of completion: | September 20, 1974 |
| Total depth: | 5,146 feet (1,564 m) |
| Perforations: | 4,961 to 5,061 feet (1,512 to 1,543 m) |
| Treatment: | Hydraulic fracturing with 650 barrels of water and 55,000 pounds of sand at an injection rate of 56.1 barrels per minute |
| Initial production: | 726 Mcf per day |
| | PRODUCTIVE AREA |
| Proved developed: | 5,840 acres |
| Spacing: | 40 acres |
| Average porosity height: | 3.25 |
| Average water saturation: | 39.69% |
| | FIELD PRODUCTION |
| Drive mechanism: | Pressure depletion |
| Producing wells as of January 1983: | 146 |
| Cumulative production at end of 1982: | 3,290,452 Mcf |
| Status of field at end of 1982: | Producing and shut-in |

was 293,650 Mcf at the end of 1982 (Harper, 1982). Reservoir characteristics of the Greenwood and Rock Creek pools are listed in Table 2.

## GEOLOGIC SETTING

The Medina Group in northwestern Pennsylvania is an entirely subsurface sequence of Lower Silurian (Berry and Boucot, 1970) sandstones and shales and minor amounts of carbonates. Within this region the group ranges in thickness from 140 to more than 200 feet (43 to 61 m). The Medina Group disconformably overlies the Upper Ordovician Queenston Shale and grades conformably upward into the Lower Silurian Clinton Group. Regional stratigraphic relationships of the Medina Group sandstones have been published by Cate (1961), Heyman (1977), and Piotrowski (1981).

On the basis of gamma-ray correlation, Piotrowski (1981) recognized four major stratigraphic units within the subsurface Medina Group. In descending order, these are: (1) the Grimsby Sandstone (interbedded sandstones, siltstones, and shales); (2) the Cabot Head Shale; (3) the Manitoulin

Table 2. *Reservoir Characteristics and Production Data for the Geneva Field*

| | |
|---|---|
| | DISCOVERY WELL |
| Name: | N-Ren Corporation, #1 Kebert Developers |
| Date of completion: | November 7, 1975 |
| Total depth: | 4,990 feet (1,521 m) |
| Perforations: | 4,798 to 4,953 feet (1,462 to 1,510 m) |
| Treatment: | Hydraulic fracturing with 1,560 barrels of water and 900 pounds of sand at an injection rate of 38.2 barrels per minute |
| Initial production: | 1,229 Mcf per day |
| | PRODUCTIVE AREA |
| Proved developed: | 2,200 acres |
| Spacing: | 100 acres |
| Average porosity-height: | 1.65 |
| Average water saturation: | 34.8% |
| | FIELD PRODUCTION |
| Drive mechanism: | Pressure depletion |
| Producing wells as of January 1983: | 22 (12 in Greenwood, 10 in Rock Creek) |
| Cumulative production at end of 1982: | 215,067 Mcf |
| Status of field at end of 1982: | Producing and shut-in |

Dolomite; and (4) the Whirlpool Sandstone. Kelley and McGlade (1969) were able to recognize the Thorold Sandstone in the subsurface of Erie County. The Thorold is stratigraphically higher than the Grimsby. New York workers generally consider the Thorold as the uppermost formation in the Medina Group (Metzger, 1982). Without samples, the Thorold and Grimsby are difficult to distinguish in the subsurface. For this reason, Piotrowski (1981) did not distinguish the Thorold from the Grimsby in his regional correlations. Figure 2B illustrates the regional stratigraphic relationships of these units in the subsurface of northwestern Pennsylvania, and correlation with the Tuscarora Formation to the south and east. This cross section, modified from Piotrowski (1981), shows that the Medina Group is characterized by a "broken sandstone" gamma-ray signature in northwestern Pennsylvania. The interval becomes less shaly to the east and southeast where it grades into the uppermost portions of the Tuscarora. The upper sandstone portion of the Grimsby appears to be correlative with the shaly Castanea Member of the Tuscarora Formation; the lower portion of the Grimsby coalesces into the principal sandstone unit of the Tuscarora. The Cabot Head Shale and the Whirlpool Sandstone are supposedly truncated by an apparent unconformity to the southeast. Piotrowski (1981) de-

fined the strike of this truncation, which occurs along the line of maximum Medina thickness, as the shoreline during the time of Medina deposition. The Manitoulin Dolomite, a minor unit in the Medina Group of Pennsylvania, is restricted to the Lake Erie region in the extreme northwest corner of the state.

Orientation of cross strata in the Medina Group shows well-defined northwestward and northeast-southwestward sediment transport directions (Martini, 1971). This is in accord with the results of Yeakel (1962) and Cotter (1982), who studied the laterally equivalent clastics to the southeast (Tuscarora Formation). Ziegler and others (1977), Johnson (1980), and Cotter (1982) place Pennsylvania approximately 25 to 30 degrees south of the equator during the Early Silurian. This interpretation puts the region under the variable influence of wet southwesterly winter winds and drier easterly summer winds (Ziegler and others, 1977). Cotter (1982) postulates that the Early Silurian climate of Pennsylvania was similar to that of the present-day Mexican Pacific coast, which has an early winter rainy season and relatively arid conditions during the remainder of year.

Lower Silurian clastics entered the Appalachian depositional basin during the last pulse of the Taconic orogeny (Cotter, 1982). Sands of moderately high quartz content were shed from foreland fold-belt highlands directly into the adjacent foreland basin (Dickinson and Suczek, 1979). The source rocks of the highlands shielded the basin from *magmatic-arc and suture-belt provenances*,[1] so that the Lower Silurian sands were initially derived from recycling of earlier sedimentary sequences (Martin, 1971) and possibly from positive areas on the craton (Knight, 1969). The sedimentary source cover was eventually stripped during the latter part of Early Silurian time, resulting in detrital contributions from the plutonic igneous rocks of the arc orogen (Folk, 1960).

The Athens and Geneva fields are located along the northwest flank of the Appalachian basin. The Findlay Arch lies approximately 200 miles (320 km) to the west, and the Allegheny Front is about 100 miles (160 km) to the southeast. Regional structure is characterized by a gentle southeasterly dip of approximately 45 feet per mile (8.5 m/km) (Figure 1). Lytle and others (1971) reported that this mild southeasterly dip is locally interrupted by minor folds and small faults. These minor fold axes trend northeast and southwest, parallel with the long axis of the Appalachian basin. Northwest-southeast- and northeast-southwest-trending lineaments are the major structural elements of the Athens and Geneva vicinity (Rodgers, 1981; Tillman, 1982; Pees, 1983b). The lineaments range from 1 mile (1.6 km) to more than 100 miles (160 km) in length and are most frequently depicted as topographic linears on raised-relief maps defined from Landsat and aerial photographs (Pees, 1983b). The Tyrone-Mount Union lineament is the major lineament that crosses Crawford County, and this feature directly

[1] Words in italics are defined in the glossary, which begins on page 113.

crosses the southwest corner of the Athens field (Figure 1). Fracture traces also appear as linear features on aerial photographs in the study area. These traces are typically less than 1 mile (1.6 km) in length, and their dominant trends are northeast and northwest (Rodgers, 1981; Pees, 1983b). Pees (1983b) noted that more than 2,000 fracture traces can occur in a 7-1/2-minute quadrangle in northwestern Pennsylvania. The lineaments and the fracture traces in the Athens and Geneva fields area are zones of secondary permeability (Rodgers, 1981; Tillman, 1982). The significance of these structures to hydrocarbon migration and accumulation have been discussed in detail by Wheeler (1980), Tillman (1982), and Pees (1983b).

## SAMPLES AND METHODS

The data presented in this report combine observations on two whole-diameter cores of the Medina Group with measurements obtained from 156 geophysical logs and selected well-cutting samples and gas logs from the Athens and Geneva fields. Core descriptions and analyses are shown graphically in Figures 3 and 4. Results of the core analyses are tabulated in Appendix 2. One-hundred eighty-six feet (57 m) of core was recovered from the Creacraft No. 1 well in the Athens field, including the entire Medina Group interval and portions of the overlying Dayton Dolomite and underlying Queenston Shale. Sixty feet (18 m) of core, representing portions of the Grimsby and all of the Whirlpool intervals, was recovered from the Kebert No. 1 well. Log calculations were made according to the procedures described by Hilchie (1978). Appendix 1 lists the results of all log calculations made for this study. Representative sample logs and gas logs from the study area are shown in Figure 5.

Analytic work included petrographic examination of samples taken from the two cores. Each core was slabbed and examined to determine gross composition, texture, and types of sedimentary structures. Fractures were also described. Sixty thin sections were examined for this study. Modal analyses were done on all samples by counting 300 points on each slide. Grain size was estimated by measuring the apparent long axis of 100 quartz or feldspar grains per slide. Estimates of sorting within each sample were made by comparing each thin section to a standard petrographic index (Beard and Weyl, 1973) and by calculating the standard deviation of grain-size measurements by moment methods (Friedman and Sanders, 1978). Selected samples were analyzed using bulk X-ray techniques. Scanning electron microscopy (SEM), in both the secondary (SE) and backscattered electron (BE) modes with energy-dispersive X-ray, was used to observe *authigenic* mineralogy, replacement textures, and pore geometry and texture. Discussions of the SEM (BE) techniques can be found in Krinsley (in preparation) and in Krinsley and others (1983, in preparation). The lateral and vertical interrelationships of the reservoir sandstones and associated lithologies were studied

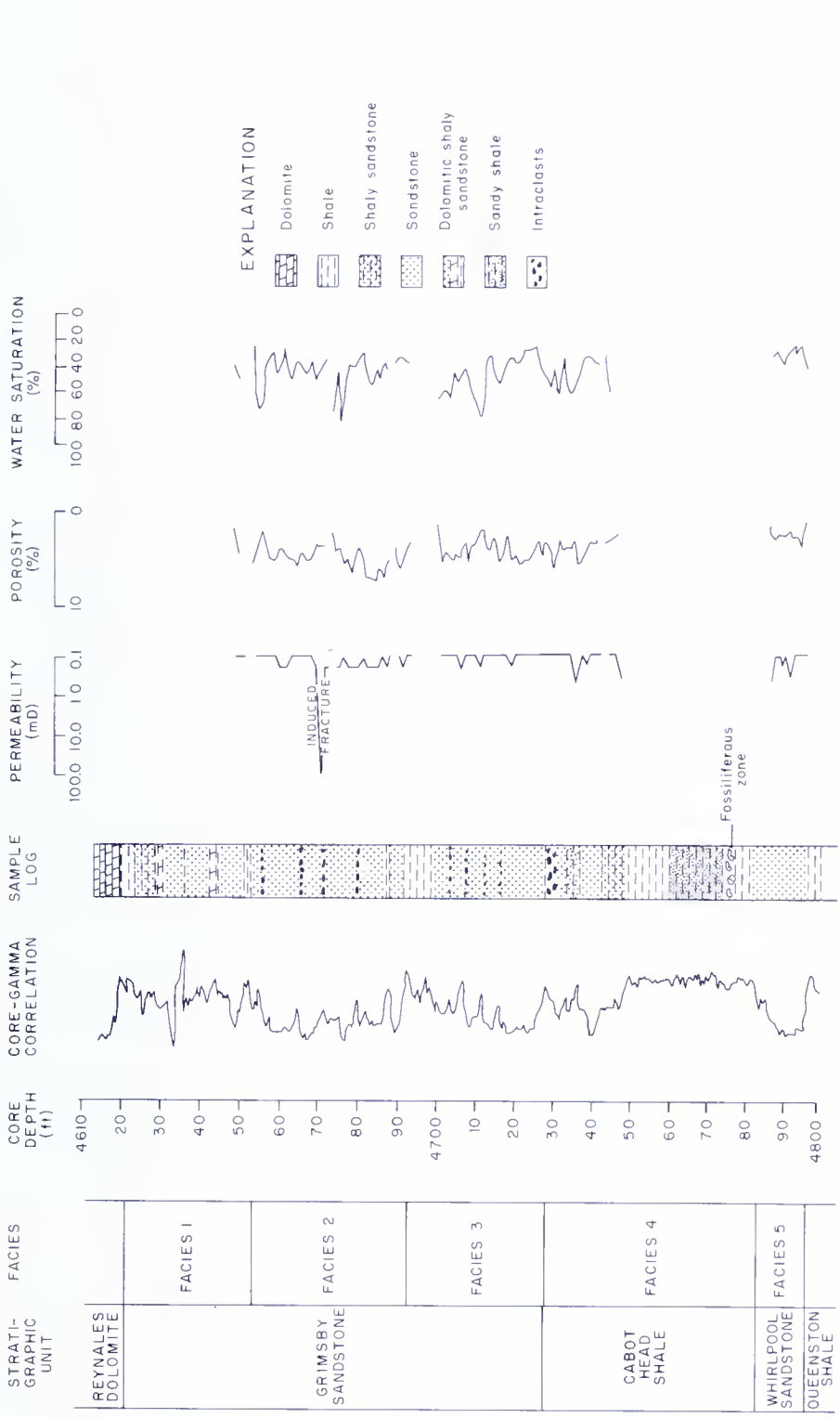


Figure 3. Graphical presentation of the results of core analyses for the Creacraft No. 1 core, Athens field (see Appendix 2 for complete core analyses). Group designations represent lithologic units or facies discussed in the text.

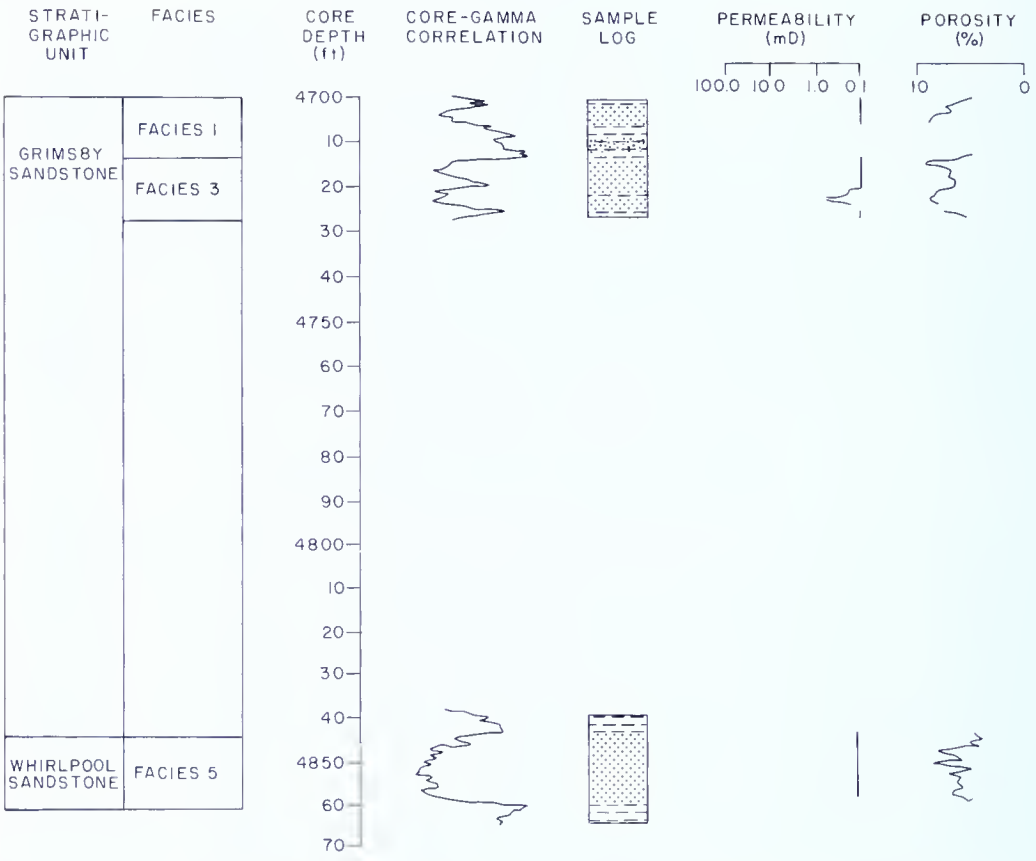


Figure 4. Graphical presentation of the results of core analyses for the Kebert Developers No. 1 well, Geneva field (see Appendix 2 for complete core analyses). Group designations represent lithologic units or facies discussed in the text. (See Figure 3 for explanation of patterns in sample log.)

through the use of multiple geophysical-log cross sections. The fluid sensitivity of the sandstones was determined by acid solubility, immersion, and iron content analyses.

Core analyses and fluid-sensitivity tests were conducted by Core Laboratories and Halliburton Services, respectively, and the data were provided through the courtesy of the Wainoco Oil and Gas Company and Cabot Oil and Gas Corporation.

The sandstone classification scheme of Pettijohn and others (1972) was used in this report (Figure 6). In this classification, two major groups of sandstones are recognized on the basis of texture: (1) *arenites*, which are sandstones composed of detrital grains and less than 15 percent matrix; and (2) *wackes*, which contain more than 15 percent matrix. The name *quartz arenite* is applied to those sandstones whose framework has 95 precent or more quartz grains. Arkosic arenites are sandstones in which there is more than 25 percent feldspar and the percentage of feldspar is greater than the percentage of rock fragments. Litharenites are sandstones in which there is

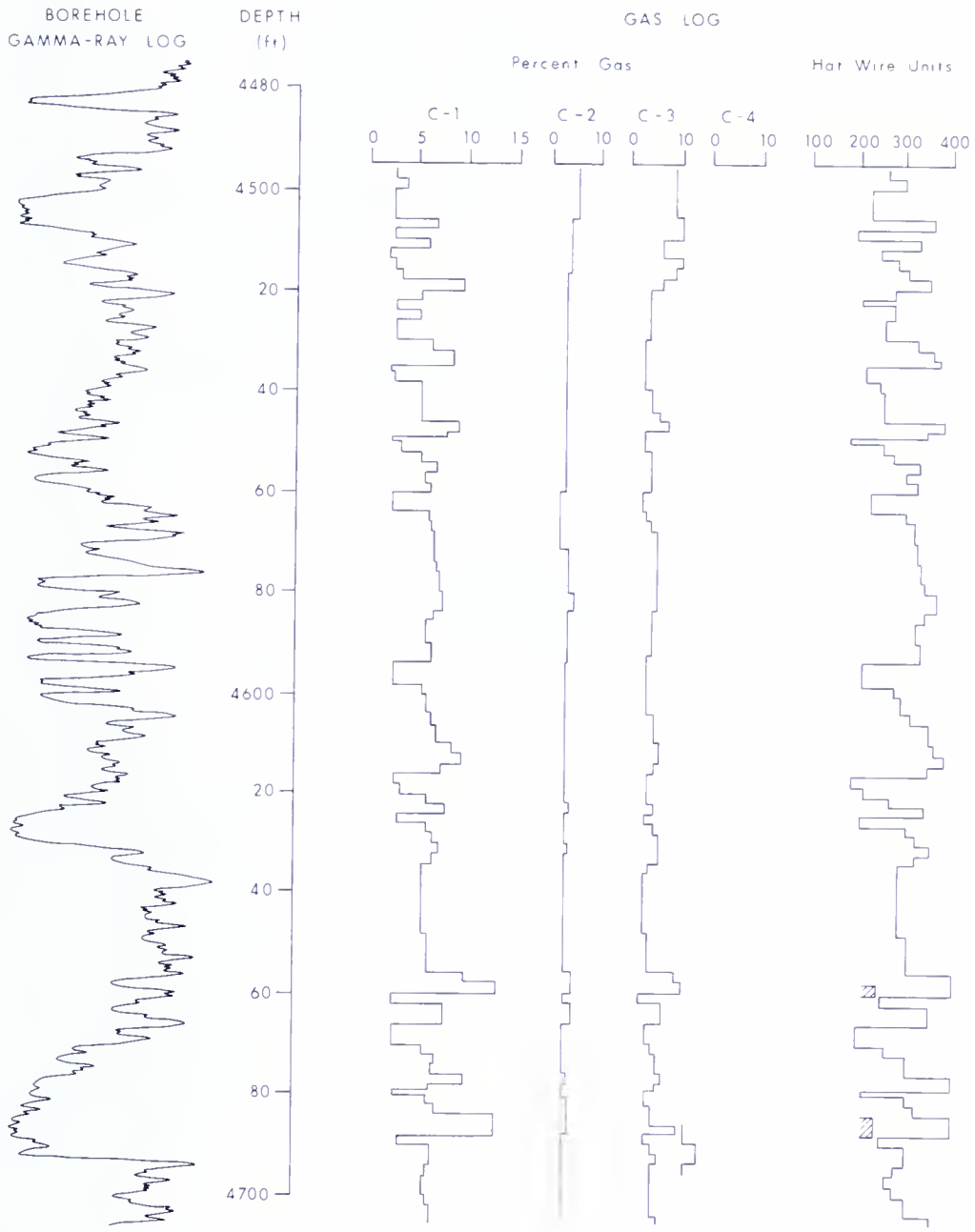


Figure 5. Representative borehole log and gas log of the Medina interval in the study area. Logs are from the Preston No. 1 well in the Athens field. Gases designated as C–1 through C–4 represent methane, ethane, propane, and butane, respectively. The relative amounts of these gases in the borehole are indicated as percentages of the total gas mixture. Hot wire units refer to the relative amount of total hydrocarbons encountered in the borehole. The gas is predominantly methane, but minor amounts of ethane, propane, and butane are present in the formation.

more than 25 percent rock fragments and the percentage of rock fragments is greater than the percentage of feldspar. Arkose and lithic arkose may be distinguished within the arkosic arenite field. *Subarkose* and *sublitharenite* are two rock types that are transitional with the quartz arenites. The wackes constitute a transitional group between the arenites and mudrocks; feldspathic and lithic graywackes are distinguished. Arkoses that have a considerable proportion of matrix are called arkosic wackes. Quartz wackes constitute an uncommon group of sandstones consisting of quartz plus some matrix.

When classified using this system, the Medina Group sandstones from the Athens and Geneva fields include 23.2 percent quartz arenites, 41 percent

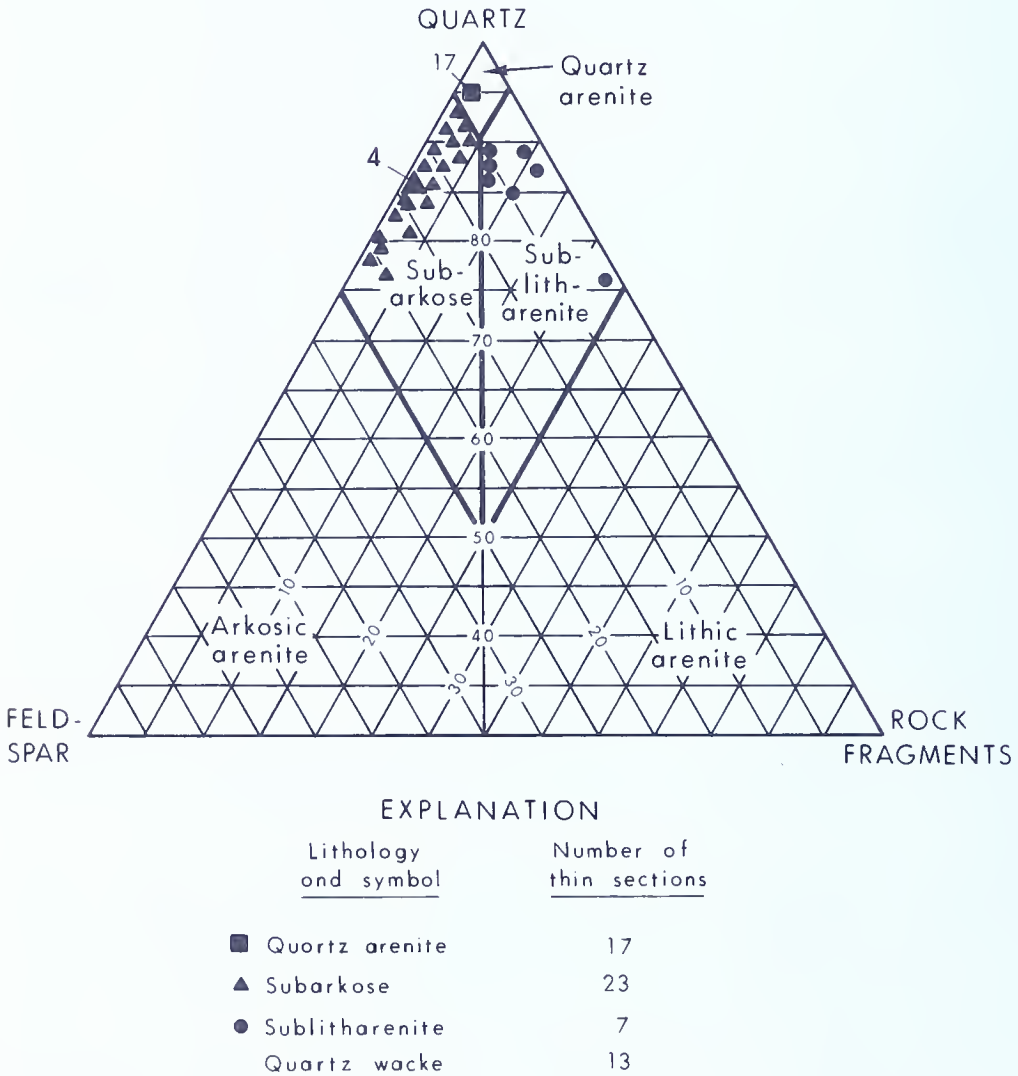


Figure 6. Ternary plot showing the composition of Medina Group sandstones based on point counts of 60 thin sections. Classification system is that of Pettijohn and others (1972).

subarkoses, 12.5 percent sublitharenites, and 23.2 percent arkosic and quartz wackes (Figure 6). The compositional varieties of specific reservoir types are presented and discussed in the following section.

## SEDIMENTARY DEPOSITIONAL ENVIRONMENTS

Medina Group sandstones at the Athens and Geneva fields can be separated into five different facies on the basis of their microscopic petrology, sedimentary structures, body and trace fossils, geometries, geophysical-log responses, and reservoir characteristics. The first three facies occur within the Grimsby Sandstone. The fourth and fifth major facies correspond respectively to the Cabot Head Shale and Whirlpool Sandstone.

### FACIES 1

This facies comprises the upper 35 feet (10.7 m) of the Creacraft well core (Figure 3) and the upper 14 feet (4.3 m) of the Kebert well core (Figure 4). This upper portion of the Grimsby is frequently identified as the upper shaly member (Heyman, 1977; Pees, 1983a), and it exhibits a characteristically argillaceous response on its gamma-ray signature (Figure 7). The upper and lower contacts of this facies are marked by an abrupt decrease in radioactivity, which reflects the transition to overlying carbonate rocks and underlying arenaceous sandstone. Geophysical-log cross sections in the study area (Figure 20) show that facies 1 has an overall sheet geometry.

#### Description

Sandstone within this facies range in thickness from 20 to 55 feet (6.1 to 16.8 m) and are composed of red to pale-green[1] arkosic wackes and quartz wackes. Figure 8 shows the various petrographic characteristics of this facies. The sandstones are poorly to moderately sorted. Mean grain size ranges from 0.1 to 0.25 mm, and the sandstones exhibit fining-upward sequences. The fining-upward trends range in thickness from 0.5 to 2 feet (0.2 to 0.6 m). They are weakly developed in the larger grain-size intervals and well developed as graded fining-upward sequences in the finer grain-size intervals. Contacts between fining-upward sequences are sharp. Detrital quartz grains are angular to subrounded and exhibit abraded overgrowths. The sandstones contain from 20 to 30 percent matrix, which is argillaceous and hematitic to sideritic and supports the framework grains. Porosity ranges from 2.2 to 4.5 percent and is largely confined to microvoids which

[1] Color designations are from *Rock-Color Chart* (The Rock-Color Chart Committee, 1970). Numerical designations from the *Rock-Color Chart* are given for the different sandstone groups in Tables 9, 10, and 11.

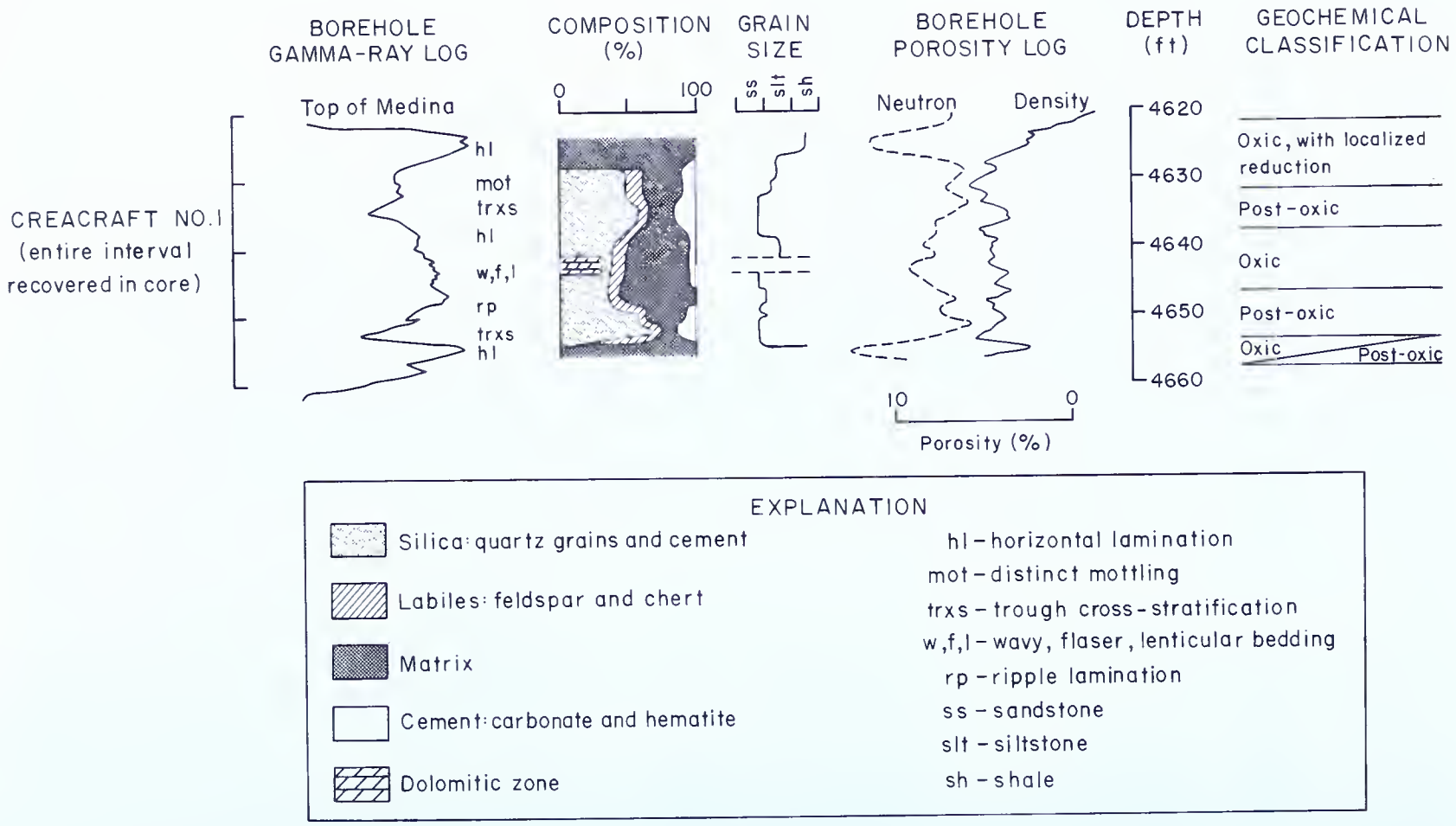
BOREHOLE GAMMA-RAY LOG
COMPOSITION (%)
GRAIN SIZE
BOREHOLE POROSITY LOG
DEPTH (ft)
GEOCHEMICAL CLASSIFICATION
CREACRAFT NO.1
(entire interval recovered in core)
Top of Medina
hl
mot
trxs
hl
w,f,l
rp
trxs
hl
0
100
ss
slt
sh
Neutron
Density
10
0
Porosity (%)
4620
4630
4640
4650
4660
Oxic, with localized reduction
Post-oxic
Oxic
Post-oxic
Oxic
Post-oxic
EXPLANATION
Silica: quartz grains and cement
Labiles: feldspar and chert
Matrix
Cement: carbonate and hematite
Dolomitic zone
hl – horizontal lamination
mot – distinct mottling
trxs – trough cross-stratification
w,f,l – wavy, flaser, lenticular bedding
rp – ripple lamination
ss – sandstone
slt – siltstone
sh – shale

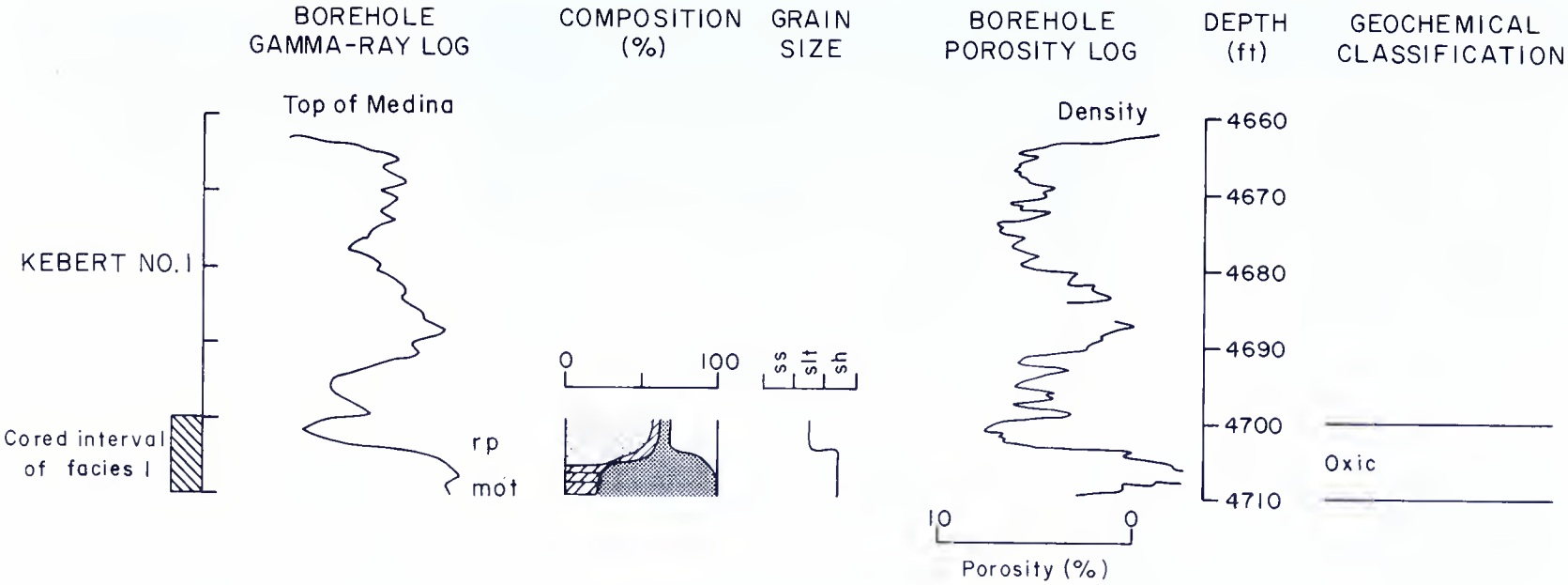


Figure 7. Geophysical logs, grain size, and compositional characteristics of Medina facies 1 sandstones penetrated in the Creacraft No. 1 and Kebert Developers No. 1 wells in Crawford County. Stable grains are quartz and unstable grains are feldspar, rock fragments, and altered accessory grains. The geochemical classification of the facies 1 sedimentary environments is based on the characteristic phases of the geochemical classification as defined by Berner (1981).

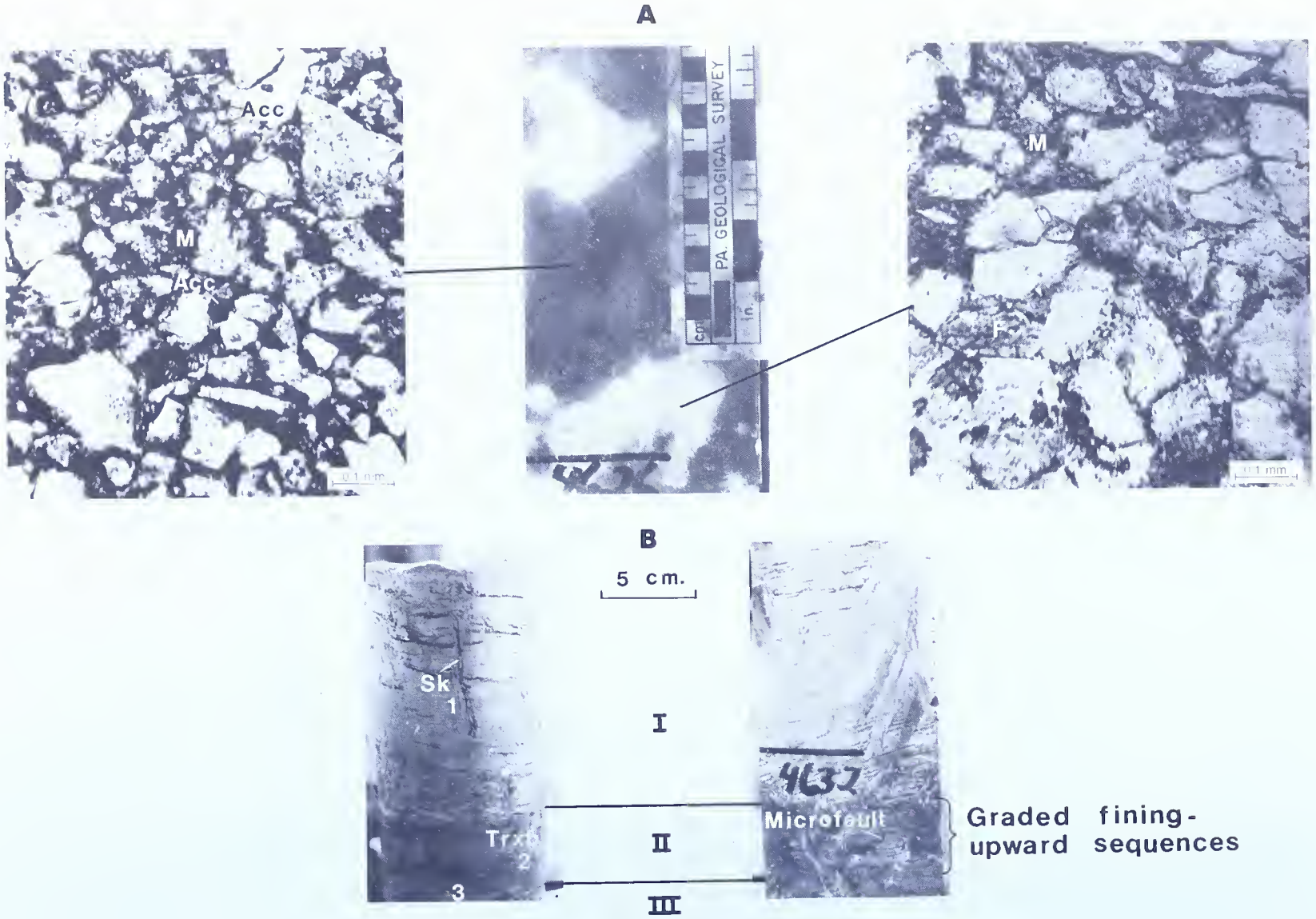
A
Acc
M
Acc
PA. GEOLOGICAL SURVEY
M
F
B
5 cm.
Sk
1
Trx
2
3
I
II
III
4632
Microfault
Graded fining-upward sequences

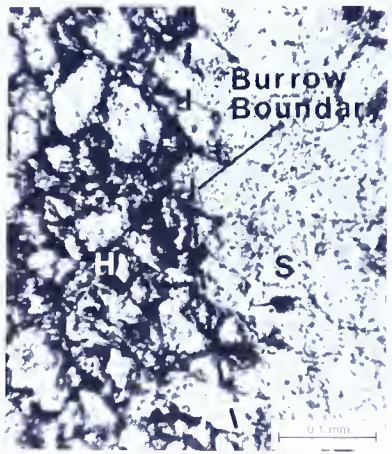


1

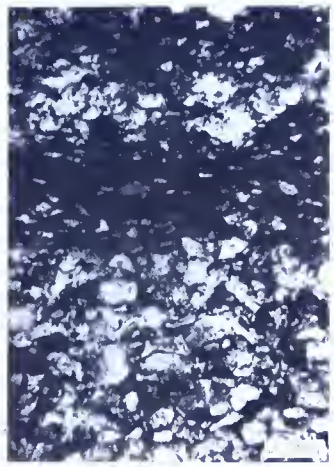

2

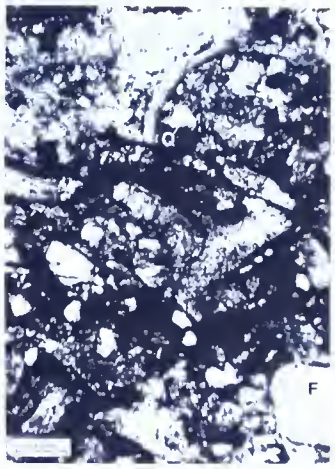


3

Figure 8. Selected petrographic characteristics of the facies 1 sandstones and associated lithologies.

A. Mottled and bioturbated, orgillaceous, hematitic sandstone. Photomicrographs on the left and right show the typically immature texture of this interval. Note the abundant amount of matrix (M), the poor sorting, and the lack of rounding in the detrital grains. Photomicrograph on the left is from the red portion of the sandstone. It is a hematitic quartz wacke. The hematite cement is finely disseminated within the argillaceous matrix. Hematite also fills intergranular pores. The hematite is believed to be derived from the intrastratal dissolution of the numerous opaque iron-bearing accessory grains (Acc) thot are present. The photomicrograph on the right is from one of the green mottles. Matrix (M) is composed of chlorite and siderite. The chloritic matrix appears to be derived, at leost in part, from the breakdown of detritol feldspar grains (F). Plane-polarized light.

B. *Skolithos*-burrowed sandstone, slabbed and unslabbed core. Three intervols (I, II, and III) are indicated, and photomicrographs from each of these intervals are shown. Interval I is choracterized by trough cross-stratification. Cross strota are interrupted by well-developed, matrix-filled *Skolithos* burrows. Sondstone is a quartz wacke. Details of the boundary between hematite-cemented and cross-bedded sandstone (H) and siderite-cemented sandstone (S) within a vertical *Skolithos* burrow are shown in photomicrograph 1. The cross-stratified sandstone is interpreted as hoving originated as a tidal-creek chonnel fill. Interval II is a graded fining-upward sequence into which the overlying tidal channel cut. The lominae of this interval are disrupted by microfaulting. Interval III is a hematitic, silty biosparrudite. Note the abundant fossil fragments, silt-sized quartz (Q) and sand-sized feldspar (F) in photomicrograph 3. The trace fossil *Rusophycus* is abundant at the base of interval III. *Rusophycus* is thought to represent the resting trace of trilobites in the soft sediment. All photomicrographs were taken under crossed nicols.

average less than 0.5 micron in diameter. The sandstones contain numerous 2-mm- to 2-cm-thick partings of argillaceous, hematitic mudstone. They also contain several thin- to medium-sized interbeds of hematitic to sideritic, argillaceous siltstone and hematitic, dolomitic, silty biosparrudite.[1] Framework grains consist of monocrystalline quartz, microcline and untwinned feldspar, and assorted accessory grains including hornblende, tourmaline, zircon, epidote, ilmenite, magnetite, and opaque iron oxides. The monocrystalline quartz exhibits straight to slightly undulose extinction. Trace amounts of polycrystalline quartz, chert, and biotite were observed. The modal analyses of the sandstones are listed in Table 3.

In the two cores examined, color variations occur as distinct mottling in the uppermost 5 to 12 feet (1.5 to 3.7 m) of this facies and as thin, horizontal, green bands in the lower, predominantly red, 9 to 23 feet (2.7 to 7 m). Petrographic observations reveal that the predominant red pigmentation of this facies is due to hematite cement, which occurs as (1) a particle coat; (2) an intergranular pore-fill; and (3) a finely disseminated mineral within the interstitial clay minerals. The localized green pigmentation owes its color to sideritic and chloritic matrix.

Numerous small-scale sedimentary structures occur within this facies. These structures include *lenticular*, *flaser*, and *wavy bedding*; small-scale trough crossbedding; very thin bedded, graded, horizontal fining-upward sequences; ripple cross-lamination; *reactivation surfaces*; and mudcracks. Microfaulted parallel laminae also occur. The trough crossbedded intervals contain basal lags of intraformational conglomerate which overlie scour surfaces. The scour surfaces are erosive into underlying argillaceous siltstone, hematitic mudstone, or carbonate.

This facies contains a diverse assemblage of trace fossils, and some intervals are very strongly bioturbated. The assemblage is dominated by the trace fossils *Skolithos* and *Monocraterion*. *Arthrophycus* is present in the lower portions of this facies. The trace fossils *Rusophycus* and *Diplocraterion* are also present.

Body fossils are common in the interbeds of muddy, silty carbonate. Pentamerid brachiopods are very abundant, as are phosphatic shell fragments.

## Interpretation

Many of the physical and biogenic structures of this facies are diagnostic of tidal-flat deposition. Structures that occur in the upper shaly member of the Grimsby have been documented in modern sediments by Klein (1977) and Reineck and Singh (1973). Interpreted processes and resultant sedimentary structures in tidal-flat sediments are listed in Table 4.

[1] Biosparrudite is a carbonate rock composed of more than two thirds calcite spar cement and less than 25 percent intraclasts and oolites. The volume ratio of fossils to pellets is greater than 3:1, and the fossil allochems are coarser than 1 mm (Folk, 1968).

Table 3. *Modal*[1] *Analyses of Facies 1 Sandstones, Athens and Geneva Fields*

(determined by petrographic examination)

| Minerals | Percentage |
|---|---|
| Quartz, total | 60 |
| Monocrystalline | 49 |
| Polycrystalline | 10 |
| Chert | 1 |
| Feldspar, total | 5 to 11 |
| Microcline | 1 to 2 |
| Plagioclase | — |
| Untwinned | 4 to 9 |
| Rock fragments, total | — |
| Sedimentary | — |
| Metamorphic | — |
| Clay matrix, total | 24 |
| Cement, total | 10 to 15 |
| **Texture** | |
| Average quartz size | 0.1 to 0.25 mm |
| Skew | Positive |
| Sorting | 1.42 to 0.78 phi |

[1] Based on point counts of 14 thin sections.

Table 4. *Interpreted Processes and Resultant Sedimentary Structures in the Facies 1 Sandstones*

| | Process | Structure |
|---|---|---|
| (1) | Alternation of bedload and suspension-load deposition | Flaser and lenticular bedding |
| (2) | Late-stage emergent runoff | Small channel scours |
| (3) | Tidal scour | Mud-chip conglomerate at channel base of trough crossbedded sandstone developed over erosive surface |
| (4) | Time-velocity asymmetry of tidal-current bedload transport | Reactivation surfaces |
| (5) | High rate of sedimentation combined with regressive sedimentation | Graded fining-upward sequence |
| (6) | Exposure and evaporation | Mud cracks |

The trace-fossil assemblage in this facies resembles the *Skolithos* ichnofacies, which indicates deposition in a sandy littoral environment in which the substrate is periodically reworked by waves and/or tidal currents (Selley, 1981; Seilacher, 1978). The overall texture of the sandstones in this facies, combined with the evidence of fluctuating marine conditions (sedimentary structures, trace fossils, and fossils in the associated interbeds), suggests deposition in an environment dominated by tidal activity.

The color differentiation observed in this facies can be explained by applying Berner's (1981) geochemical classification of sedimentary environments (Figure 7). In the upper part of the facies, the sandstone is very strongly bioturbated, and the pale-green mottles are associated with burrow trails. The green mottles contain siderite and chlorite, which are indicative of reducing conditions, whereas the surrounding sandstone is cemented by hematite, which forms under oxidizing conditions. The green mottles are interpreted as having formed as localized reduction spots associated with decaying organic matter within a generally oxidizing environment. Most of the organic matter in the original sediments probably was destroyed through oxic decomposition by aerobic microorganisms prior to burial. Fine-grained ferric oxides within the sediment were not reduced and account for the predominantly red coloration of the sandstones. The *in situ* death of burrowing organisms, however, resulted in the partial removal of oxygen from the buried organic matter by oxidation, and the local reduction of iron oxides to other minerals. In the lower part of this facies, the vertical arrangement of thick red sediments and thin pale-green bands represents the oxic and post-oxic geochemical environments which developed sequentially at shallow burial depths.

## FACIES 2

This second facies of Medina reservoir sandstones and associated lithologies makes up the central one third of the Grimsby Sandstone in the Athens field. It is present in the Creacraft No. 1 well core from 4,654 to 4,694 feet (1,419 to 1,431 m). This facies does not occur in the Geneva field. The characteristic gamma-ray response of this facies is shown in Figures 3 and 9. The upper and lower boundaries of the interval are marked by abrupt increases in radioactivity. The gamma-ray signatures of the individual sandstone units exhibit blunt bases and slightly sloping tops with internal interdigitate patterns.

### Description

The sandstones of this facies range in thickness from 30 to 55 feet (9.1 to 16.8 m) and are composed mostly of grayish-red subarkoses and sublitharenites. A thin, 2- to 5-foot- (0.6- to 1.5-m-) thick interval of light-gray quartz arenite occurs conformably interbedded within the red sandstones near the top of the facies interval (Figure 10, D and E). Figure 10 shows the petrographic characteristics of this facies. The sandstones are moderately well to very well sorted. Mean grain size ranges from 0.35 to 0.5 mm. The sandstones display multiply stacked, 1- to 3-foot- (0.3- to 0.9-m-) thick fining-upward sequences. Detrital quartz grains are subrounded to rounded, and feldspars and rock fragments are subangular to rounded. The sandstones lack any appreciable matrix and are grain supported. Point and, to a

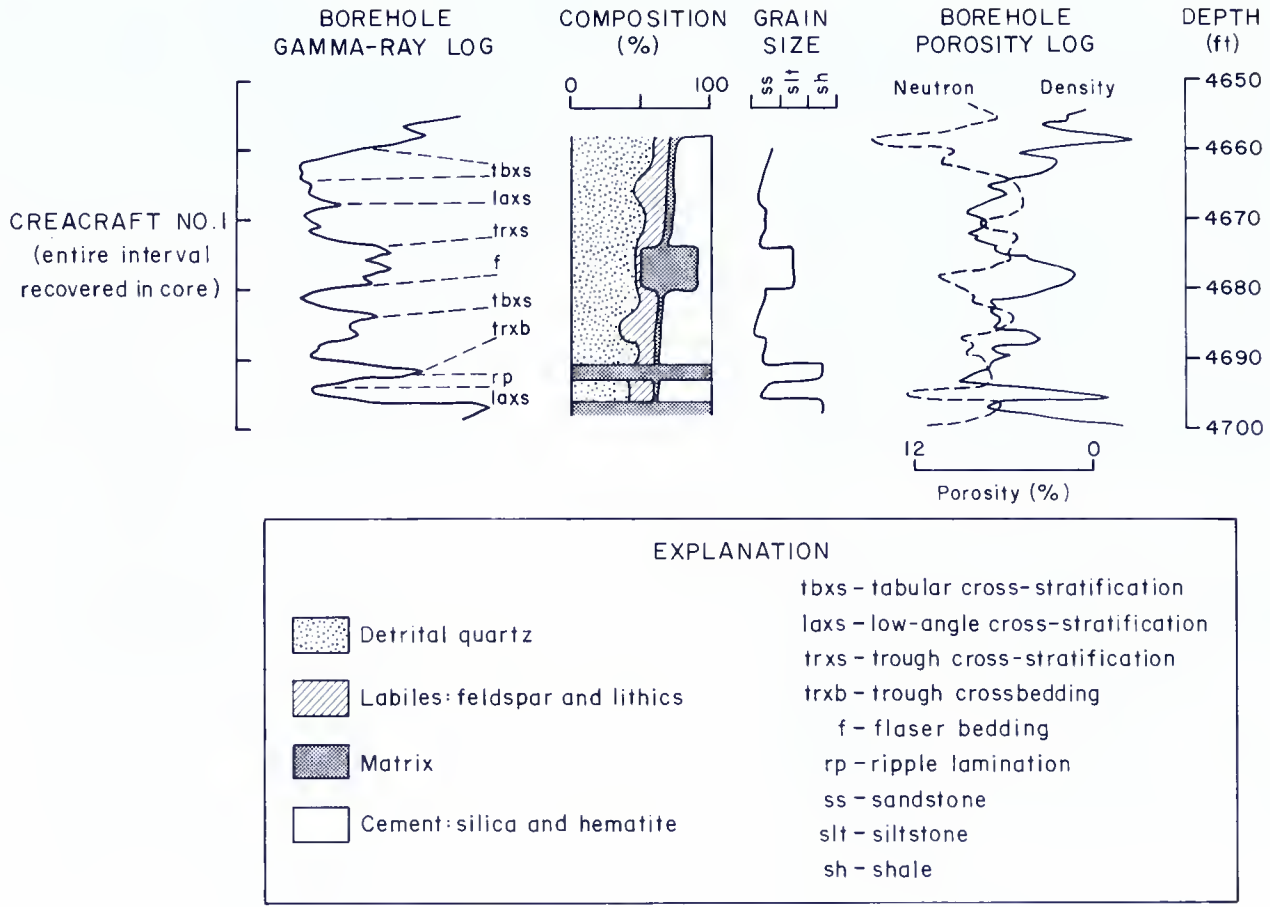


Figure 9. Geophysical logs, grain size, and compositional characteristics of Medina facies 2 sandstones penetrated in the Creacraft No. 1 well, Crawford County.

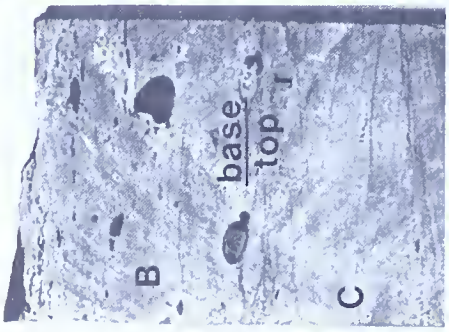


A


B

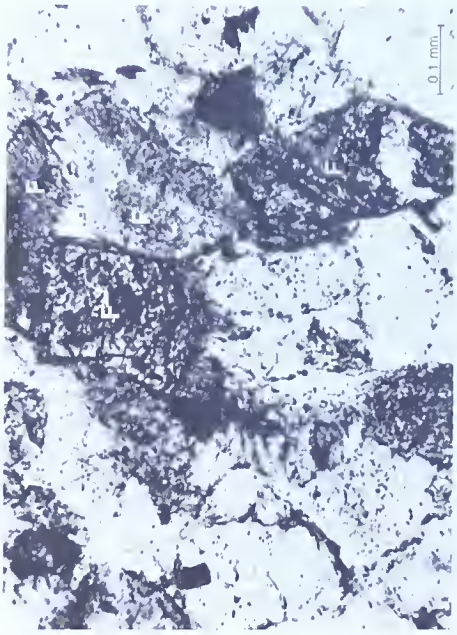


C

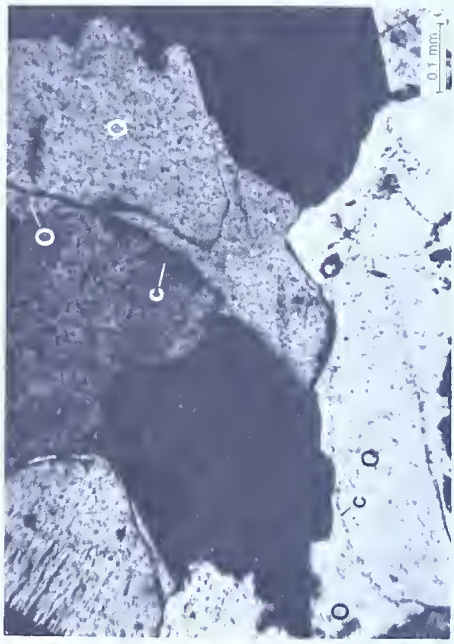


E

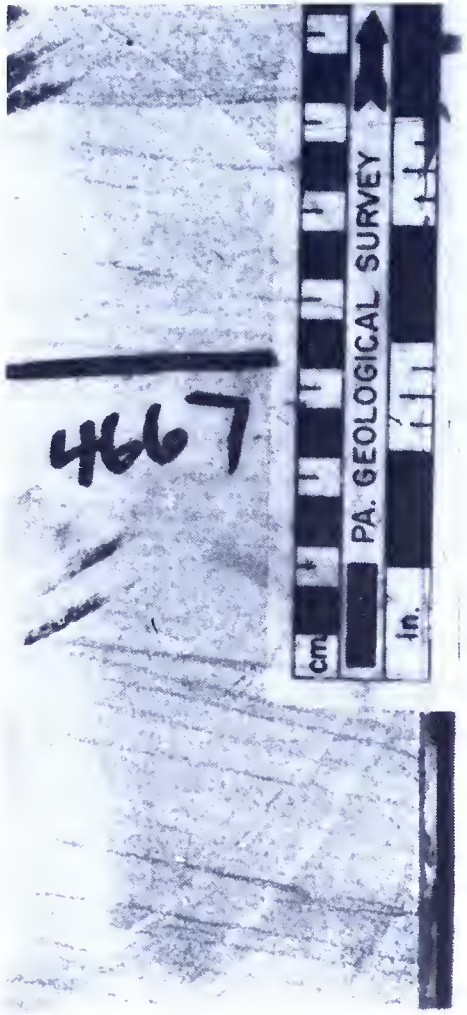


D

Figure 10. Selected petrographic characteristics of facies 2 sandstones and associated lithologies.

A. Crossbedded and rippled hematitic sandstone from the Creacraft well in the Athens field. Note the nonerosive base of a fining-upward sequence (base) marked only by a lag of mudstone chips. Ripples (r) occur at the top of the subjacent fining-upward sequence.

B. Photomicrograph of the sandstone at the base of a fining-upward sequence in the Grimsby facies 2 sandstones from the Athens field. The sandstone is a sublitharenite. Note the siltstone rock fragment (RF), the altered feldspar grains (F), the rounded detrital quartz grains (Q) and silica overgrowths (O), and the patches of hematite cement (H). Plane-polarized light.

C. Typical subarkose in the facies 2 sandstones. Feldspars (F) are highly altered. Plane-polarized light.

D. Light-gray quartzose sandstone which occurs interbedded with the red sublithic and subarkosic sandstones of facies 2. Note the low-angle trough cross-stratification.

E. Photomicrograph of sandstone in D. Specimen is a quartz arenite. Note the detrital quartz (Q), authigenic chlorite rims (c), and quartz overgrowths (O). Crossed nicols.

lesser extent, long grain contacts are dominant. A few concavo-convex and sutured grain contacts can be observed. Authigenic feldspar, chlorite, quartz, and hematite form the main cementing agents. Porosity ranges from 2.1 to 7.3 percent, and permeability ranges from less than 0.1 to 0.2 mD (millidarcy). The sandstones contain a few discontinuous partings of hematitic mudstone and infrequent interbeds of argillaceous, hematitic mudstone and siltstone.

Framework grains consist of monocrystalline quartz with straight to slightly undulose extinction, microcline, perthite, untwinned feldspar, mudstone and siltstone rock fragments, and assorted accessory grains including hornblende, zircon, epidote, ilmenite, and sphene. The modal analyses of the sandstones in this facies are listed in Table 5.

Sedimentary structures are dominated by 2- to 10-foot- (0.6- to 3-m-) thick sets of trough and planar cross-stratified beds. Erosive scour surfaces overlie argillaceous mudrock interbeds at the base of some crossbedded sets, but most of the trough cross-stratified sets are vertically stacked and display concave-upward erosive bases, which are marked only by basal lags of mud-chip conglomerate and reactivation surfaces within the foresets at the top of the subjacent crossbedded sandstones. Foresets within the crossbedded sandstones exhibit inverse grading. A few sets of low-angle cross-stratified and ripple-laminated sandstone also occur. Interbeds of argillaceous siltstone are flaser and lenticular bedded. Hematitic mudstone partings and interbeds are structureless.

Body fossils and trace fossils are conspicuously absent in this facies.

Facies 2 sandstones appear to have an elongate belt-shaped geometry, as indicated by the isolith map for this interval shown in Figure 11. The isolith map and the cross section of this interval (Figure 20) show that the belt is approximately 6 miles (9.7 km) wide and is composed of a laterally continuous sequence of sandstone bodies which is generally of uniform thickness but does contain localized, thicker sandstone pods. Although the facies 2 interval represents a laterally continuous and distinctive depositional cycle, it appears as if the individual sandstones cannot be traced laterally from well to well for any great distance.

## Interpretation

Facies 2 sandstones are interpreted as originating in a braided fluvial channel system which intermittently prograded across a littoral environment. Erosive bases and fining-upward grain-size sequences have been characterized as criteria for the recognition of channel deposits by Potter (1967) and Collinson (1978). The medium-grained, cross-stratified, feldspathic and lithic red beds of the facies 2 sandstones are similar to the braided-channel sands described by Miall (1977). Individual fining-upward sequences represent the accumulation of transverse and migrating linguoid bars in a

Table 5. *Modal[1] and Bulk X-ray Diffraction Analyses of Facies 2 Sandstones*

| MODAL ANALYSES [2] | |
|---|---|
| Detrital minerals | Percentage |
| Quartz, total | 80.4 |
| Monocrystalline | 79.3 |
| Polycrystalline | 0.9 |
| Chert | 0.2 |
| Feldspar, total | 7.8 |
| Microcline | 2.5 |
| Plagioclase | 0.5 |
| Untwinned | 4.8 |
| Rock fragments, total | 7.6 |
| Sedimentary | 7.6 |
| Metamorphic | — |
| Accessory grains, total | 3.0 |
| Matrix, total | 1.2 |
| **Texture** | |
| Average quartz size | 0.35 to 5.0 mm |
| Skew | Positive |
| Sorting | 0.95 to 0.37 phi |
| **CEMENT** (percentage of whole rock) | |
| Cementing mineral | Percentage |
| Quartz | 29.8 |
| Dolomite | <1.0 |
| Anhydrite | 0.3 |
| Hematite | 8.4 |
| Calcite | <1.0 |
| Chlorite | 2.1 |
| Illite | 2.0 |
| **BULK MINERALOGY** (determined by X-ray diffraction) | |
| Minerals | Percentage |
| Quartz | 82 to 89 |
| Feldspar | <1 to 2 |
| Clay | 5 to 8 |
| Calcite | <1.0 |
| Ca-Dolomite | <1.0 |
| Siderite | 0.1 |
| Hematite | 4 to 9 |
| Other | — |

[1] Based on point counts of 12 thin sections.

[2] Determined by petrographic examination and recalculated to represent detrital percentages.

broad, shallow fluvial system. Muddy overbank deposits, represented by the hematitic mudstone partings and interbeds, are poorly preserved because they were frequently ripped up to form cohesive lithic intraclasts

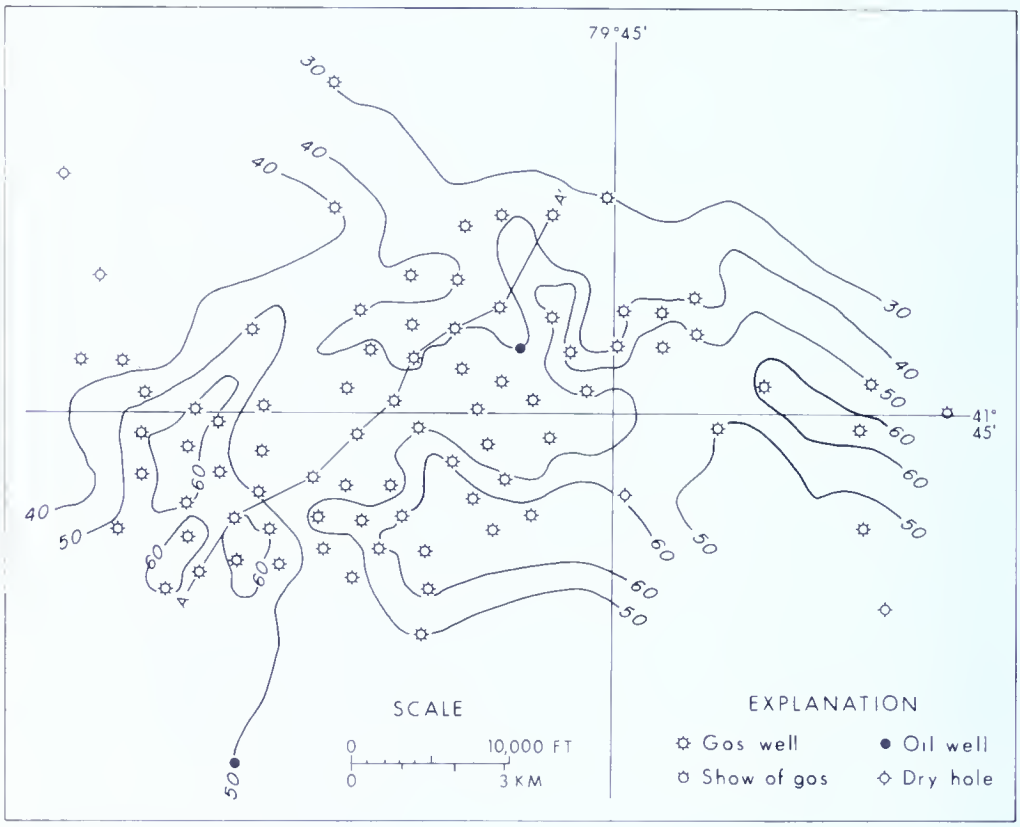


Figure 11. Isolith map of the facies 2 sandstones in the Athens field, based on a 40 percent sand cutoff on the gamma-ray log. Contour interval is 10 feet. See Figure 20 for geophysical-log cross section A-A'.

which form the mud-chip conglomerates concentrated at channel bases. The sand bodies of this facies are developed perpendicular to depositional strike, and the map and cross-sectional geometries exhibited by this interval resemble the braided-channel patterns outlined by Coleman and Prior (1982). Interbeds of flaser and lenticular cross-stratified siltstone resemble one of the previously described lithologies of the facies 1 sandstones. This suggests that the braided fluvial system cut across and through the tidal-flat sediments. The presence of the 2- to 4-foot- (0.6- to 1.2-m-) thick sequence of very well sorted, pure quartz arenite within the red sandstones suggests that progradation of the fluvial sediments across the tidal flats and into the littoral zone sometimes resulted in the rapid reworking of the sand by waves and longshore currents, which removed the labile constituents from the sand deposits.

## FACIES 3

This facies of sandstones forms the lower one third of the Grimsby Sandstone in the Athens field and the lower two thirds of the Grimsby in the Ge-

neva field. It is present in the Creacraft No. 1 core from 4,694 to 4,727 (1,431 to 1,441 m) and in the Kebert Developers No. 1 core from 4,714 to 4,727 feet (1,437 to 1,441 m). The gamma-ray signature of individual sandstones within this facies is characterized by blunt bases and blunt tops. Interdigitate patterns are also present. Figures 3, 4, and 12 show the distribution of this facies in the subsurface of the study area and the gamma-ray log signatures of the sandstones.

## Description

The sandstones of this facies range in thickness from 15 to 40 feet (4.6 to 12.2 m). They are composed of light-gray quartz arenites and sublithare-

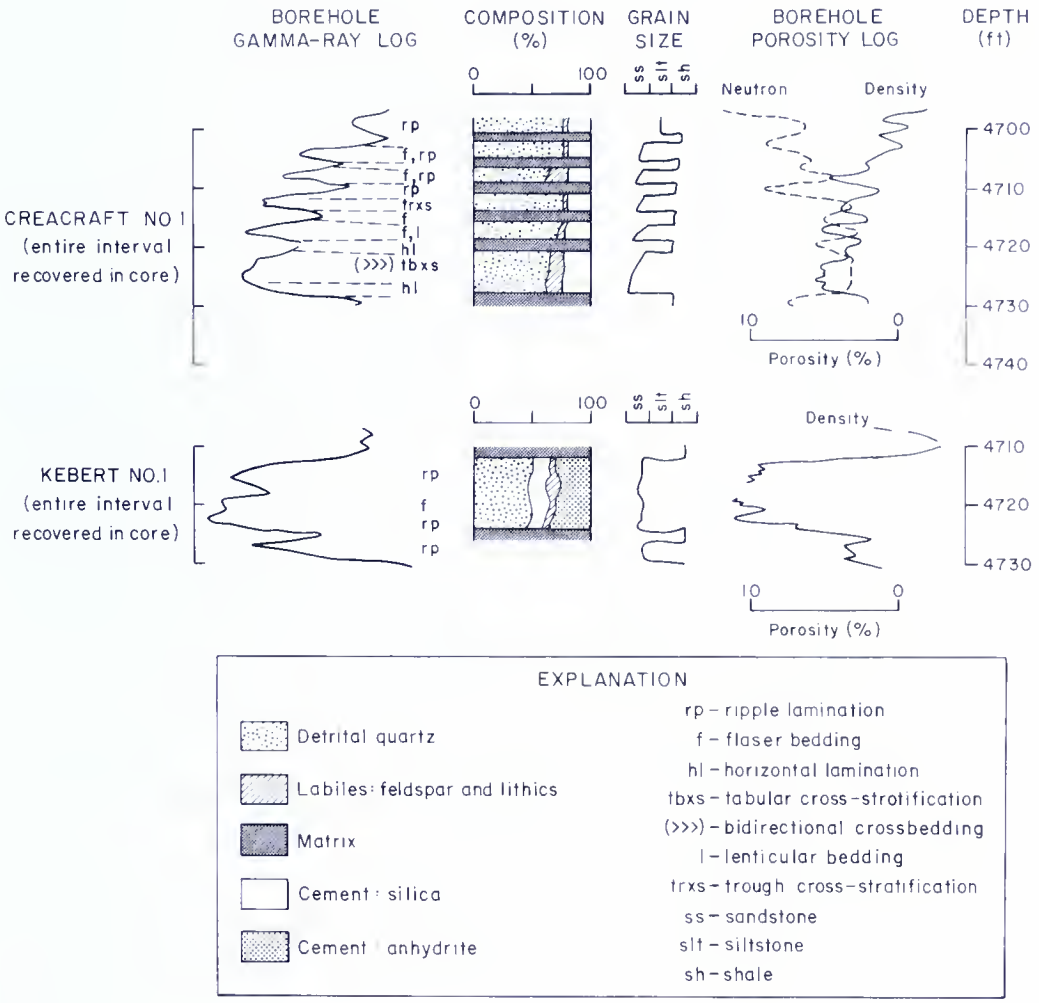


Figure 12. Geophysical logs, grain size, and compositional characteristics of Medina facies 3 sandstones penetrated in the Creacraft No. 1 and Kebert Developers No. 1 wells in Crawford County.

nites. Figure 13 shows the petrographic characteristics of this facies. The sandstones are well sorted to very well sorted. Mean grain size ranges from 0.25 to 0.35 mm, and the detrital quartz grains are rounded to well rounded. The fabric is grain supported, and the grain contacts are predominantly long and sutured. A few concavo-convex contacts occur. The sandstones contain little or no matrix and consist of thin to very thick beds that display fining-upward sequences. Porosity ranges from 1.6 to 8.9 percent, and permeability ranges from less than 0.1 to 0.2 mD. The sandstones contain a few dark-gray illitic mudstone partings and interbeds. Clay drapes occur intercalated within ripple laminae at the top of fining-upward sequences.

Framework grains consist of monocrystalline quartz, locally concentrated mud-chip conglomerate, and minor amounts of potassium feldspar along with zircon and epidote[1] accessory grains. Glauconite constitutes between 0.5 and 1.0 percent of the detrital fractions. The quartz grains exhibit straight to slightly undulose extinction. Authigenic illite, anhydrite, quartz, calcite, and dolomite are the principal cementing agents. The modal analyses of the sandstones in this facies are listed in Table 6.

Facies 3 sandstones in the Creacraft core, from the Athens field, display a distinct sequence of sedimentary structures (Figure 12). The basal sandstones of this facies are horizontally laminated and contain scattered mudstone clasts. These sandstones are overlain by bidirectional tabular cross-stratified sets of quartz arenite. These sandstones, in turn, are overlain by dark-gray massive mudstone and flaser- and lenticular-bedded siltstones. The uppermost sandstones of the sequence exhibit trough cross-stratification with basal lags of mud-chip conglomerate overlying scour surfaces. Well-developed *climbing ripples* are superimposed on the trough cross-stratified sets. Sandstones at the very top of the sequence, in the Creacraft core, are intricately ripple-laminated and contain reactivation surfaces.

Facies 3 sandstones recovered from the Kebert core consist of thin to medium beds of tabular cross-stratified and small-scale ripple cross-laminated quartz arenite. Reactivation surfaces are common.

Neither body fossils nor trace fossils were found in this facies.

Facies 3 sandstones have an elongate ribbon-shaped geometry (Figure 14). The sandstones are developed parallel to the depositional strike. Individual sandstone units can be traced laterally from well to well for short distances.

---

[1] T. M. Berg (personal communication, 1983) reported that *no* epidote was found in heavy mineral concentrations from the Tuscarora Formation of central Pennsylvania. It is unlikely that the small amounts of epidote observed in the Medina Group (this report and Fisher, 1954) were derived from the southeastern source area. Epidote is a moderately stable heavy mineral derived mainly from altered igneous rocks and crystalline metamorphic terrains (Pettijohn and others, 1972). This author suggests that perhaps a northern source terrain, the Canadian Shield and/or Adirondacks, provided the epidote found in the Medina rocks.

Table 6. *Modal[1] and Bulk X-ray Diffraction Analyses of Facies 3 Sandstones*

| MODAL ANALYSES[2] Detrital minerals | Percentage |
|---|---|
| Quartz, total | 96.5 |
| Monocrystalline | 96.0 |
| Polycrystalline | 0.5 |
| Chert | — |
| Feldspar, total | 2.25 |
| Microcline | 0.35 |
| Plagioclase | — |
| Untwinned | 1.9 |
| Rock fragments, total | 0.5 |
| Sedimentary | 0.5 |
| Metamorphic | — |
| Accessory grains, total | 0.5 |
| Matrix, total | 0.25 |
| **Texture** | |
| Average quartz size | 0.25 to 0.35 mm |
| Skew | Positive |
| Sorting | 0.42 to 0.36 phi |

| CEMENT (percentage of whole rock) | Percentage | |
|---|---|---|
| Cementing mineral | Athens | Geneva |
| Quartz | 20.5 | 19.6 |
| Dolomite | — | <1.0 |
| Anhydrite | <1.0 | (1.5 to 31.0) |
| Hematite | <1.0 | — |
| Calcite | 0.5 | <1.0 |
| Chlorite | 0.5 | — |
| Illite | 2.25 | 1.2 |

| BULK MINERALOGY (determined by X-ray diffraction) | Percentage | |
|---|---|---|
| Minerals | Athens | Geneva |
| Quartz | 95.0 | 65.0 |
| Feldspar | 2.0 | — |
| Clay | 3.0 | <1.0 |
| Calcite | <1.0 | 3.0 |
| Ca-Dolomite | — | — |
| Siderite | — | <1.0 |
| Hematite | — | — |
| Anhydrite | — | 31.0 |

[1] Based on point counts of 13 thin sections.

[2] Determined by petrographic examination and recalculated to represent detrital percentages.

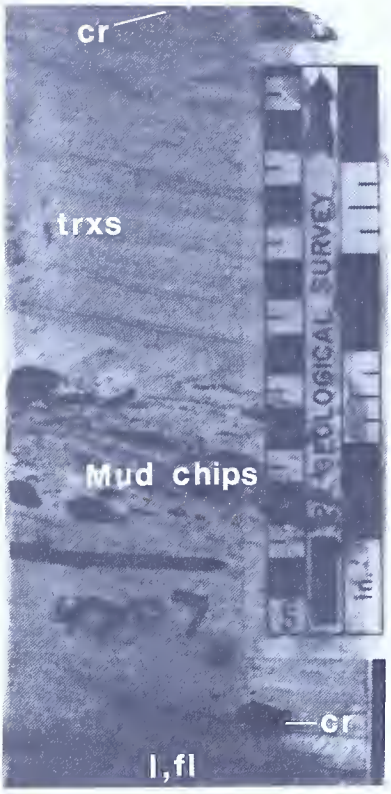


A

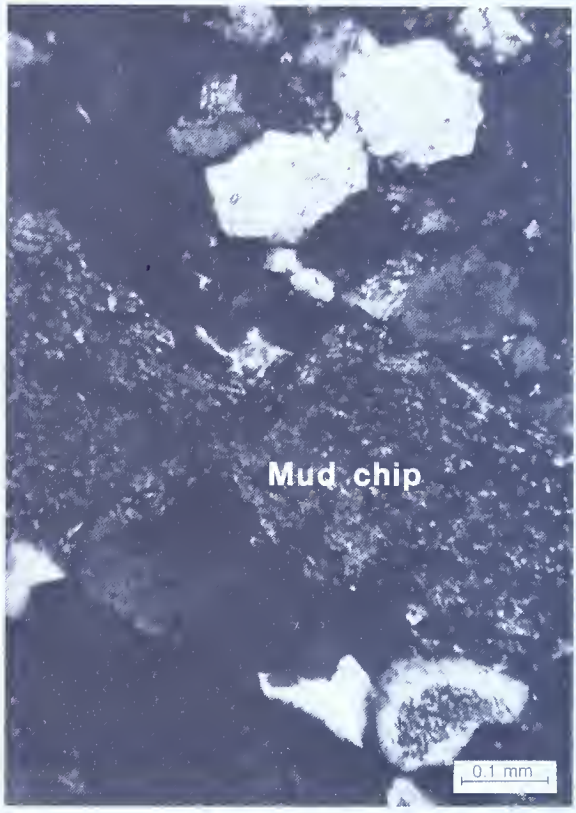


B

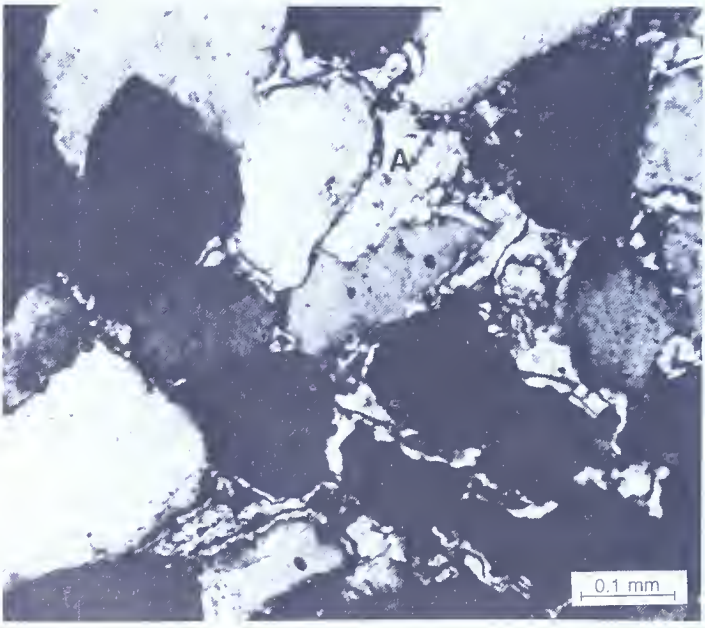


C

Figure 13. Selected petrographic characteristics of the facies 3 sandstones and associated lithologies.
A. Tidal-creek channel-fill sequence from the Creacraft core. Flaser (fl), lenticular (l), and current ripple (cr) bedding characterize the bottom portion of the sample. Abundant mud-chip conglomerate resulted from the erosion of cohesive lagoonal mud by tidal scour in the channel. Trough cross-stratification (trxs) passes upward into climbing current-ripples that contain thin flakes of mudstone on the stoss side of the ripples (incipient flasers).
B. Photomicrograph of the sublitharenite from the sequence shown in A. Mudstone lithic grain has been partially deformed by compaction. Note the tight, interlocking texture of the quartz. Crossed nicols.
C. Quartz arenite containing anhydrite-cemented nodules (A) and quartz cement. Crossed nicols.

## Interpretation

Facies 3 sandstones are interpreted as having been deposited in a littoral marine environment as barrier bars and as tidal deltas formed at barrier inlets. Some of the sand bodies may have developed through shore-parallel inlet migration. The vertical sequence of sedimentary structures in the Creacraft core is similar to the hypothetical regressive sequence for a flood-tidal delta complex proposed by Hayes (1976). In the Creacraft core, the thick basal sequence of horizontal and bidirectional, tabular cross-stratified sandstones represents the development of megaripples within a tidal inlet channel. Overlying sets of trough and planar cross-stratified sandstone represent megaripples and sand waves which fill the inlet channel and later develop on the flood ramp. Overlying mudstones are deposited as back-barrier mud-flat and lagoonal sediments. These, in turn, may be cut by the channel deposits of back-barrier tidal creeks. Mud-chip conglomerates form as basal lags in response to tidal scour of underlying argillaceous sediments. Similar ancient sequences have been described in the Cretaceous Gallup Sandstone of northwestern New Mexico (Campbell, 1971) and in the Cretaceous Blood Reserve and St. Mary River Formations of southern Alberta (Reinson, 1979).

A complete vertical sequence of sedimentary structures was not recovered in the Kebert core. The mineralogical maturity and tabular cross-stratification of the sandstones, however, suggest that the depositional environment was characterized by high energy. The intricately braided ripple-laminated sets are diagnostic of bedding features formed as the result of wave action (Reineck and Singh, 1973). The common reactivation surfaces indicate tidal-current bedload transport. The sandstones display log signatures that are typical of littoral deposits (Selley, 1981), and the strike-parallel geometry of the sands in the Geneva field strengthens the barrier-bar interpretation. Predominantly marine conditions are also indicated by the presence of glauconite.

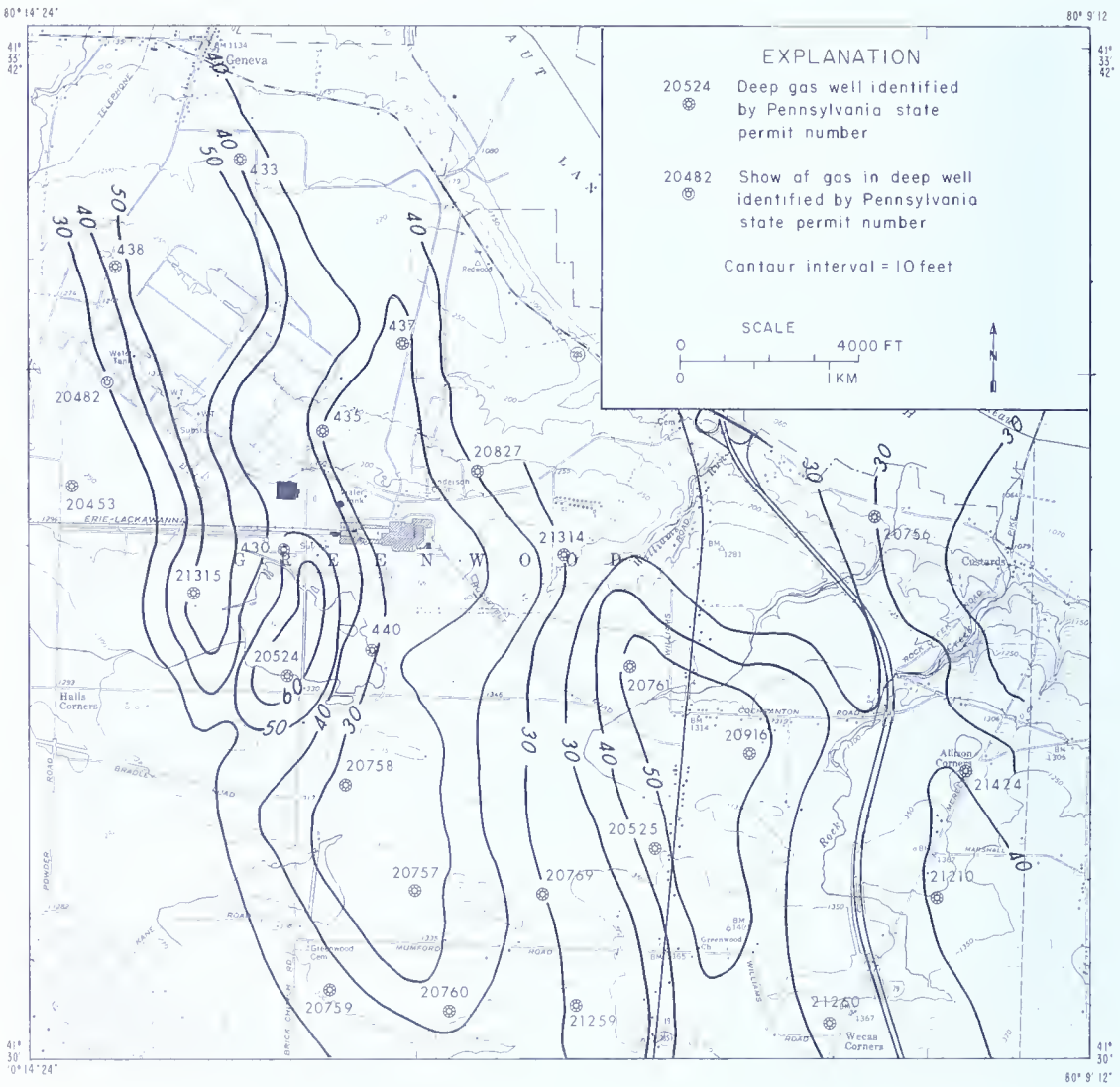


Figure 14. Isolith map of the Medina facies 3 sandstones in the Geneva field, based on the 50 percent sandstone gamma-ray cutoff.

## FACIES 4

Facies 4 corresponds to the Cabot Head Shale. Facies 4 can be subdivided into five subfacies which are present as distinct lithologic units. The sandstones of this facies occur within and near the top of the Cabot Head Shale. The sandstone, where present, is generally referred to as the Cabot Head or Tracy sandstone (Kelley and McGlade, 1969). It is present in the Creacraft core, from the Athens field, between 4,736 and 4,742 feet (1,444 and 1,445 m). Where well developed, the sandstone exhibits a blocky gamma-ray pattern characterized by a blunt top and blunt base. As the sandstone becomes shaly, towards its lateral margins, the gamma-ray signature exhibits a blunt top and sloping base (Figures 3 and 15).

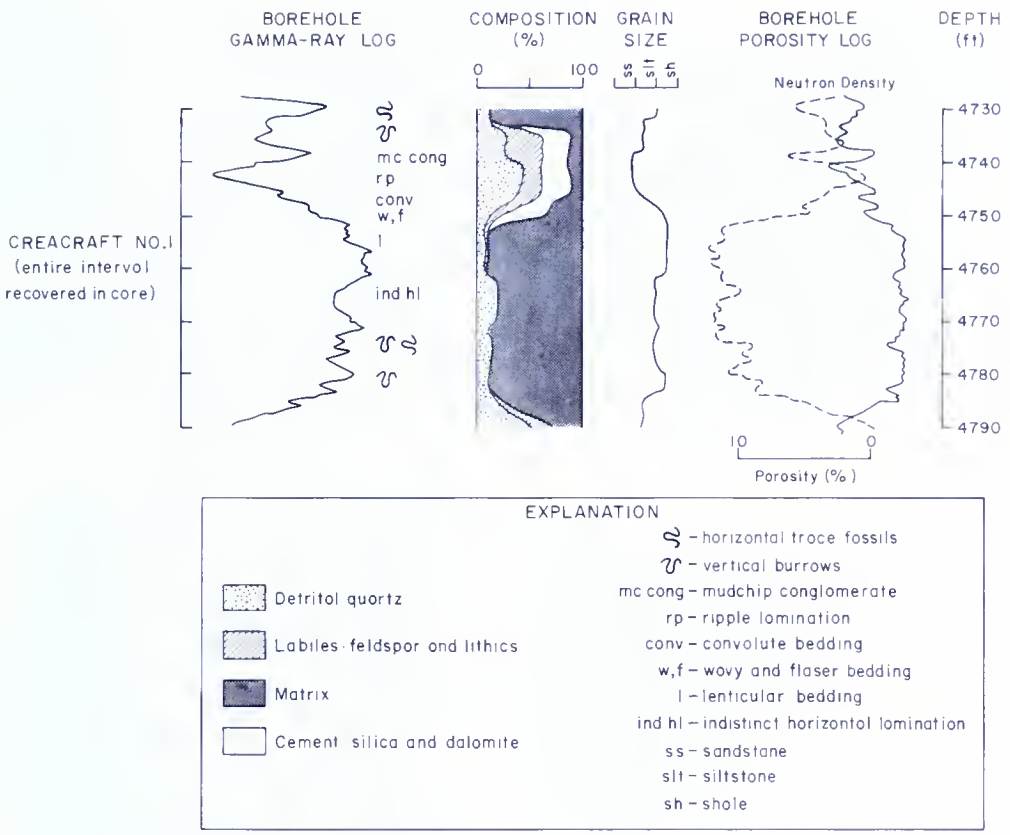


**Figure 15. Geophysical logs, grain size trend, and compositional characteristics of the Medina facies 4 sandstones and associated lithologies in the Creacraft No. 1 well in Crawford County.**

In the Creacraft core, the Cabot Head Shale consists of the following beds, in descending order:

| | *Unit (subfacies)* | *Thickness (feet)* |
|---|---|---|
| (1) | Mudstone, silty, bioturbated | 2 |
| (2) | Sandstone, massive, fine-grained, containing abundant mud-chip clasts | 6 |
| | Sandstone, ripple-laminated, fine-grained, glauconitic, containing a few scattered mud-chip clasts | 5 |
| | Sandstone, ripple-laminated, flaser-bedded, fine-grained, glauconitic; has reactivation surfaces | 3 |
| (3) | Sandstone and mudstone, convolute-bedded, very fine grained | 1 |
| (4) | Sandstone, ripple-laminated, containing thin mudstone laminae. *Chondrites* trace fossils; burrowed | 3 |
| (5) | Mudstone, containing rippled lenses of very fine grained sandstone, very fossiliferous | 39 |

The bioturbated silty mudstone (unit 1) contains the trace fossil *Arthrophycus*. The amount of organic reworking is extensive, but there is an indistinct horizontal appearance to the bedding. The trace fossil *Chondrites* is very abundant in unit 4. The body fossils in the mudstones of unit 5 include various gastropods, crinoid stems, and rugose corals.

A

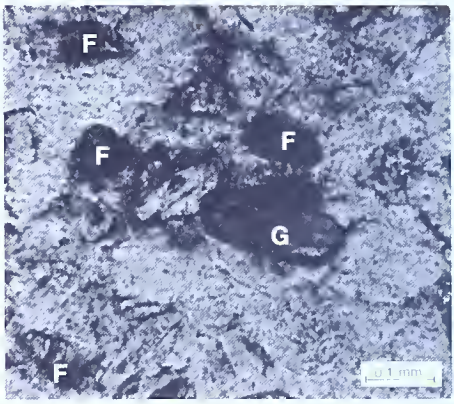


B

convolute bedding

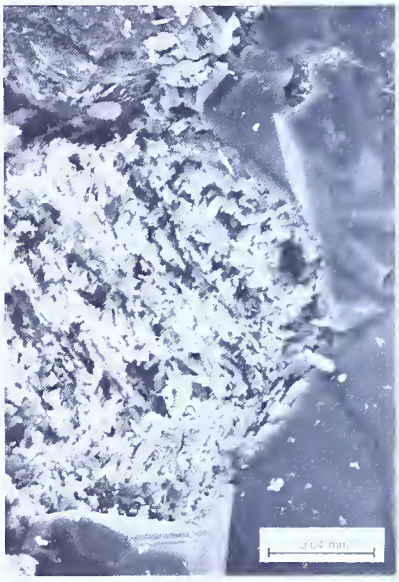

C

wavy, flaser, lenticular, bedding

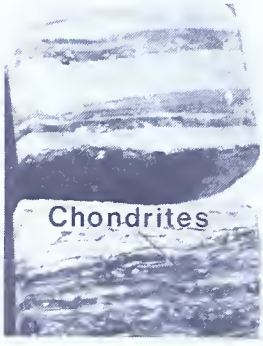


lenticular, bedding

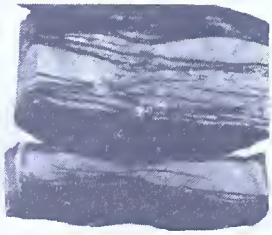

D

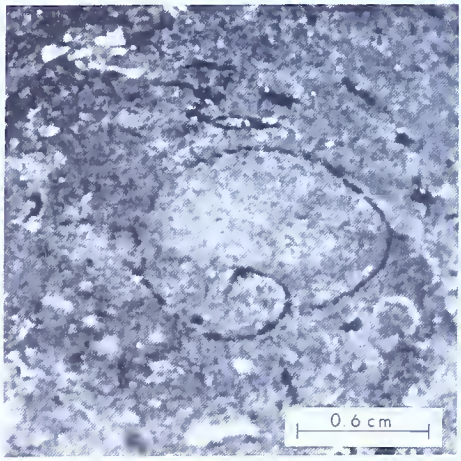


E

Figure 16. Selected petrographic characteristics of the facies 4 sandstones and associated lithologies.
A. Cabot Head or Tracy sandstone. Mud-chip conglomerate developed at the top of a coarsening-upward sequence in an offshore sandstone which is encased in the Cabot Head Shale.
B. Photomicrograph of the Cabot Head sandstone sample shown in A. Sample was taken a few centimeters below the accumulation of mudstone chips. Grain in the center of the photomicrograph is glauconite (G). A few altered feldspar (F) grains are also present. Plane-polarized light.
C. SEM view of partially altered glauconite from the sample shown in B.
D. Convolute, ripple, and lenticular bedding in thin sandstone beds within the Cabot Head Shale. Note the upward increase in sand content.
E. Fossiliferous, bioturbated Cabot Head Shale.

Unit 2 has a distinct signature on the gamma-ray log (Figures 3 and 15). For purposes of subsurface recognition, this unit is arbitrarily called facies 4 sandstone. The sandstones of facies 4 exhibit a distinct sequence of sedimentary structures. The sequence is gradational with the surrounding lithologies of the Cabot Head mudrocks.

## Description

The sandstones within this facies range in thickness from 5 to 25 feet (1.5 to 7.6 m). They are composed of light-gray sublitharenites, subarkoses, and quartz arenites. Figure 16 illustrates the petrographic characteristics of this facies. The mean grain size of the sandstones is 0.2 mm. The sandstones are moderately well to well sorted. Detrital grains are subrounded to well rounded. The fabric is grain supported. Small amounts of illitic matrix occur within the principal sandstone body. The amount of matrix increases toward the upper, lower, and lateral margins of the sand body, which is completely enclosed in dark-gray mudstone. Grain contacts are long, concavo-convex, and sutured. Mechanical compaction has caused plastic deformation of some lithic grains, yielding localized patches of pseudomatrix. The sandstones of this facies display distinct coarsening-upward grain-size trends. Porosity ranges from 3.3 to 6.5 percent, and permeability is less than 0.1 mD.

Framework grains consist of monocrystalline quartz, microcline and untwinned feldspar, mudstone lithic grains, and glauconite. The sandstones are cemented by authigenic illite and quartz. Modal analyses of the sandstones in this facies are presented in Table 7.

Facies 4 sandstones have an elongate, ribbon-shaped geometry oriented perpendicular to depositional strike. These sand bodies can extend for over 20 miles (32 km) in their long direction (Charles Grapes, personal communication, 1983).

## Table 7. *Modal[1] and Bulk X-ray Diffraction Analyses of Facies 4 Sandstones*

| MODAL ANALYSES[2] Detrital minerals | Percentage |
|---|---|
| Quartz, total | 80.2 |
| Monocrystalline | 80.2 |
| Polycrystalline | — |
| Chert | — |
| Feldspar, total | 3.8 |
| Microcline | 0.7 |
| Plagioclase | — |
| Untwinned | 3.1 |
| Rock fragments, total | 8.9 |
| Sedimentary | 8.9 |
| Metamorphic | — |
| Accessory grains, total | 3.0 |
| Matrix, total | 0.3 |
| **Texture** | |
| Average quartz size | 0.2 mm |
| Skew | Slightly positive |
| Sorting | 1.1 to 0.62 phi |
| **CEMENT (percentage of whole rock)** Cementing mineral | Percentage |
| Quartz | 19.5 |
| Dolomite | 5.0 |
| Anhydrite | — |
| Hematite | — |
| Calcite | <1.0 |
| Chlorite | — |
| Illite | 2.15 |
| **BULK MINERALOGY (determined by X-ray diffraction)** Minerals | Percentage |
| Quartz | 81.0 |
| Feldspar | 3.0 |
| Clay | 10.0 |
| Calcite | 1.0 |
| Ca-Dolomite | 5.0 |
| Siderite | <1.0 |
| Hematite | — |
| Other | — |

[1] Based on point counts of three thin sections.

[2] Determined by petrographic examination and recalculated to represent detrital percentages.

### Interpretation

Facies 4 sandstones are interpreted as tide- and storm-deposited offshore bars. The fossiliferous mudstones of the Cabot Head represent offshore marine-shelf deposits. The occurrence of rippled, fine-grained sandstone lenses within the mudstone, overlain by rippled sandstone containing thin mudstone laminae, represents the early incursion of sand onto the mud-dominated shelf. The sand first occurred as discontinuous patches of rippled sand and later, in response to variable depositional energies, formed subaqueous straight-crested rippled beds. Burrowing organisms were active during low-current periods. The principal sandstone body originated as a low-relief sand-dune bed form which developed in response to sustained bottom currents. The coarse lag of mud chips at the top of the sandstone formed in response to storm activity as storm-generated currents scoured the muddy interbar bottom sediments and ripped up the partially cohesive muds. The offshore bars were capped by horizontally laminated and bedded silt and mud which was later reworked by burrowing organisms. The vertical sequence of sedimentary and biogenic structures in the facies 4 sandstones is similar to the sequences described by Berg (1975) and Hobson and others (1982) for the Upper Cretaceous Sussex Sandstone in Wyoming. The Cabot Head and Sussex sandstone reservoirs differ in orientation; the Cabot Head sandstones are oriented perpendicular to depositional strike whereas the Sussex sandstones are developed as shore-parallel bars. Cotter (1983; personal communication, 1982) has suggested that these Medina Group offshore sand bodies could have developed as shoreface-connected sand ridges, similar to the sand bodies on the western Atlantic shelf described by Swift and others (1978).

## FACIES 5

The sandstones of facies 5 correspond to the Whirlpool Sandstone (Figures 3 and 4). This facies occurs in the Creacraft core from 4,787 to 4,797.6 feet (1,459 to 1,462.3 m) and in the Kebert core from 4,847 to 4,863 feet (1,477 to 1,482 m). The gamma-ray signature exhibits a blunt base and a blunt to slightly sloping top (Figure 17).

### Description

These sandstones range in thickness from 10 to 20 feet (3 to 6.1 m) and are composed of light-gray quartz arenites and subarkoses. Figure 18 shows the petrographic characteristics of these sandstones. Mean grain size ranges from 0.15 to 0.17 mm. In the Creacraft core, the Whirlpool is well sorted to very well sorted and the grains are rounded to well rounded. The fabric is grain-supported and contacts are sutured, long, and concavo-convex. In the Kebert core, the Whirlpool is texturally inverted; that is, the grains are

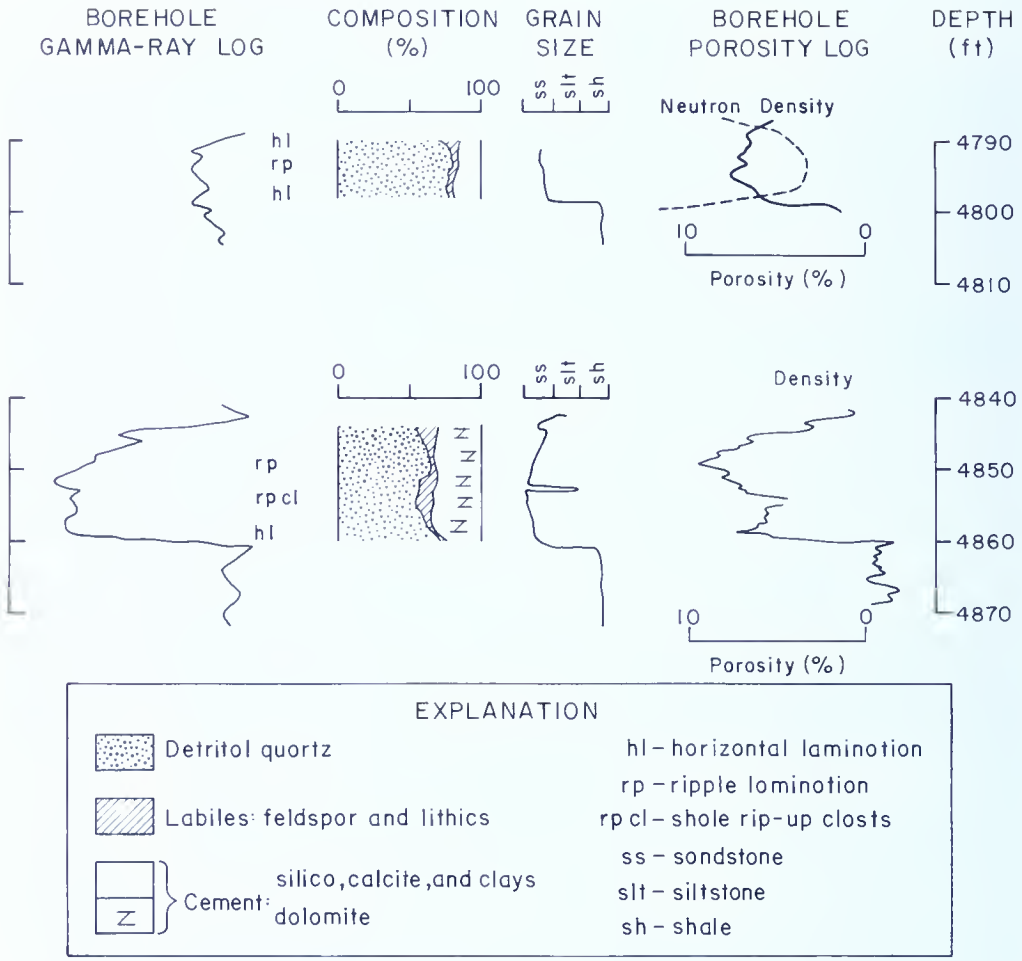


Figure 17. Geophysical logs, grain size trend, and compositional characteristics of the Medina facies 5 sandstones in the Athens and Geneva fields in Crawford County.

rounded to well rounded, there is no matrix, and the sandstone has a bimodal grain-size distribution (Figure 18). Quartz grains are sutured where they are in contact. Much of the framework, however, is supported by extensive dolomite cement. Porosity ranges from 1.6 to 4.3 percent in the Creacraft core and from 3.8 to 8.7 percent in the Kebert core.

Framework grains consist of monocrystalline quartz, potassium feldspars, glauconite, and accessory zircon, tourmaline, and epidote. The quartz exhibits straight to slightly undulose extinction. Phosphatic granules are scattered throughout the sandstones. The modal analyses for these sandstones are listed in Table 8.

Sedimentary structures include planar and tabular cross-stratification, ripple cross-lamination, and parallel lamination. Parting lineations occur on some horizontal surfaces. Possible *synaerial shrinkage cracks* also occur.

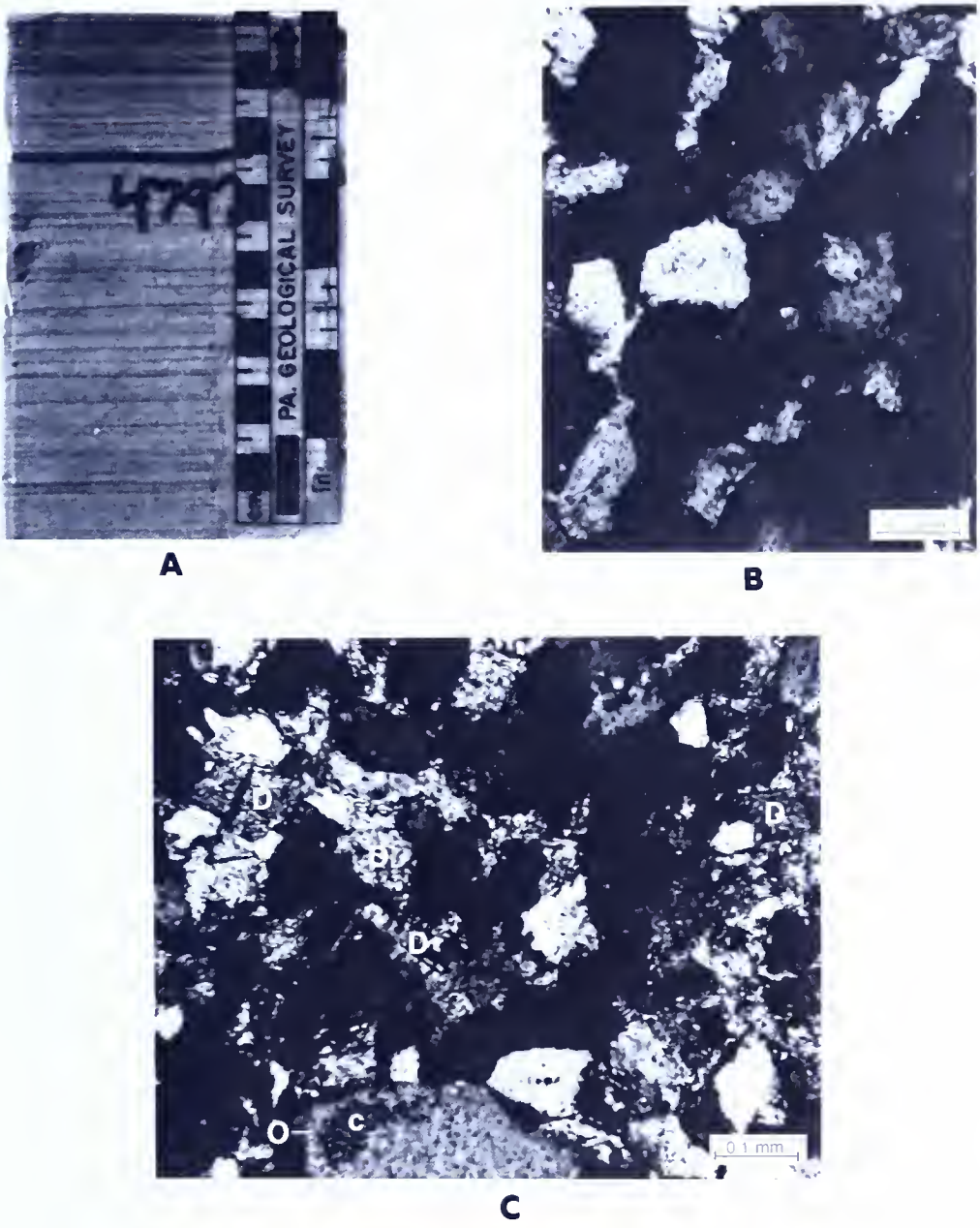


Figure 18. Selected petrographic characteristics of the facies 5 sandstones and associated lithologies.

A. Evenly laminated sandstone and mudstone in the Whirlpool Sandstone (Creacraft core).

B. Photomicrograph of Whirlpool quartz arenite from the Creacraft core. Crossed nicols.

C. Photomicrograph of the Whirlpool Sandstone. Note the bimodal grain-size distribution, quartz overgrowths (O), vermicular chlorite (c), and rhombic dolomite cement (D). Crossed nicols.

## Table 8. *Modal[1] and Bulk X-ray Diffraction Analyses of Facies 5 Sandstones*

| MODAL ANALYSES[2] Detrital minerals | Percentage |
|---|---|
| Quartz, total | 94.3 |
| Monocrystalline | 94.2 |
| Polycrystalline | 0.1 |
| Chert | — |
| Feldspar, total | 1.7 |
| Microcline | 0.6 |
| Plagioclase | — |
| Untwinned | 1.1 |
| Rock fragments, total | — |
| Sedimentary | — |
| Metamorphic | — |
| Accessory grains, total | 3.0 |
| Matrix, total | 1.0 |
| **Texture** | |
| Average quartz size | 0.15 to 0.17 mm |
| Skew | Positive |
| Sorting | 0.5 to 0.39 phi |

CEMENT
(percentage of whole rock)

| Cementing mineral | Percentage Athens | Geneva |
|---|---|---|
| Quartz | 19.7 | 4.0 |
| Dolomite | — | 18.0 |
| Anhydrite | <1.0 | 2.0 |
| Hematite | — | — |
| Calcite | 1.0 | 3.0 |
| Chlorite | — | — |
| Illite | 2.2 | 3.0 |
| Gypsum | — | 1.0 |

BULK MINERALOGY
(determined by X-ray diffraction)

| Minerals | Percentage Athens | Geneva |
|---|---|---|
| Quartz | 95.0 | 66.0 |
| Feldspar | 2.0 | 4.0 |
| Clay | 3.0 | 6.0 |
| Calcite | <1.0 | 3.0 |
| Ca-Dolomite | — | 18.0 |
| Siderite | — | <1.0 |
| Hematite | — | — |
| Anhydrite | — | 2.0 |
| Gypsum | — | 1.0 |
| Pyrite | Trace | — |

[1] Based on point counts of 18 thin sections.

[2] Determined by petrographic examination and recalculated to represent detrital percentages.

Body fossils and trace fossils are absent. The sandstones exhibit a sheet geometry, are laterally continuous in cross-sectional view, and are easily traced from well to well.

In the two cores examined, the Whirlpool can be divided into lower and upper sections on the basis of sedimentary structures, textural trends, and composition. The lower Whirlpool (Figures 17 and 18) is composed of quartzose and feldspathic sandstones which are very fine grained, well sorted, and coarsen upward. The coarsening-upward trends are abruptly followed by a fining-upward tail in vertical sequences. The lowermost 2 to 4 cm (0.8 to 1.6 in.) of the Whirlpool is horizontally laminated, and horizontal surfaces exhibit parting lineations. Mud chips of underlying Queenston lithology are abundant in the basal Whirlpool samples. The horizontal lamination of the basal Whirlpool grades upward into low-angle and tabular cross-stratification and further upward into ripple cross-lamination. The upper Whirlpool is composed of interlaminated, very fine grained quartz arenite and illitic mudstone. Laminae of these lithologies alternate rhythmically as evenly laminated and graded beds. The upper and lower parts of the Whirlpool are very distinct in core samples but are difficult to discern in the geophysical logs. For this reason, the entire Whirlpool is considered to be facies 5 sandstone.

### Interpretation

The sandstones of facies 5 are interpreted as sublittoral sheet sandstones. The petrographic and sedimentologic characteristics of the sandstones match several of the diagnostic criteria listed by Johnson (1978) for shallow marine siliciclastic deposits. These include (1) marine authigenic minerals (glauconite and phosphatic granules); (2) high textural maturity; (3) sedimentary structures indicative of wave action; and (4) sheet geometry. Martini (1971), Piotrowski (1981), and Metzger (1982) have all inferred a sublittoral to littoral origin for the Whirlpool Sandstone.

## SANDSTONE DISTRIBUTION

Knowledge of the three-dimensional distribution of sandstone is critical to the interpretation of the depositional histories of clastic sequences. At the Athens and Geneva fields, the Medina Group averages 50 percent sandstone and 40 percent mudstone (Figure 19 and 20). In both fields, the Grimsby sandstones are distributed as elongate northwest-striking lobes of high sandstone content separated by areas of higher mudstone content (Figure 19). Regional maps constructed by Piotrowski (1981, Plates 6 and 7) show that the Whirlpool displays a sheet geometry in the Athens and Geneva vicinity, whereas the Cabot Head sandstones are characterized by a northwest-trending elongate ribbon-shaped geometry.

Isolith maps of the various Medina sandstone facies, as discussed in the preceding pages, illustrate that both northwest-trending and northeast-

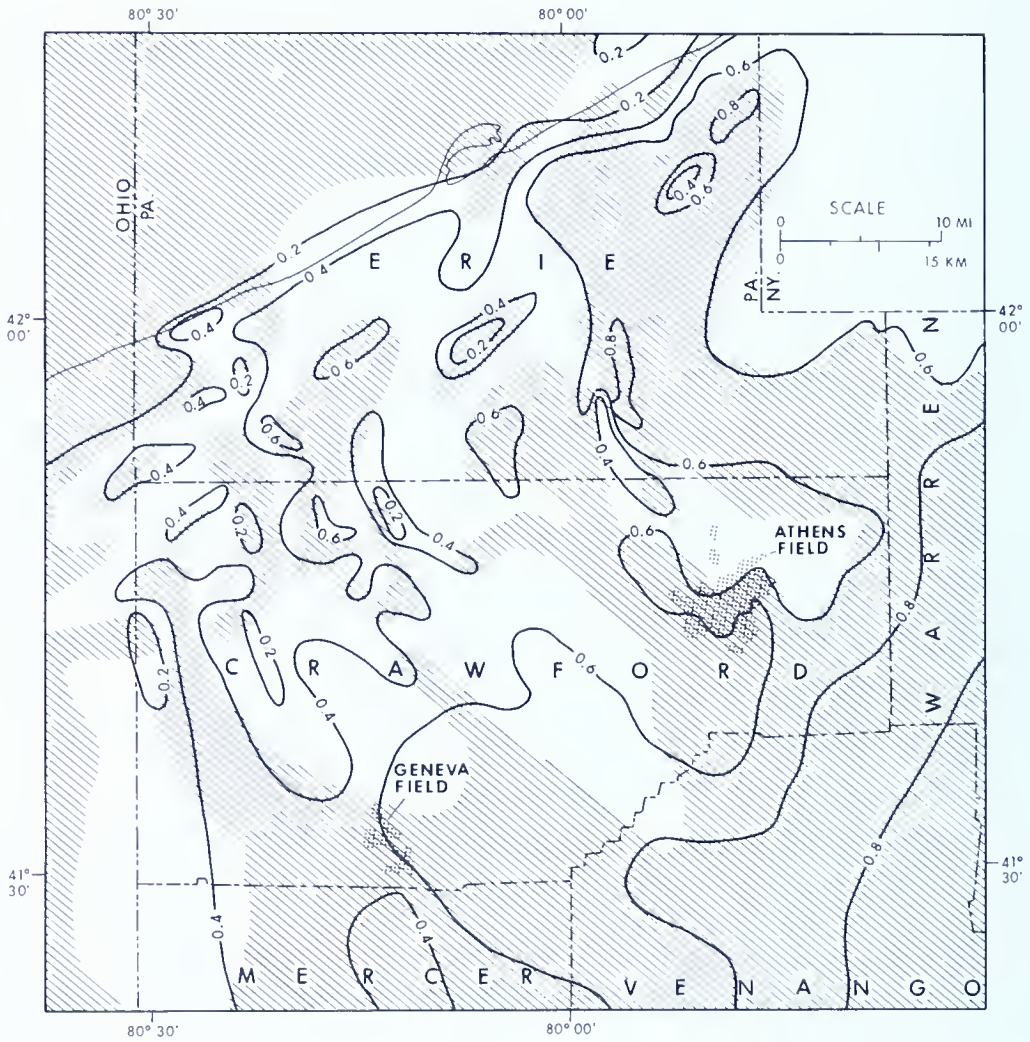


Figure 19. Subsurface distribution of Medina Group clastics in northwestern Pennsylvania. Striped areas are regions underlain by 50 percent clean sandstone as measured on gamma-ray logs. Contours represent the sand/shale ratio (from work maps used by Piotrowski (1981), on file in the Pennsylvania Geological Survey, Pittsburgh office). Stippled areas depict the Athens and Geneva fields.

trending belts of sandstone and shale can be mapped in the subsurface of the study area. The intersection of the two contrasting trends must mark the location of important facies changes produced along the boundary of contrasting environments. The preceding core descriptions show that the zone of high sandstone content in the Athens field is composed of low-sinuosity channel deposits, littoral deposits, and sublittoral deposits. Sandstones in the Geneva field are composed of littoral and sublittoral deposits. The intersections of the various types of sandstone deposits in the Athens and Geneva fields mark the sites of nearshore environments favorable for the accumulation and entrapment of hydrocarbons.

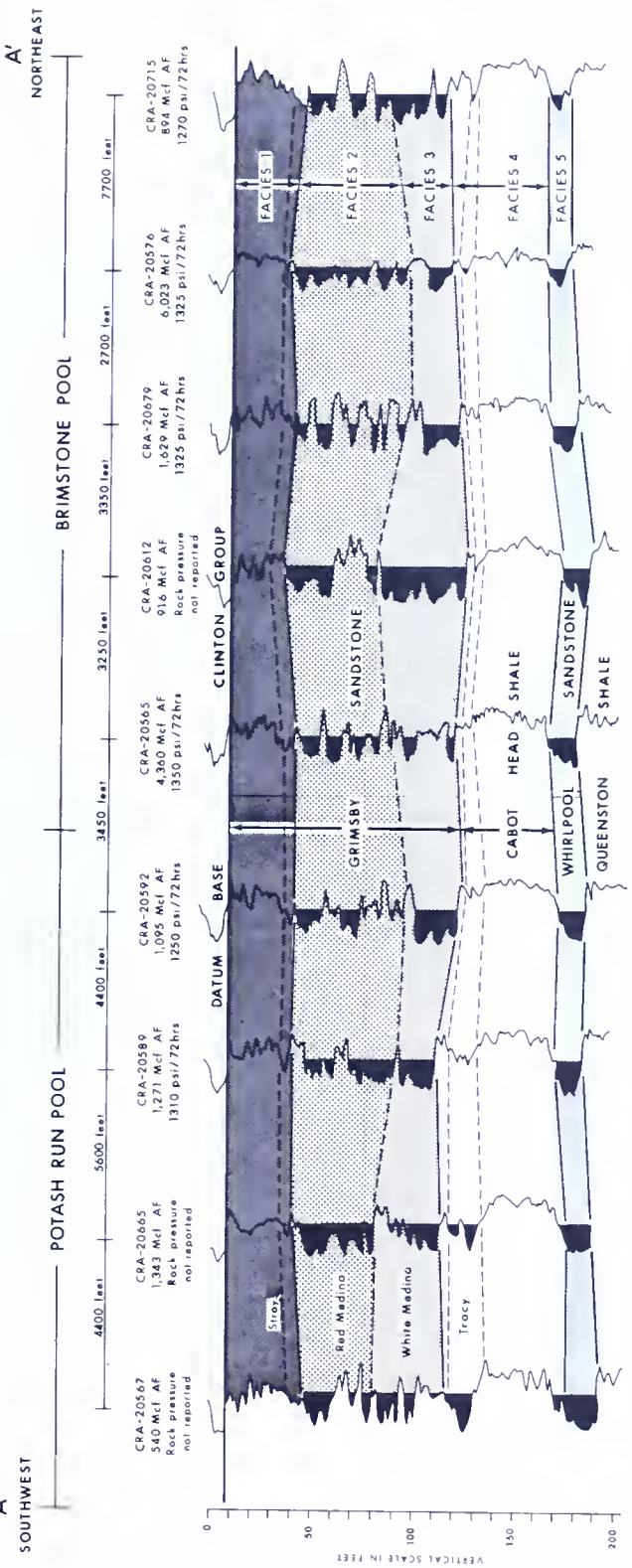


Figure 20. Geophysical-log cross section of the Medina Group in the Athens field. The lines of section are indicated in Figure 11.

## ENVIRONMENTAL RECONSTRUCTION

Martini (1971) presented a detailed sedimentological analysis of the Medina Group based on outcrop studies along the Niagara Escarpment in western New York and southern Ontario. He demonstrated that the Medina was deposited in a shelf/longshore-bar/tidal-flat/deltaic complex (see Martini, 1971, p. 1252, Figures 3 and 4). The observed facies sequences of the Athens and Geneva fields are remarkably compatible with those of Martini's model (Figure 20). For example, the core cut from the Athens gas field exhibits a vertical sequence which is almost identical to the Medina sections at Niagara Gorge in western New York State and at Niagara Glen in Ontario. The Kebert core shows a sequence of facies similar to those in the sections described by Martini (1971) west of Stoney Creek, Ontario.

No single modern analogue is appropriate for comparison with the stratigraphic sequences observed in the Medina Group of northwestern Pennsylvania. A combination of models of ancient and modern depositional environments, however, provides several instructive parallels with the processes and environments that influenced the Medina depositional system. Facies interpretations of the Medina Group in the Athens and Geneva fields are shown in Figure 21. The Whirlpool Sandstone is present as a basal transgressive sandstone which was deposited on top of the older deltaic and coastal-plain sediments of the Queenston Shale. Offshore and longshore bars of the Whirlpool (facies 5 sandstones) migrated up the shoreface to the southeast along with the transgressing sea. A stabilized shoreline developed along the line of thickest Medina development from central Warren County to central Beaver County. Shelf muds of the lowermost Cabot Head Shale were deposited over the sandy shelf sediments of the distal Whirlpool. The progradation of the shoreline resulted in the deposition of transitional silty sands and lower shoreface sands of the upper Cabot Head (facies 4 sandstones and adjacent units). These units were, in turn, overlain by middle and upper shoreface and nearshore sands of the lowermost Grimsby Sandstone (facies 3 sandstones). Varicolored red and green argillaceous sandstones of the uppermost Grimsby (facies 1 sandstones), which formed within a prograding coastal sand/mud complex, were generally deposited on top of these coastal sands. This entire vertical sequence, as just described, is similar to the vertical sequence of retrogradational and progradational facies described for the coast of Nayarit, Mexico, by Curray and others (1969), and is also similar to the prograding sandy shoreline sequences that have been documented in the Cretaceous Gallup Sandstone of New Mexico (Harms and others, 1982). This sequence is applicable to Martini's (1971, Figure 3, p. 1252) interdistributary regions and is illustrated in Figures 19 and 21.

Narrow belts of bedded fluvial deposits (facies 2 sandstones), which are developed normal to the shoreline, intermittently interrupt the vertical sequence just described. In map view, these units appear as flattened, lobate

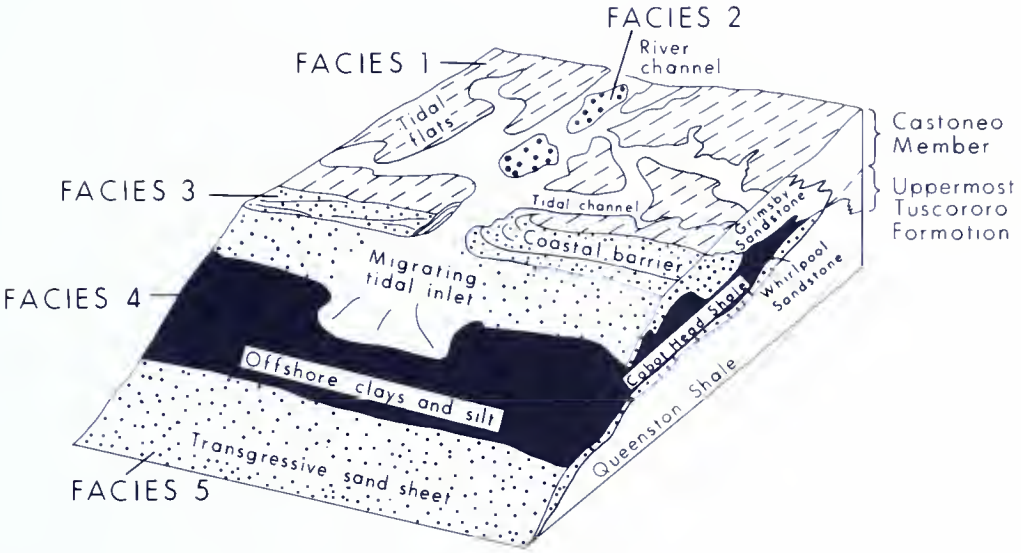


Figure 21. Generalized paleogeographic reconstruction of the depositional environment and facies relationships during deposition of the Lower Silurian Medina Group in the vicinity of the Athens and Geneva fields in northwestern Pennsylvania.

extensions of sandstone (striped area of Figure 19). Selected facies characteristics of these sandstones and associated sediments are described in Table 9. These sandstones were deposited in fluvial channels that had cut into the underlying littoral and shoreface deposits during a period of relatively stable shoreline conditions, thereby permitting the development of small deltas at river mouths. The deltaic units consist, in ascending order, of distributary-mouth bar, channel, tidal-flat, nearshore, and tidal-flat deposits. This sequence resembles the upper portions of the modern-day Klang River Delta of Malaysia (Coleman, 1976). A more suitable analogue may be found in the Gascoyne Delta of western Australia, which was described by Johnson (1982). Here, the climate is semiarid and the Gascoyne River flows intermittently into Shark Bay. The Gascoyne deltaic sequence forms a regressive terrigenous wedge which cuts into basal littoral deposits. The deltaic sequence itself contains channel-bar, delta-bay, and strandplain-sheet sediments. The subaerial sequence of the Gascoyne Delta consists of a "narrow, axial belt of channel sands and levee silts flanked by extensive red-brown muds" (Johnson, 1982, p. 547). Laughrey and Donahue (1982) compared the remarkably straight channel orientation, dominance of trough and planar crossbeds, and hematitic clay drapes in the fluvial Medina to some of the facies characteristics of the Nubia Sandstone in southwest Egypt.

An abrupt transition from dolomitic shales to fossiliferous and argillaceous dolostones typically marks the contact between the upper Medina Group and the overlying Clinton Group. The marine deposits of the Clinton

Table 9. *Summary of Lithologic Facies and their Sedimentary Characteristics in the Grimsby Sandstone in Northwestern Pennsylvania*

| | FACIES 1 | FACIES 2 | FACIES 3 |
|---|---|---|---|
| LITHOLOGY | Grayish-red (5R4/2) to pale-green (5G7/2), very fine to fine-grained quartz wackes interbedded with very light gray (N8), silt-sized quartz arenites, hematitic mudstones, and dolomitized, hematitic, silty biosparite. | Grayish-red (10R4/2) to light-gray (N7), fine- to medium-grained subarkoses, sublitharenites, and quartz arenites interbedded with dark-reddish-brown (10R3/4) hematitic mudstones. | Very light gray (N8) to light-gray (N7), fine-grained quartz arenites and sublitharenites interbedded with greenish-gray (5G6/1), very fine grained quartz wackes and medium-light-gray (N6) mudstones. Some glauconite. |
| SANDSTONE TEXTURE | Poorly to moderately well sorted; variable grain size trends; positive skew; grains are subangular to subrounded; fabric is matrix supported. | Moderately well to very well sorted; fining-upward sequences; slightly positive skew; subrounded to well-rounded grains; fabric is grain supported and displays predominantly point and concavo-convex particle contacts; hematitic clay drapes are common at the top of fining-upward sequences; foreset laminae commonly exhibit inverse grading. | Well-sorted to very well sorted; fining-upward sequences; slightly positive skew; rounded to well-rounded grains; grain-supported fabric; predominantly concavo-convex, long, and sutured grain contacts. |
| SEDIMENTARY STRUCTURES | Medium to very strongly bioturbated; distinct mottling; lenticular, flaser, and wavy bedding; trough cross-stratification; small-scale ripple cross-lamination; mud cracks; microfaulted parallel laminae. | Tabular cross-stratification; low-angle cross-stratification; trough cross-stratification; ripple cross-lamination is superimposed on some of the tabular cross-stratified sets; minor flaser and lenticular bedding; some mud cracks; scour surfaces overlain by abundant mud clasts are common. | Planar and tabular cross-stratification with mud clasts common as basal lags; low-angle cross-stratification with internal, intricately braided cross-laminae; climbing ripple cross-laminae with mud drapes; lenticular and flaser bedding. |

| | | | |
|---|---|---|---|
| FOSSILS AND TRACE FOSSILS | Brachiopods (*Lingula* sp.); gastropods (unidentified); phosphatic shell fragments; *Arthrophycus*; abundant *Skolithos*; *Monocraterion*; possible *Rusophycus*; possible *Diplocraterion*. | Some horizontal burrows are present in the thin, flaser- and lenticular-bedded intervals. | None. |
| GEOMETRY | Widespread, uniformly thick (40 to 50 feet, or 12 to 15 m) sheet geometry. | Thick (30 to 45 feet, or 9 to 14 m), narrow sandstone bodies oriented perpendicular to the shoreline. | Linear sandstone bodies, 25 to 35 feet (7.6 to 10.7 m) thick, oriented parallel to depositional strike. |
| GROUP ASSOCIATIONS | Conformably underlies the Lower Silurian Clinton Group marine carbonate rocks and mudstones; may overlie facies 2 or 3. | Underlies facies 1 and overlies facies 3. | Underlies facies 1 or 2; overlies the Cabot Head Shale. |
| ENVIRONMENTS OF DEPOSITION | Coastal sand/mud flats: tidal plain; tidal creeks; coastal lagoon. | Deltaic: mixed fluvial and paralic setting; ephemeral braided fluvial channel; tidal plain; beach ridge. | Littoral marine: barrier inlet sand body developed through shore-parallel inlet migration. |

Table 10. *Summary of Lithologic Units and their Sedimentary Characteristics in the Cabot Head Shale (Facies 4) in Northwestern Pennsylvania*

| | UNIT 1 | UNIT 2 | UNIT 3 | UNIT 4 | UNIT 5 |
|---|---|---|---|---|---|
| LITHOLOGY | Light-brownish-gray (5YR6/1) to medium-dark-gray (N4), argillaceous siltstone and interbedded mudstone. | Light-gray (N7), very fine to fine-grained subarkose and sublitharenite. Glauconitic. | Light-gray (N7), very fine grained subarkose; medium-dark-gray (N4) mudstone laminae are spaced throughout the unit. | Interlaminated very fine grained to coarse silt-sized arkosic wacke and mudstone. Light gray (N7) to medium dark gray (N4). | Medium-gray (N5) to medium-dark-gray (N4), sandy and silty, illitic-chloritic mudstone. Nonfissile. |
| SANDSTONE TEXTURE | None. | Moderately to moderately well sorted; coarsens upward, and mud clasts are concentrated at the top of the upward-coarsening sequence; grains are subrounded to rounded; fabric is grain supported, and concavo-convex contacts are the most common. | Moderately sorted; no apparent grain size trend; grains are subrounded; grain-supported fabric; sutured grain contacts. | Moderately sorted; graded sand and silt laminae pass up into mud-grade material. Grains are subrounded; fabric is matrix supported. | None. |
| SEDIMENTARY STRUCTURES | Extensively burrowed to bioturbated; indistinct wavy and irregular laminations. | Intricately braided sets of cross-laminae; hummocky sets of cross-laminae; near-horizontal fine laminae; indistinct low-angle cross-stratification. | Ripple bedding: small-scale oscillation-ripple cross-lamination is distinctly developed; mudstone laminae drape some ripple forms; thin, single, flat laminae | Ripple lamination; flasers and lenticular laminae. Wavy and irregular bedding. | Indistinct horizontal laminations and bedding. Very strongly bioturbated. |

| | | | | | |
|---|---|---|---|---|---|
| | | | and low-angle eross-laminae also occur; convolute bedding. | | |
| FOSSILS AND TRACE FOSSILS | *Arthrophycus*. | Minor burrows. | Abundant *Chondrites*. | Abundant *Chondrites*. | Very fossiliferous: gastropods; erinoids; eorals; *Chondrites*. |
| GEOMETRY | Thin, elongate bed always associated with unit 2. | Narrow, elongate sandstone ribbons developed perpendieular to depositional strike. | Thin sheets and pods. | Extremely diseontinuous pods and lenses. | Thiek blanket deposit. |
| UNIT ASSOCIATIONS | Overlies unit 2; underlies Grimsby Sandstone units. | Always oeeurs developed within the Cabot Head shaly lithologies. Underlies unit 1 and overlies unit 3. Upper contaet is abrupt but eomformable. Lower contaet is gradational with unit 3. | Gradational upward and downward with units 2 and 4. | Gradational upward with unit 3; gradational downward with unit 5. | Underlies unit 4; overlies Whirlpool Sandstone. |
| ENVIRONMENTS OF DEPOSITION | Offshore marine: interpreted to have eapped the bar units deseribed in unit 2. Originally formed as ripple-laminated silt and elay and later was reworked by burrowing organisms. | Shallow marine: sandstone originated as low-relief sand dune whieh developed in response to sustained bottom currents. | Shallow marine: rippled sand layers oeeasionally blanketed by mud; formed as subaqueous straight-erested ripple forms whieh developed in response to notably variable depositional energies; burrowers were active during low-current periods. | Shallow marine: formed as discontinuous patches of rippled sand on mud-dominated shelf. | Offshore marine: shelf mud aeeumulation. |

Table 11. *Summary of the Facies 5 Sandstones and their Sedimentary Characteristics in the Whirlpool Sandstone in Northwestern Pennsylvania*

| | UPPER WHIRLPOOL | LOWER WHIRLPOOL |
|---|---|---|
| LITHOLOGY | Light-gray (N7), very fine grained quartz arenite interlaminated with medium-gray (N5) mudstone. Glauconitic. | Light-gray (N7), very fine grained subarkoses and quartz arenites. Glauconitic. |
| SANDSTONE TEXTURE | Individual sandstone laminae are well sorted; sandstone and mudstone laminae alternate rhythmically; individual sandstone laminae average 1.0 cm in thickness and are inversely graded; the number of mudstone laminae increase upward; sand grains are well rounded; fabric of individual sandstone laminae is grain supported and contacts are long to sutured. | Well sorted; grain size coarsens, then fines upward; positive skew; rounded to well-rounded grains; grain-supported fabric; predominantly long and sutured grain contacts. |
| SEDIMENTARY STRUCTURES | Graded bedding; even laminations; individual sandstone laminae are parallel laminated and some have parting lineations developed along internal surfaces. | Planar lamination; low-angle cross-stratification; ripple cross-laminations; tabular cross-stratification; parting lineations; synaerial shrinkage cracks. |
| FOSSILS AND TRACE FOSSILS | None. | None. |
| GEOMETRY | Thin, widespread unit which is transitional between lower Whirlpool and overlying Cabot Head Shale. | Sheet sandstone, 10 to 20 feet (3 to 6 m) thick. |
| FACIES ASSOCIATIONS | Conformably underlies the Cabot Head Shale and transitionally overlies the lower Whirlpool. | Underlies the upper Whirlpool; disconformably overlies the Queenston Shale. |
| ENVIRONMENTS OF DEPOSITION | Offshore marine: storm influenced deposition in deeper water than the sublittoral sheet-sand complex of the lower Whirlpool. | Offshore marine: sublittoral sheet sand. |

Group formed during a rise in the Upper Llandovery sea level and a shift of the paleoshoreline to the north (Brett, 1982). The facies and sedimentary characteristics of the Medina Group in the area are listed in Tables 9, 10, and 11.

# DIAGENESIS

Postdepositional diagenetic effects, which have altered the pore systems of the Medina sandstones, are superimposed on the physically deposited spectrum of sandstone types. Diagenesis is defined as the compositional and textural changes that occur postdepositionally in sediments and sedimentary rocks under low temperatures (<200 °C) and low pressures (<2000 kg/cm$^2$), exclusive of weathering and metamorphism (Davies, 1979; Blatt, 1979). Hayes (1979) summarized much of the current research on sandstone diagenesis and the application of these studies in the petroleum industry. As noted by Hayes (p. 127), "Present-day porosity and permeability of a potential reservoir are the products of diagenetic modification of original porosity." Secondary porosity in sandstones may be more abundant than primary sandstone porosity (Schmidt and McDonald, 1979). The diagenetic occlusion of primary porosity and the development of secondary porosity in sandstones parallel the principal phases of hydrocarbon generation in sedimentary basins (Al-Shaieb and Shelton, 1981). Diagenetically precipitated minerals in sandstones occur as pore linings and pore fills. These minerals can effectively block pore throats, inhibit fluid introduction and hydrocarbon extraction, and react with drilling, stimulation, and recovery fluids in such a manner as to damage the reservoir. It is obvious that an understanding of sandstone diagenesis is critically important in any study of sandstone reservoirs. The successful exploitation of tight gas sands, such as the Medina reservoirs, is particularly dependent upon an understanding of their diagenesis (Wescott, 1983).

This portion of the report includes a description of the kinds of diagenetic alterations that are observable in the Medina Group reservoirs, a recount of the diagenetic history of the sandstones, an outline of the distribution of various diagenetic minerals in the rocks, and a discussion of the effects of the diagenesis on reservoir qualities.

## BURIAL AND THERMAL HISTORY

Many of the diagenetic reactions by which sediments are transformed are related to the burial histories of the sediments (Siever, 1983). Temperatures increase as sediments are buried. The subsurface temperature of a sediment is a function of the burial depth and the geothermal gradient. Thermal gradients vary with the tectonic state of the earth's crust and mantle. At any given place in the earth's crust, the geothermal gradient is related to heat flow and thermal conductivity (Tissot and Welte, 1978). Diagenetic reac-

tions involving inorganic and organic constitutents of a sediment are thermally controlled (Schmidt and McDonald, 1979; Al-Shaieb and Shelton, 1981). The burial history, thermal regime, and rate of diagenetic reactions of sediments are related by their time-temperature history (Waples, 1980; Siever, 1983).

Tissot and Welte (1978) have listed the general rules for the evaluation of present and ancient geothermal gradients. The present geothermal gradient can be obtained by making a sufficient number of temperature measurements in boreholes. Reliable results are obtained when formation temperature measurements are taken in boreholes in which thermal equilibrium between the formation and the well has been reestablished. Temperature logs taken immediately after the completion of drilling are generally low by about 10 to 20°C (Blatt, 1979). Ancient geothermal gradients may be estimated from geochemical data such as vitrinite reflectance, electron-spin resonance, conodont color alteration, carbonization of polymorphs, hydrocarbon composition, fluid inclusions, and diagenetic mineral assemblages (Tissot and Welte, 1978; Hunt, 1979; Al-Shaieb and Shelton, 1981).

After deposition, the Medina Group in northwestern Pennsylvania was buried progressively deeper beneath younger Paleozoic rocks (Figure 46). For the Athens and Geneva fields, the thermal history due to burial has been deduced from several sources. The maximum temperatures of the Medina sandstones and shales during burial were inferred from their diagenetic mineral assemblages and the composition of the hydrocarbons produced. Regional conodont color alteration maps (Harris, 1979) and vitrinite reflectance data from adjacent areas in northwestern Pennsylvania are compatible with the inferred estimates of ancient temperature.

Maurath and Eckstein (1981) measured present-day heat flow and heat production in northwestern Pennsylvania. Their data provided reliable temperature-gradient estimates. The geothermal gradient in the vicinity of the Athens and Geneva fields currently averages 25°C/km (1.4°F/100 ft). This value yields formation temperatures of approximately 50°C to 65°C (122 to 149°F) for the Medina in the study area.

The present-day geothermal gradient cannot account for the maturity of the hydrocarbons (Figure 5) and the diagenetic mineral assemblages observed in the Medina sandstones in the Athens and Geneva fields (Heroux and others, 1979). The geothermal gradient in northwestern Pennsylvania must have been significantly higher in the geologic past. Other workers have made similar conclusions. Weaver and Beck (1971) suggested that a higher paleogeothermal gradient was responsible for the diagenetic mineral assemblages in the shales of the central Appalachian basin. On the basis of fluid-inclusion studies, Tillman and Barnes (1983) suggested a paleogeothermal gradient of about 40°C/km (116°F/mi) for the central and northern Appalachian basin in late Paleozoic or early Mesozoic time. This gradient was used in the construction of the geothermal grid shown in Figure 46. The

burial history of the Medina Group sandstones, based on compacted stratigraphic thicknesses of overlying Paleozoic rocks, is shown superimposed on the temperature grid. Striped and dotted patterns drawn along the burial curves represent the oil and dry-gas thermal-generation windows, respectively. These windows were determined by estimating the thermal history of the Medina Group according to the time-temperature calculation methods of Waples (1980). The proposed elevated geothermal gradient in late Paleozoic–early Mesozoic time would have pushed the Medina sediments into the dry-gas stage of thermal maturity despite their shallow burial depth. This hypothetical approach to the burial history of the Medina sediments could explain the apparent contradiction of dry, thermally generated gas occurring in shallow "cool" reservoirs in the Athens and Geneva fields. Such a thermal history, as will be seen, is also compatible with the diagenetic history of the Medina Group sandstones.

## DIAGENETIC ALTERATIONS

Petrographic analyses of core samples from the Medina intervals in the Athens and Geneva fields permitted the recognition of eight diagenetic events: (1) precipitation of feldspar overgrowths; (2) nodular anhydrite, calcite, and siderite cementation; (3) clay-mineral authigenesis; (4) silica cementation; (5) titanium-mineral authigenesis; (6) compaction and pressure solution; (7) dolomitization; and (8) hematite cementation.

### Precipitation of Feldspar Overgrowths

Detrital feldspar is a common component of the sandstones of the Medina Group in the Athens and Geneva fields. Most of the feldspar has been considerably altered by vacuolization and illitization. Careful petrographic and SEM observations, however, permit the distinction of the original detrital cores from the later authigenic feldspar overgrowths. In most instances, the detrital feldspar cores have been largely altered to clay minerals by hydrolysis, whereas the overgrowths have undergone direct dissolution (Figure 22). In addition, a few slightly altered to unaltered, authigenic, euhedral feldspar crystals can be observed in the sandstones (Figure 22).

In the Medina sandstones, degradation of the detrital potassium feldspars by hydrolysis may have provided the necessary potassium, aluminum, and silica ions for the formation of authigenic feldspar overgrowths; i.e., detrital feldspars, which are intermediate in the alkali feldspar series and less stable at low temperatures than the pure end members, underwent partial alteration during hydrolysis, followed by reprecipitation (Pettijohn and others, 1972, p. 429–430). Feldspar authigenesis, which requires alkaline pore waters, and hydrolysis may have occurred both above and below the water table at shallow burial depths (Walker, 1967).

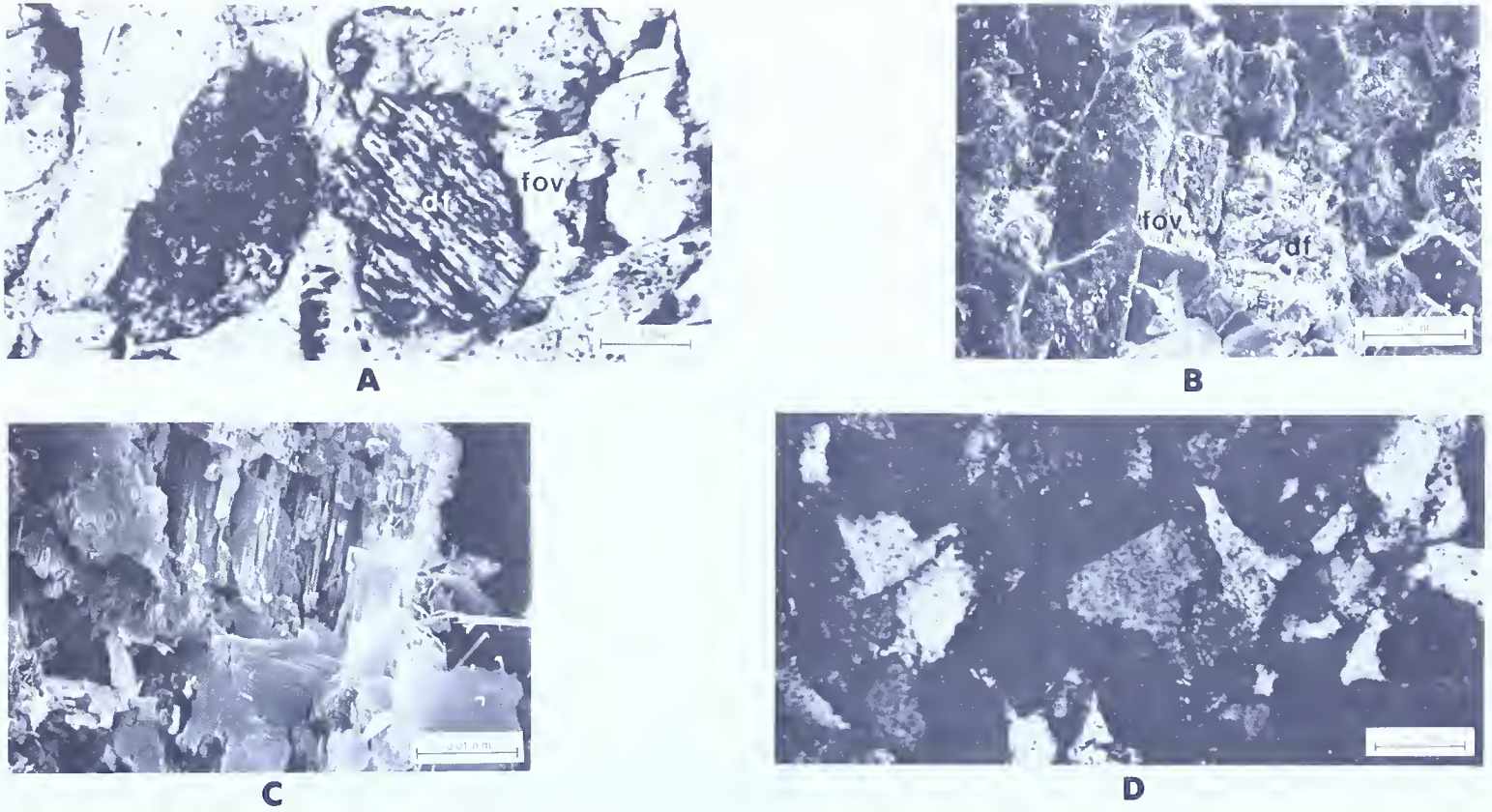


Figure 22. Authigenic feldspars in the Medina Group reservoir sandstones. Photomicrograph A shows several highly altered detrital feldspar grains (df) and authigenic overgrowths (fov). The detrital grains have partially altered to clay. The overgrowths composed of potassium feldspar have undergone partial dissolution. The two SEM views of the same sample (B and C) show a detrital feldspar core that is almost completely illitized. The potassium feldspar overgrowth has undergone direct dissolution and slight illitization. Photomicrograph D shows a euhedral, authigenic potassium feldspar crystal which has partially altered to clay.

## Nodular Anhydrite, Calcite, and Siderite Cementation

Anhydrite occurs as a *poikilotopic* cement which locally forms dense white nodules. It occupies from 0.05 to 2.0 percent of the rock volume of the Grimsby Sandstone samples recovered in the Athens field. In Grimsby samples recovered from the Geneva field, anhydrite occupies as much as 31 percent of the rock volume. Whirlpool samples from the Geneva field contain anhydrite cement that occupies from 1 to 2 percent of the rock volume.

The anhydrite-cemented nodules display the following petrographic characteristics (Figure 23):

(1) The nodules are sparsely to closely disseminated and have an average diameter of 1.0 cm (0.4 in.).
(2) The nodules are not *fabric selective*.
(3) The nodules are composed of significantly etched and corroded detrital grains in a matrix of poikilotopic cement.
(4) The nodules lack later diagenetic modifications.
(5) The nodules are low in preserved primary porosity.
(6) The anhydrite cement locally disrupts the original packing of the sandstone.

The presence of anhydrite cement in a sandstone indicates that evaporite conditions prevailed at the time of sedimentation or that hypersaline pore waters from overlying formations moved through the sandstones during burial (Pettijohn and others, 1972, p. 430). In the Medina sandstones, the patchy distribution and nodular habit of the anhydrite cement, as well as the absence of other early authigenic minerals within the nodules, suggest that the first of these two mechanisms was responsible for the occurrence of evaporite-mineral cements. Anhydrite cements of similar texture and distribution have been described by Mou and Brenner (1982) in the Pennsylvanian Tensleep Sandstone of Wyoming. These authors consider the texture of nodular anhydrite cements to be indicative of slow precipitation in a stable chemical environment from stagnant connate pore waters during initial burial. Gypsum may have been the original evaporite cement that precipitated and, during deeper burial, was converted to anhydrite (Pettijohn and others, 1972, p. 430). Minor amounts of gypsum (< 1.0 percent of the rock volume) were detected by bulk X-ray diffraction analyses in some of the Whirlpool Sandstone samples.

Calcite cement is a quantitatively insignificant component of the Medina Group sandstones in the Athens and Geneva fields, although it may have been present in greater amounts at an earlier time in the burial history. Calcite cement has been largely dolomitized in the Kebert core (Figure 18D) and replaced by silica cements in the Creacraft core (Figure 23). Calcite now constitutes from less than 1 to 3 percent of the rock volume in the Medina sandstones. It is present as a poikilotopic cement and as a secondary mineral replacing feldspar (Figure 23). In some cases, the calcite has etched and

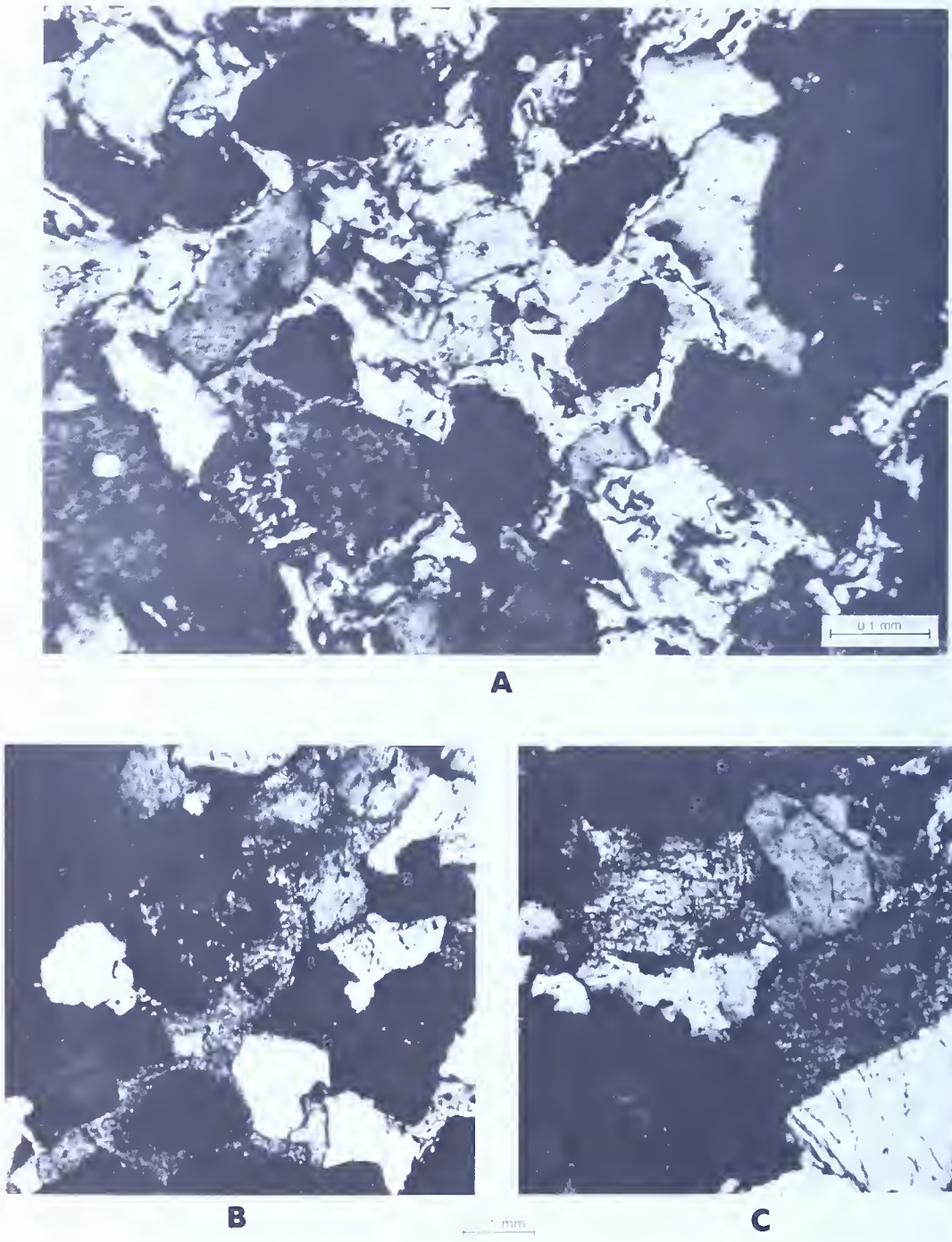


Figure 23. Anhydrite and calcite cements in the Medina sandstones. Photomicrograph A shows anhydrite-cemented nodules in the Grimsby Sandstone from the Kebert No. 1 well. Photomicrograph B shows an isolated patch of calcite cement in the Grimsby Sandstone (Creacraft well core). Photomicrograph C illustrates calcite replacing potassium feldspar in the Grimsby Sandstone (Creacraft well core).

corroded detrital quartz grains. Calcite precipitation in the sandstones required pore fluids of relatively high pH. Calcium and carbonate ions could have been provided to the system by normal marine pore waters, dissolution of fossil shell material, clay membrane filtration, or pressure solution of adjacent limestone units (Blatt, 1979). This latter mechanism is a likely possibility for the Medina Group sandstones in the Athens and Geneva fields. Overlying carbonate rocks within the Clinton Group display extensively developed stylolite and compaction seams. Shinn (1983) has recently shown that limestone compaction can be rather extensive at relatively shallow burial depths. As noted by Blatt (1979, p. 152), ". . . it is conceivable that excess ions from pressure solution of limestone at depth can be supplied to adjacent sandstones for precipitation in sandstones." In the argillaceous Grimsby sandstones of facies 1, the iron carbonate mineral siderite precipitated instead of calcite. The occurrence of siderite within the chemically reduced portions of facies 1 was discussed previously.

## Clay-Mineral Authigenesis

Authigenic clay minerals make up between 3.0 and 10.0 percent of the total rock volume of the Medina reservoir sandstones in the Athens and Geneva fields. The following authigenic clays are present: (1) illite; (2) iron-rich chlorite; (3) mixed-layer chlorite/illite; and (4) corrensite (mixed-layer chlorite/smectite). The illite and chlorite occur as neoformed pore linings and pore fillings. Illite also occurs as a feldspar replacement product and as a recrystallized grain-coating. Mixed-layer chlorite/illite and corrensite are also feldspar replacement products. Figures 24 and 25 show the petrographic and morphologic habits of the authigenic clays in the Medina Group.

### *Illite Neoformation*

Illite is common as neoformed grain-coats in the Medina sandstones in the Athens and Geneva fields. Individual flakes are irregular and have elongate spines. Aggregates of these illite flakes may form pore-lining sheets. Lathlike projections are quite delicate, which precludes a detrital origin. Illite laths reach lengths of as much as 20 microns and frequently bridge the adjacent pore spaces. Authigenic illites appear to have developed from the pore walls into the pore openings, which they characteristically fill.

Illite is also common as a product of feldspar alteration. Illite laths are often observed extending directly out into pore spaces from severely vacuolized feldspar grains and overgrowths.

Illite plays an important role in promoting pressure solution, which results in the observed sutured grain contacts in the sandstones (Heald, 1982). Potassium is lost from the illite structure due to complex ion exchange. This takes place along the edges of sheets where the weakest bonds occur. Cations, capable of replacing potassium, enter the system via pore-water solutions charged with carbon dioxide. Loss of potassium from the illite struc-

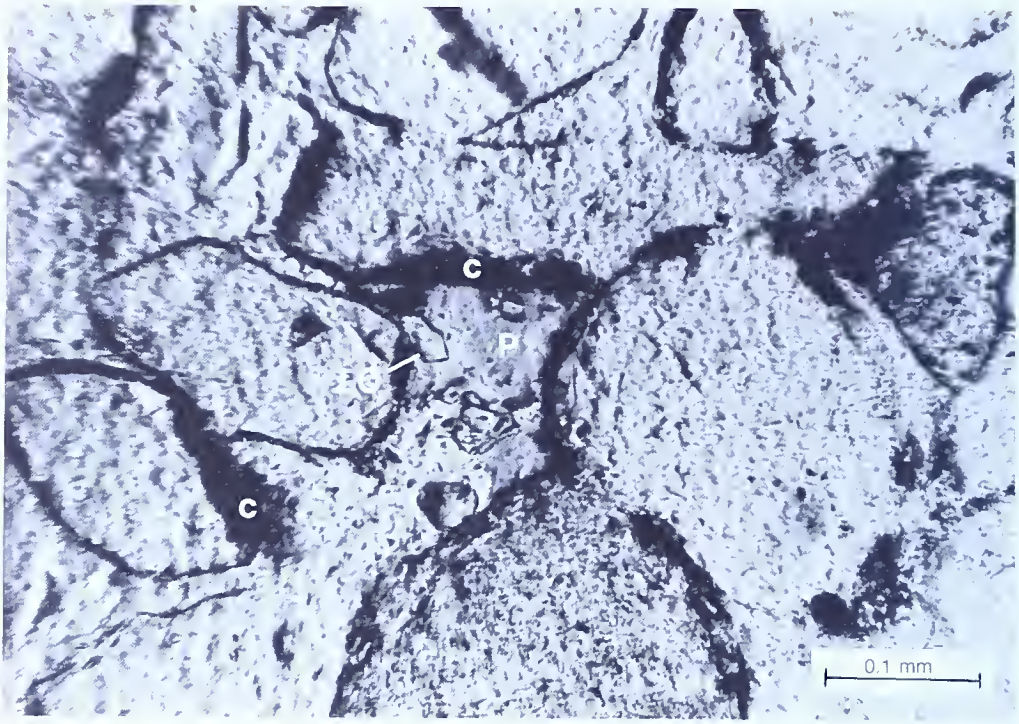


A

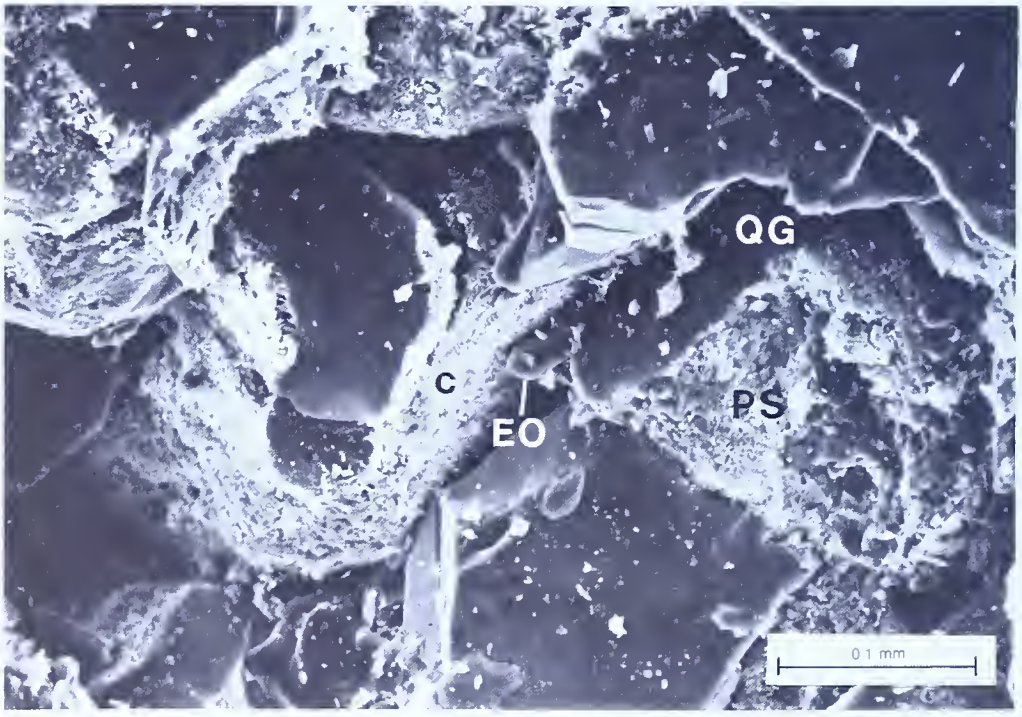


B

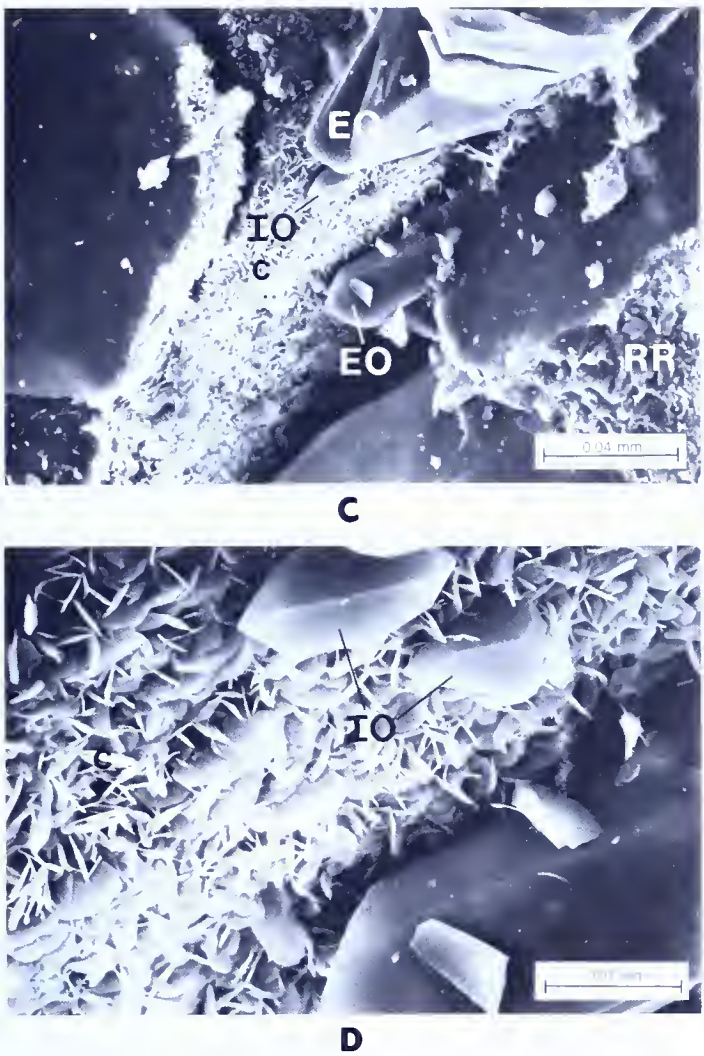


Figure 24. Nature of authigenic chlorites in the Medina Group sandstones.

A. Relict primary pore space (P) lined with authigenic chlorite (c). Doubly terminated incipient quartz overgrowths (IO) occur on top of the chlorite.

B. SEM view of sample shown in A. Chlorite (c) coats the grain in the center of the photomicrograph. Adjacent grains show the effects of pressure solution. Note the pressolved surface (PS) on the quartz grain (QG) and the small euhedral quartz overgrowth (EO) on the grain.

C. SEM view of B at a greater magnification. Note the ridge-and-runnel morphology (RR) of the pressolved quartz grain, the rosette arrangement of the chlorite (c) clays, the doubly terminated incipient quartz overgrowths (IO), and the euhedral quartz overgrowths (EO).

D. Detailed SEM view of the authigenic chlorite (c) rosettes and the doubly terminated incipient quartz overgrowths (IO).

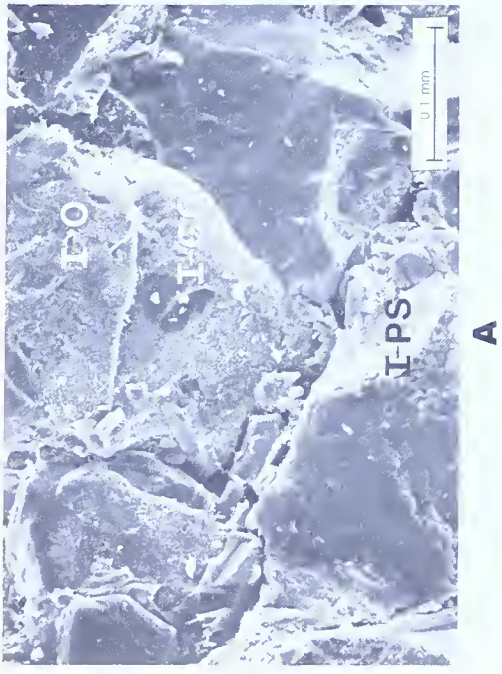
0.1 mm
T-PS
A

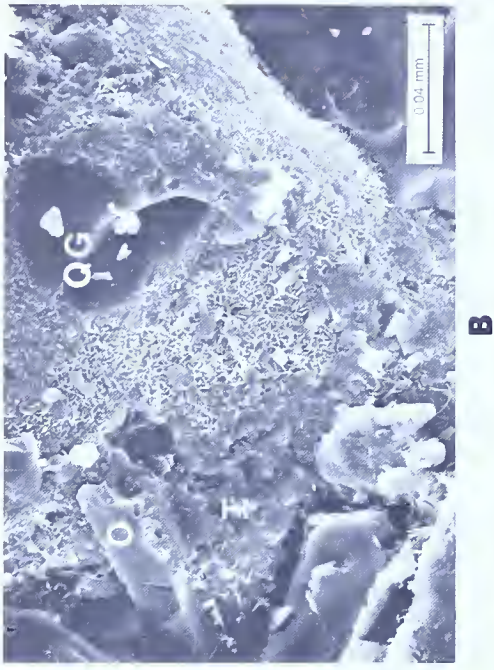
0.04 mm
QG
B


0.01 mm
C

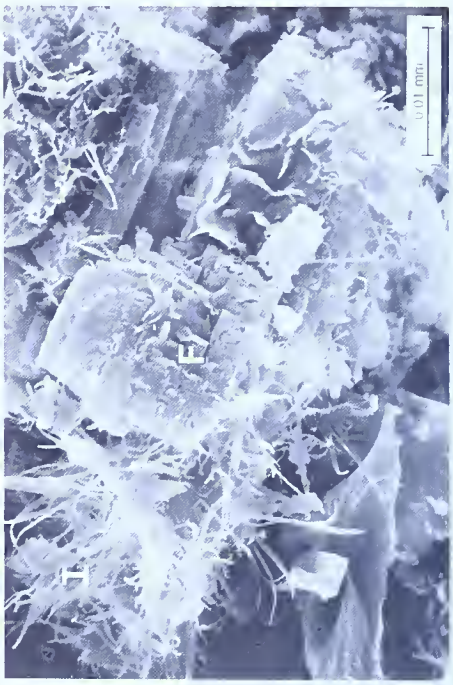
0.01 mm
D


Figure 25. Nature of authigenic illites in the Medina Group sandstones.

A. SEM view of grain-coating authigenic illite (I-GC), authigenic illite coating a quartz overgrowth (I-O), and illite associated with pressure-solution pits in detrital quartz grains (I-PS).

B. Close-up SEM view of the center quartz grain shown in A reveals that pressure solution has removed part of a quartz overgrowth (O) which had partially enveloped the detrital quartz grain (QG). Note the presence of illite (I) along the partially dissolved quartz overgrowth (O).

C. Detailed SEM view of the authigenic illite grain coats. Note the delicate morphology of the illite and the abundant microporosity associated with this authigenic clay.

D. Neoformed illite (I) which formed through the diagenetic alteration of potassium feldspar (F). Note that the illites extend as wispy laths out into the pore space.

E. Illite associated with pressure solution. Sutured grain contact (SC) is shown in the lower left. Pressure solution pit (PS) is lined with wispy laths of very crystalline neoformed illite.

F. Extremely delicate neoformed laths (I) developed on a pressolved quartz overgrowth (O) surface. Also note the presence of authigenic chlorite (c).

ture results in the formation of increasingly alkaline pore fluids which promote silica dissolution at quartz grain contacts in the area of highest pH. In the Medina sandstones, recrystallized illite occurs adjacent to sutured quartz grain contacts and pressolved surfaces. It is present as irregular, overlapping laths which curl away from their points of attachment and extend as wispy projections into the pore spaces. The illite is believed to have squeezed out from between the points of grain contact during compaction and recrystallized as clay coats and ridges.

Illites form authigenically in sandstones through the alteration of precursor detrital or authigenic grains, cements, and clays (Wilson, 1982). They also can be generated by burial transformations of smectite clay (Wilson, 1982). The neoformation of illite from precursor materials is clearly evident in the Medina sandstones. As described above, illite recrystallized near sutured grain contacts from which it was squeezed, formed as an alteration product of feldspar, and precipitated directly on detrital grains. These events were most likely enhanced by increasing carbon dioxide concentrations and the release and availability of potassium, sodium, calcium, and magnesium ions in the pore fluids (Al-Shaieb and Shelton, 1981).

### *Chlorite Neoformation*

Authigenic chlorite occurs as grain-coating pseudohexagonal flakes in a rosette arrangement and also occurs as a pore-filling cement. In thin section, the chlorite appears pale green, and the perpendicular growth of the crystals along the longest dimension of the sand grains can be observed. Chlorite rosettes are also developed as clusters along the crystal faces of euhedral quartz overgrowths (see Frontispiece). Individual rosettes or fans are generally 3 to 5 microns in diameter, but may reach diameters as large as 15 microns. Energy-dispersive X-ray analyses indicate that the chlorite in the Medina sandstones is iron rich.

Chlorite neoformation in sandstones requires that the pore waters contain an adequate supply of ferrous iron and have a negative Eh. The ferrous iron is provided through the dissolution of ferric oxides, hydroxides, and amorphous material, which are unstable under the reducing conditions that prevail in the shallow burial realm of paralic sediments (Wilson, 1982). Authigenic chlorite can also form at the sediment-water interface in a low-energy anoxic environment (Hurst and Irwin, 1982). The dissolution of ferric materials can occur intrastratally in the sandstones or in adjacent siltstones and mudstones, the principal source of the fluids flushed through the sandstone during compaction (Wilson, 1982, p. 2873). This latter mechanism requires that the pore-fluid system be open during chlorite authigenesis. Intrastratally derived chlorite would require static and stagnant pore fluids and would form in the anoxic, low-energy environment described by Hurst and Irwin (1982).

Petrographic examination of the argillaceous, fine-grained clastics of Grimsby facies 1 reveals that the iron-bearing minerals underwent localized, intrastratal dissolution. Partially to almost completely dissolved hornblende, magnetite, hematite, epidote, garnet, and tourmaline occur within and adjacent to the green mottles or reduction spots in these otherwise hematitic rocks. The mottles are associated with distinct burrows and bioturbation, and, as discussed earlier, probably represent endemic reduction areas which formed through the decomposition of the organic material of the burrowing organisms. Authigenic chlorite is only present in those facies 2 sandstones that are interbedded with the red argillaceous sediments of facies 1. Facies 2 sandstones are also the coarsest grained rocks (medium grained) that were recovered in the cores. Iron, which was originally contained in the detrital grains of the argillaceous sediments, was in the oxidized state at the time of deposition. This iron was later mobilized by release in the ferrous state from the localized reduction spots. The ferrous iron was subsequently flushed through the more porous, intercalated sandstones during early burial and compaction. The ferrous iron was able to form stable compounds, such as chlorite, under reducing conditions in the more permeable sands through which fluids were readily transmitted. Chlorite neoformation thus was fabric selective.

### *Mixed-Layer Chlorite/Illite and Corrensite*

Mixed-layer chlorite/illite and corrensite are present as complex feldspar alteration products. Standard SEM observations of the chlorite/illite reveal its presence as a dense pore lining or pore filling where most of the original feldspar has been altered to illite. The clay-filled moldic pores often retain the outline of the original feldspar's cleavage. Low-angle backscatter SEM observations (Figure 26) reveal the curved nature of illite layers within chlorite/illite stacks that partially replace originally twinned detrital feldspar grains. Most of the feldspar grain shown in Figure 26 has been replaced by another mixed-layer clay, namely corrensite. Corrensite is a clay composed of chlorite interstratified with another clay that swells in a liquid. Smectite is the swelling clay in Figure 26.

## Silica Cementation

Silica cement is present in the Medina sandstones as (1) doubly terminated, incipient quartz overgrowths (Figure 24); (2) irregular, encrusting quartz overgrowths (Figure 27); and (3) well-developed euhedral quartz overgrowths (Figure 27 and Frontispiece). The quartz overgrowths have retained crystallographic continuity with their detrital hosts. The Medina sandstones in the Athens field have reached an advanced stage of overgrowth cementation. Thin-section and SEM observations reveal that nearly all of the original pore space has been filled by quartz cement. The bound-

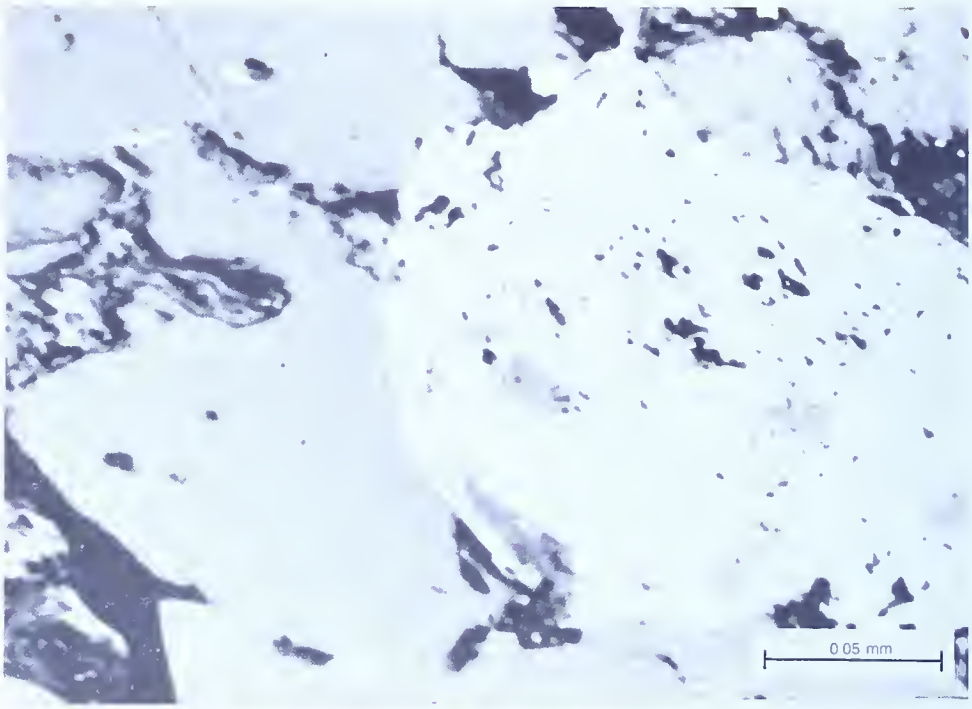


Figure 26. Mixed-layer chlorite/illite and corrensite clays replacing a detrital feldspar grain.

aries between overgrowth cement and the detrital grain nuclei are only weakly visible except where outlined by earlier chlorite cement. Later hematite cement sometimes coats the early chlorite crystals and highlights the development of extensive silica overgrowths (Figure 27). Contacts between adjacent overgrowths form irregular boundaries as a result of common interference during quartz crystal growth. Silica cements in the Athens field sandstones appear to have encroached upon and engulfed the earlier calcite cements (Figure 23).

Silica cementation was not as extensive in the sandstone reservoirs of the Geneva field. These sandstones contain about one third of the silica cement found in the Athens reservoir sandstones. Quartz cement is present as incipient and *syntaxial* overgrowths. Dolomite cementation is more prevalent in these sandstones and is discussed on page 71.

During diagenesis, silica cementation required pore fluids enriched in dissolved silica. Possible sources of dissolved silica include pressure solution, silica released during clay-mineral diagenesis and feldspar alteration, biogenic silica incorporated with the sediments, and silica dissolved in meteoric waters that circulated through the sandstones during shallow burial (Blatt, 1979). Silica may also enter sandstones as dissolved ions flushed from adjacent shales during compaction (Pettijohn and others, 1972). The solubility of silica decreases with decreasing temperature. Silica may precipitate from slowly rising groundwater or from pore fluids that become more supersatu-

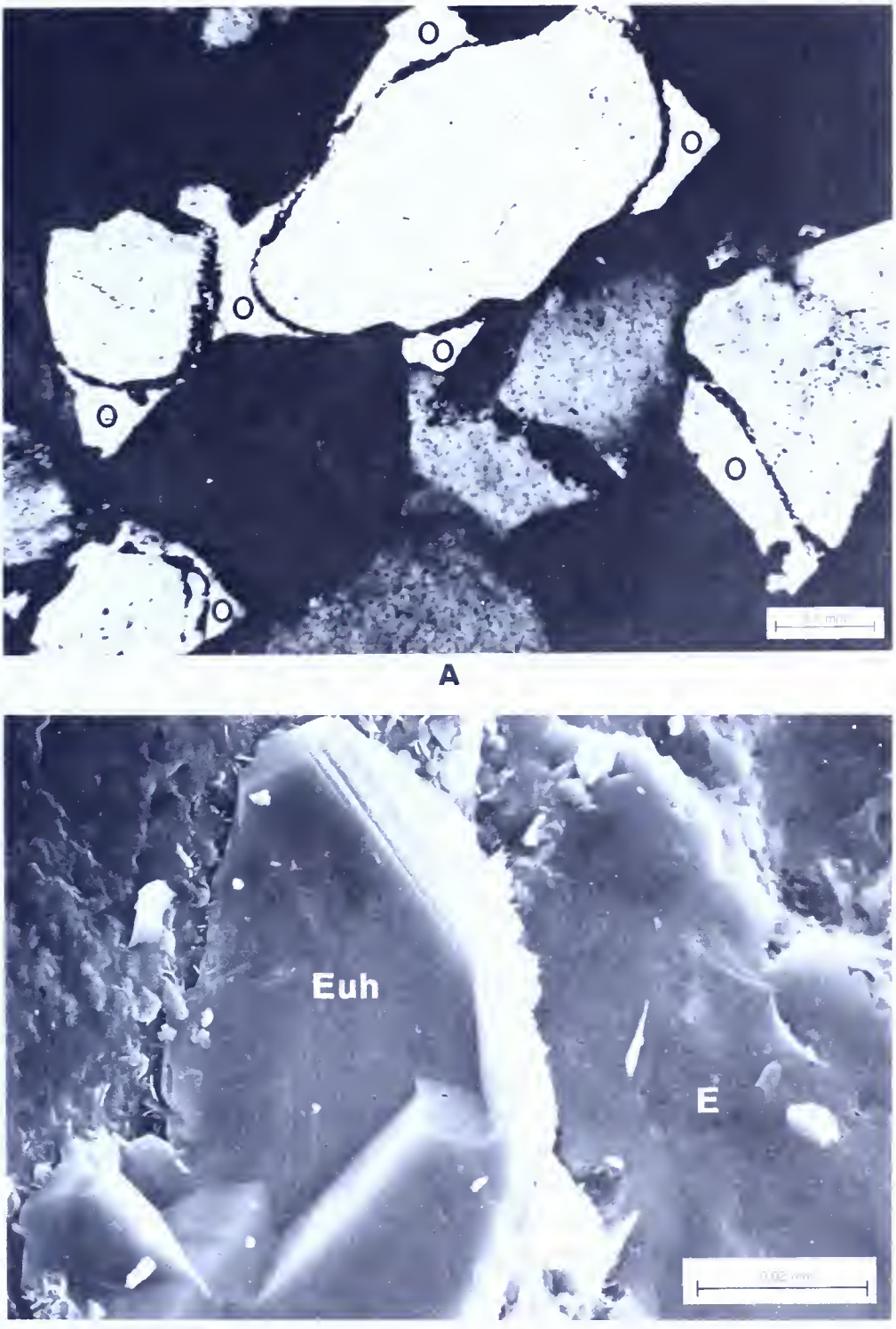


Figure 27. Photomicrograph A showing quartz overgrowths (O) and SEM photomicrograph B showing encrusting (E) and euhedral (Euh) habits of quartz cement.

rated as they cool during episodes of tectonic uplift (Pettijohn and others, 1972, p. 427). These latter two mechanisms are thought to be possible explanations for "late diagenetic quartz that follows an earlier paragenesis of quartz and carbonate" (Pettijohn and others, 1972, p. 427).

## Titanium-Mineral Authigenesis

Petrographic and X-ray diffraction analyses reveal the presence of several titanium-mineral species in the Medina sandstones. The titanium-mineral species identified during the course of this investigation are ilmenite ($FeTiO_3$), sphene ($CaTiO[SiO_4]$), rutile ($TiO_2$), and leucoxene (a term used to denote nondifferentiated microcrystalline titanium-mineral aggregates). A detrital origin for the rutile is suggested because, although remnants of a prismatic outline and pyramidal terminations are evident, most grains appear to have been rounded somewhat by abrasion (Figure 28). Rutile grains appear partly corroded and dissolved. Ilmenite also appears as partially altered grains. The dissolution of ilmenite frequently resulted in the formation of secondary voids. Ilmenite was altered to cryptocrystalline leucoxene during dissolution through the release of iron from its structure. The resultant leucoxene may have lined the dissolution pore (Figure 28) or further mobilized to fill the dissolution pore. Leucoxene pseudomorphs after ilmenite grains also occur. Associated lumps of cryptocrystalline leucoxene and sphene are occasionally found within interstitial cementing materials, particularly hematite. Much of the titanium-mineral authigenesis has resulted in the corrosion and dissolution of adjacent silica cements and grains (Figure 28).

## Compaction and Pressure Solution

Petrographic evidence of mechanical and chemical compaction can be observed in the Medina reservoir sandstones of the Athens and Geneva fields. The mechanical squeezing of the ductile argillaceous lithic grains was an early diagenetic event associated with burial compaction (Figure 13 and 16). The mechanical rotation and fracturing of grains is also evident. The deformation of argillaceous rock fragments did produce some minor amounts of pseudomatrix which locally reduced porosity and permeability. Most ductile rock fragments, however, appear to be little affected by mechanical compaction. This observation implies that mineral cements precipitated early enough in the burial sequence to support the detrital framework and preserve the essential shape of ductile lithic grains.

Compaction through pressure solution is evidenced by the presence of stylolites and sutured grain contacts. Intergranular stylolites occur in the intervals of very fine and fine-grained sandstone. Suture amplitudes are smaller than the mean grain size of the sandstone. The stylolite seams appear to have originated as clay laminae. Stylolites are present as fine sutures at detrital quartz contacts. Here, the sand grains underwent dissolution at

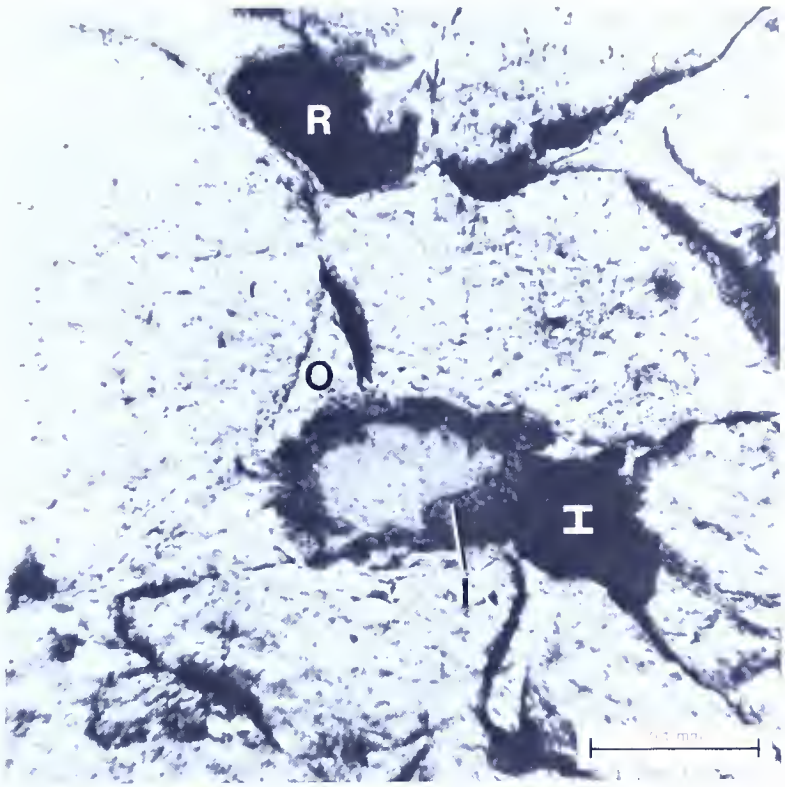


Figure 28. Titanium-mineral authigenesis: rutile (R) grains are partially corroded, and ilmenite (I) dissolution resulted in the development of secondary voids lined with cryptocrystalline leucoxene (1). Note the partially corroded quartz overgrowth (O).

points and interfaces of contact. SEM examination of the chemically compacted Medina sandstones reveals that the sites of pressure solution appear as circular and elliptical spots marking the points of contact between visible pressolved grains and formerly adjacent grains which were removed during sample preparation. The pressolved surfaces consist of ridges with corresponding furrows, and knobs with corresponding depressions. The ridge-and-furrow network is thought to have conducted dissolved silica away from the stressed area (Pittman, 1972, p. 514–515).

## Dolomitization

Calcian dolomite is the dominant cement in the Whirlpool sandstones in the Geneva field (Figure 18). It occupies an average of 18 to 20 percent of the rock volume. The dolomite cement fills intergranular pores. The dolomite is present as partly interlocked, rhombic crystals. The rhombs exhibit sweeping extinction under cross-polarized light, and the crystal faces and cleavage surfaces appear slightly curved. The dolomite crystals are turbid.

These compositional and petrographic characteristics are typical of "saddle dolomite" (Radke and Mathis, 1980). The dolomite cement appears to replace earlier calcite cement.

Three lines of evidence suggest that the dolomite cement formed late in the burial history of the Medina Group sandstones in the Geneva field:

(1) Dolomite replaces the earlier calcite cement.
(2) Dolomite can be found replacing all of the other cements described in this report so far.
(3) "Saddle dolomite" is believed to be indicative of late diagenetic formation by sulfate reduction processes in hydrocarbon reservoirs (Radke and Mathis, 1980).

The dolomite cement present in the Medina sandstones is thought to have formed through the dolomitization of earlier calcite cement. Friedman and Sanders (1978, p. 159–160) suggest that the dolomitization of earlier calcite cements occurs in response to increased pressures and temperatures during maximum burial.

## Hematite Cementation

Hematite occurs as both early and late diagenetic cements in the Medina Group sandstones. It is present as an early cement in the red, argillaceous, *Skolithos*-burrowed sandstones of Grimsby facies 1 (Figure 8). It occurs as a late diagenetic cement in the medium-grained subarkoses and sublitharenites of Grimsby facies 2. Minor amounts of late diagenetic hematite occur in the Grimsby facies 3.

In facies 1, hematite cement occurs as a diagnostic indicator of the early diagenetic stage of burial within an oxidized geochemical environment (Berner, 1981). The hematite is present as a finely disseminated cement in the argillaceous sandstones. X-ray diffraction peaks are sharp for the hematite, indicating a high degree of crystallinity (Gary Cooke, personal communication, 1982). The red, hematite-cemented intervals of this facies alternate vertically with the gray and green intervals of siderite- and chlorite-cemented sandstones, which represent the stable diagenetic minerals of the nonsulfidic, post-oxic geochemical environment (Berner, 1981). Green mottling within the hematite-cemented intervals of facies 1 represents localized reduction associated with decaying organic matter. This was discussed in detail under the previous section titled "Chlorite Neoformation."

Hematite is present as a late stage diagenetic cement in the sandstones of facies 2 and 3. Its relative position in the diagenetic sequence is suggested because (1) hematite cement fills some of the fractures that cut across all of the other cements as well as the grains; (2) hematite replaces all of the previously described cements; and (3) hematite fills secondary voids.

Figure 29 shows the petrographic details of hematite cementation in the sandstones.

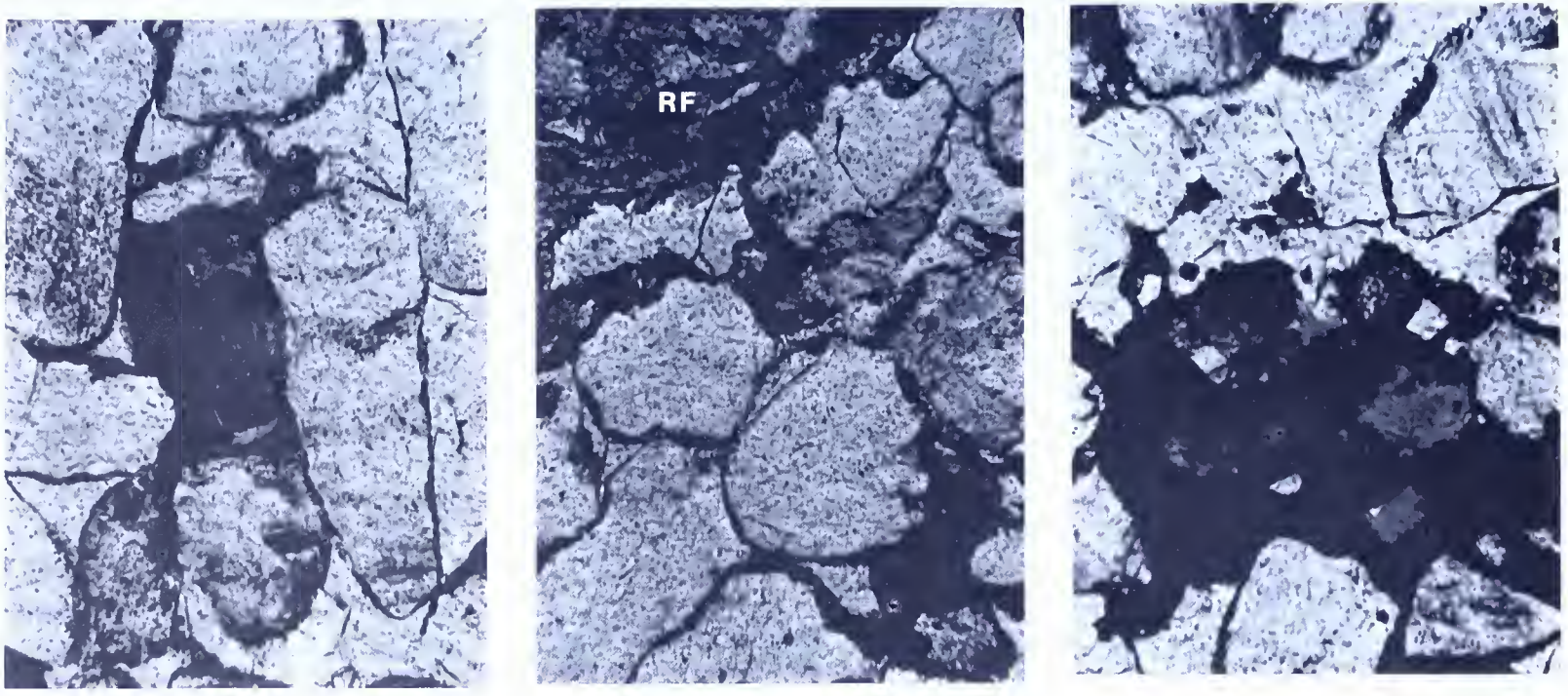


Figure 29. Hematite cementation in the Grimsby Sandstone.
A. Intrastratal dissolution of detrital hornblende provided the iron for hematite formation in the dissolution pore.
B. Intergranular pore-filling hematite cement. Note the partial corrosion of the siltstone rock fragment (RF).
C. Hematite filling a secondary void.

Hematite cement formed in the sandstones through two mechanisms:

(1) Intrastratal dissolution of iron-bearing minerals. Hematite can be observed replacing detrital grains of hornblende, ilmenite, biotite, and sideritic rock fragments.

(2) Direct precipitation from solution. Hematite fills many intergranular pores and moldic pores and also coats early stage chlorite crystals that line detrital and secondary quartz surfaces.

Blatt (1979) states that hematite formation in sandstones requires a source of iron atoms and sufficient circulation of oxidizing pore waters. In the Medina sandstones, the source of the iron atoms was obviously internal, as evidenced by the association of hematite cement with partially altered iron-bearing minerals. Oxidizing fluids apparently entered the sandstones through the vertical fractures in the rocks. Figure 35A shows a series of bands, representing an oxidizing front, which radiate out from a vertical fracture in a facies 2 sandstone.

This author's proposal that meteoric water has invaded the Medina sandstone reservoirs in the study area is supported by geochemical data obtained in an unrelated investigation by A. W. Rose and E. P. Dresel at The Pennsylvania State University. These investigators analyzed brine samples taken from Medina reservoirs in the study area. Their data on Medina brine compositions in the study area indicate that the original connate waters underwent mixing and dilution (A. W. Rose, personal communication, 1984). The Medina brines that they analyzed contain measurable quantities of dissolved sulfate. Stable isotope analyses of the sulfur in this component show that the sulfur is isotopically "light" (rich in $^{32}S$ relative to the amount of $^{32}S$ in a standard). Sulfur in sulfates is normally isotopically "heavy" (rich in $^{34}S$ relative to a standard), whereas the sulfur in sulfides is usually "light." The presence of isotopically "light" sulfur in the sulfate indicates that the sulfur was derived from sulfide minerals. Oxidation of sulfide mineral species, such as pyrite, provided the sulfur that is now present in the dissolved sulfate of the brine.

## POROSITY

The extensive amount of authigenic cementation in the Medina Group sandstones discussed so far resulted in the almost complete occlusion of primary intergranular porosity. Reservoir porosity is, therefore, largely secondary. Seven porosity types are recognized: (1) *relict primary porosity*; (2) *secondary intergranular porosity*; (3) *moldic porosity*; (4) *fabric-selective interlaminar porosity*; (5) *intraconstituent porosity*; (6) *microporosity*; and (7) *fracture porosity*. The porosity of the sandstones is extremely heterogeneous and is controlled by compaction, dissolution, and cementation.

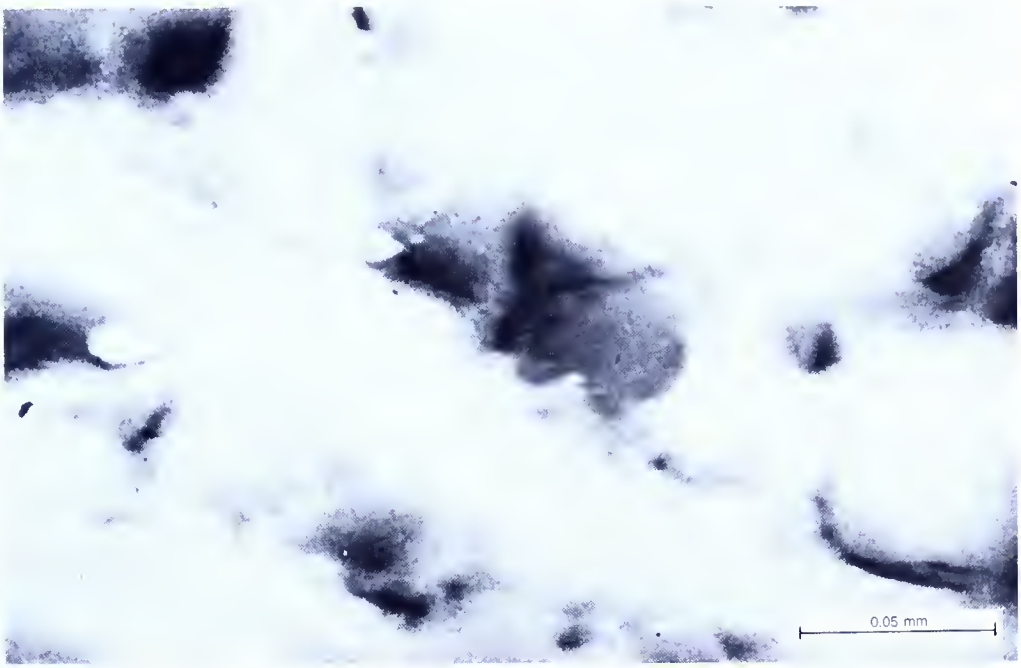


Figure 30. Relict primary voids in the Grimsby Sandstone.

## Relict Primary Porosity

Textural parameters of the detrital fraction of the Medina Group sandstones (Tables 3, 5, 6, 7, and 8) allow us to make the following estimations of the original porosity and permeability of the reservoirs at the time of their deposition (Beard and Weyl, 1973):

| *Texture of Medina Group sandstones* | *Porosity and permeability at time of deposition* |
|---|---|
| Medium grained, moderately to very well sorted | 34.2–41.7 percent; 14–119 darcys |
| Fine grained, moderately to very well sorted | 33.9–43.5 percent; 3.5–29 darcys |
| Very fine grained, moderately to well sorted | 33.1–40.2 percent; 1.1–4.7 darcys |
| Very fine grained, poorly sorted | 30.5 percent; 0.1–0.21 darcys |

These figures, derived from textural measurements of modern sands, help us to realize how extensively the pore spaces have been altered by compaction and cementation in the Medina sandstones. The present porosities range from less than 2.0 percent to almost 9.0 percent, and the average permeability of the reservoirs is less than 0.1 mD.

Thin-section and SEM observations reveal that primary intergranular porosity in the Medina sandstones was greatly reduced during diagenesis. Relict primary porosity is present as extremely reduced intergranular voids (Figure 30). Relict pores occurs as small triangular voids where quartz overgrowths have closed off a pore (Figure 30). Relict primary porosity is also present as lamellar voids which average a few microns in width. Relict pri-

mary porosity accounts for only 0.03 to 0.06 percent of the total porosity in the sandstones (determined by point count). A comparison of these values with the estimates of original depositional porosity given above suggests that the Medina Group sandstones have experienced nearly 100 percent reduction in primary porosity and permeability.

## Secondary Intergranular Porosity

Secondary intergranular porosity is present in all pay horizons and accounts for 1.0 to 3.0 percent of the total porosity of the sandstones. Secondary intergranular voids formed through the partial dissolution of mineral cements and detrital grains. Two types of secondary intergranular porosity, described by Schmidt and McDonald (1979), are present in the Medina sandstones: (1) enlarged intergranular porosity; and (2) reduced intergranular porosity. The enlarged intergranular pore texture formed through the enlargement of previously reduced intergranular void space by the dissolution of cement and grain margins. Both carbonate and silica cements were apparently affected by dissolution, as were the margins of some feldspar grains and sedimentary rock fragments. Adjacent grains and cements in these secondary enlarged pores are significantly corroded, and pore boundaries are largely concave. Later cementation by hematite frequently reduced the enlarged secondary voids (Figure 31).

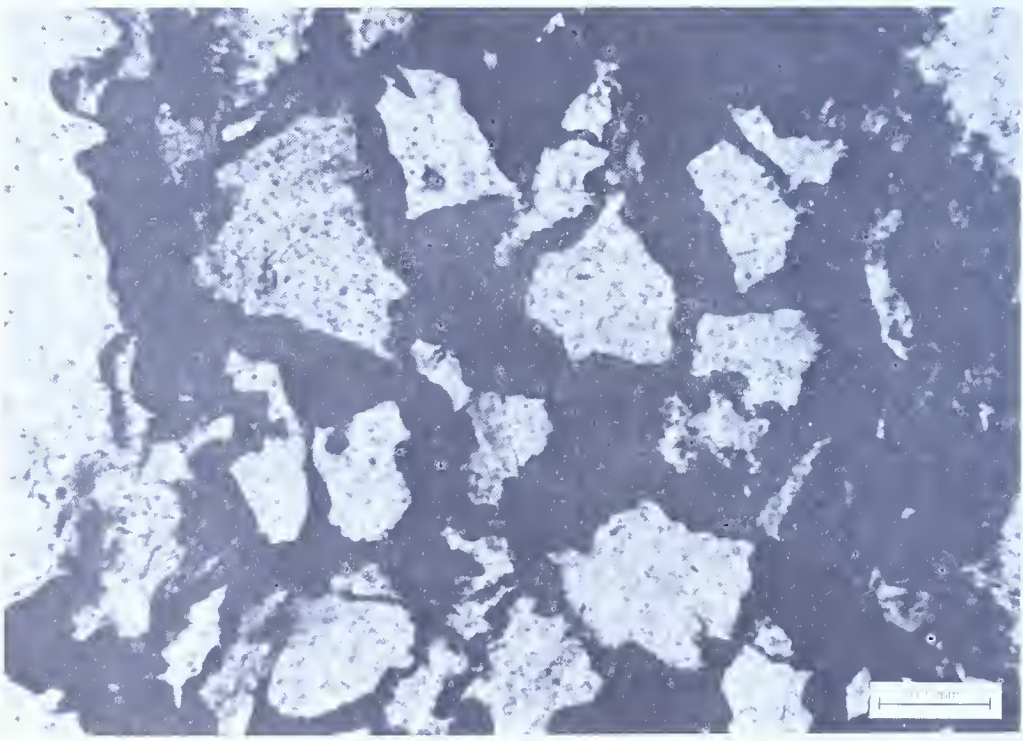

Figure 31. Enlarged secondary void filled with late stage hematite cement.

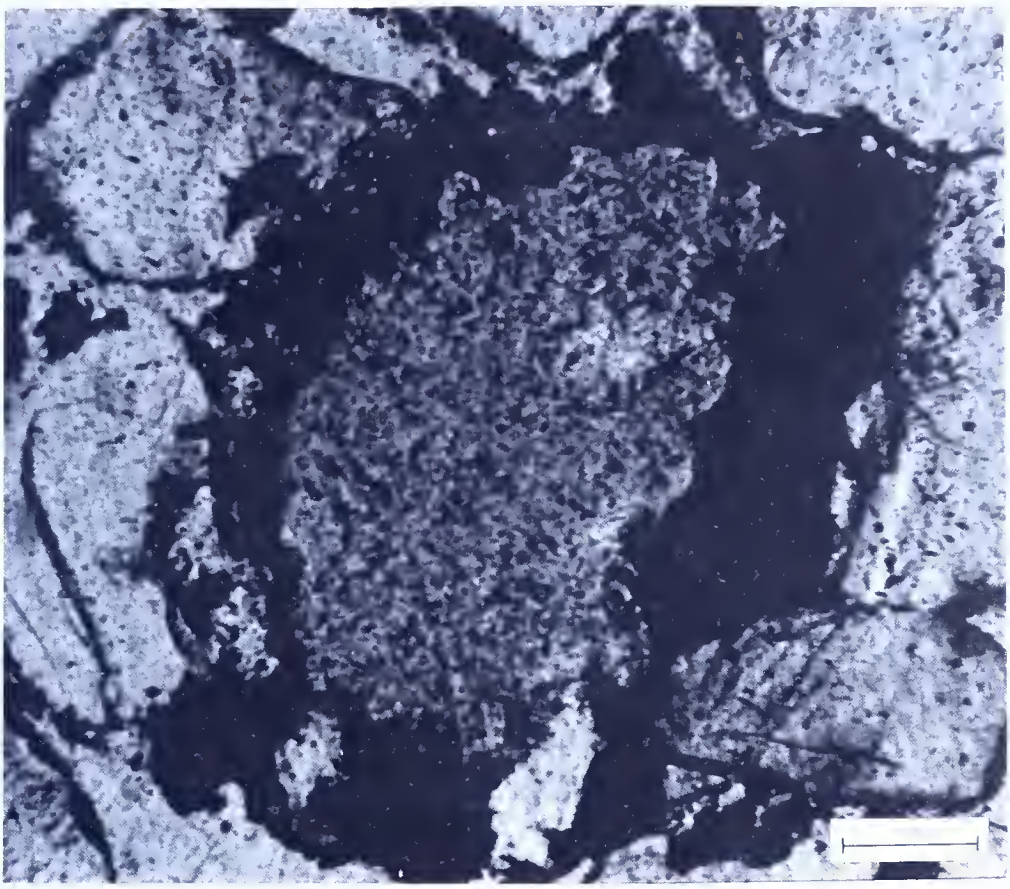

Figure 32. Moldic secondary pore which formed through the dissolution of a sedimentary rock fragment.

## Moldic Porosity

*Moldic secondary pores* are common in all of the sandstones examined. They are most significant in the fluvial Grimsby sandstones of the Athens field, where they form up to 5 percent of the total porosity. These grain-mold void textures developed where selective dissolution of feldspars (see Frontispiece) and lithic grains (Figure 32) resulted in isolated pores that are surrounded by other grains, matrix, and cement. Where labile grains were in direct contact with each other, they jointly dissolved to form oversized intergranular pore textures.

## Fabric-Selective Interlaminar Porosity

Fabric-selective interlaminar porosity is the dominant void type in Grimsby facies 3 and in the Whirlpool Sandstone in the Geneva field. It accounts for up to 8.9 percent of the porosity in the Kebert core samples (Figure 33). In these sandstones, thin, porous laminae are interbedded with thin, tight laminae. The interlaminar pores are distributed in bands oriented parallel to

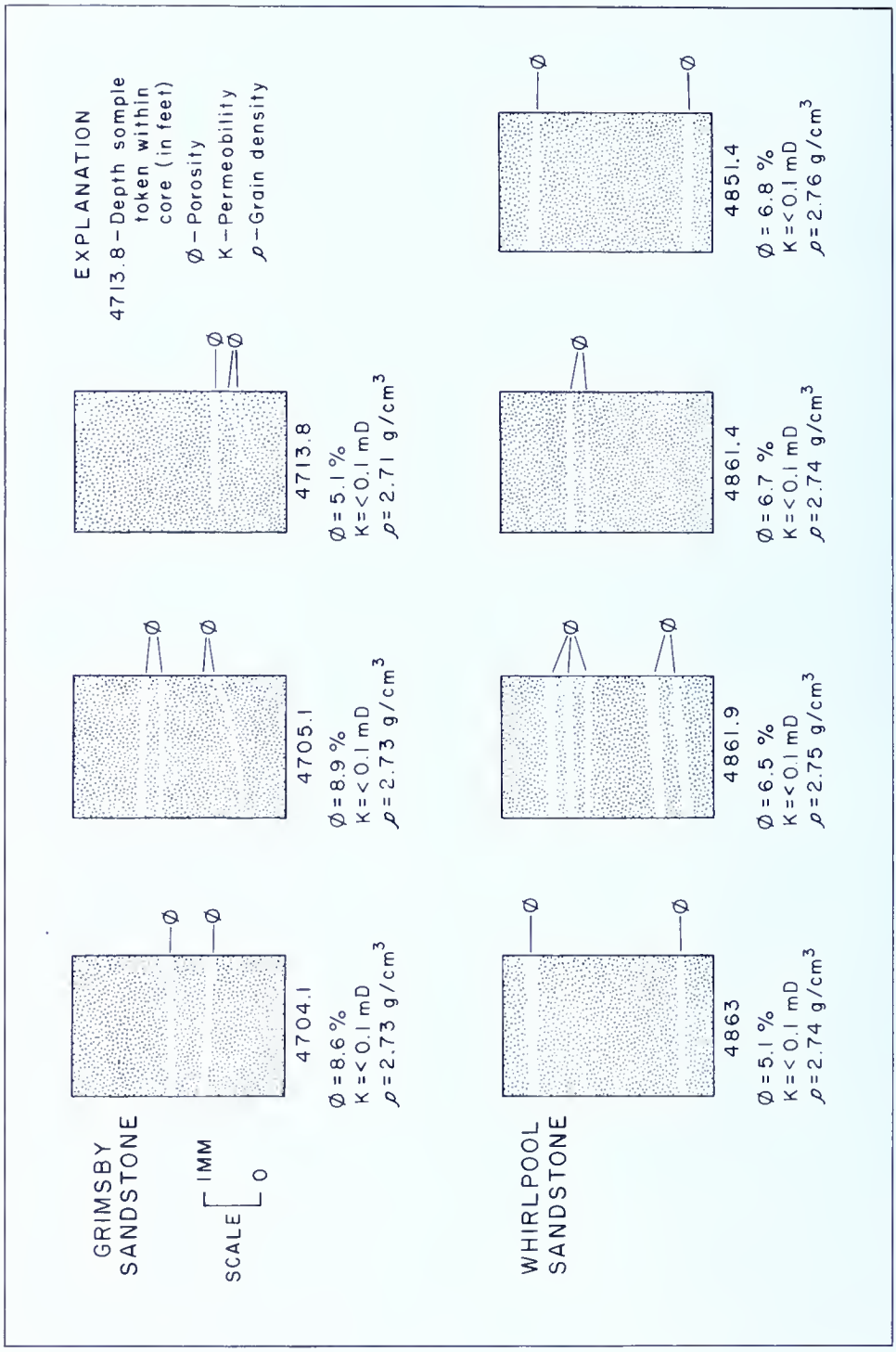


Figure 33. Fabric-selective interlaminar porosity in the Kebert Developers No. 1 Medina core samples.

crossbedding and are separated by thicker belts of tightly cemented sandstone. The interlaminar pores formed through the dissolution of feldspar grains and calcite cement along selectively coarser laminae.

## Intraconstituent Porosity

Intraconstituent voids occur within detrital grains and secondary mineral cements (Figure 36). They range in size from less than a micron to almost the size of the host material. These voids are widely scattered in occurrence and do not contribute to any significant porosity in the sandstones.

## Microporosity

Microporosity is defined as porosity in which the pore-aperture radii are less than 0.5 micron (Pittman, 1979). Micropores in the Medina Group reservoirs occur at the pore-throat restrictions in the sandstones (see Frontispiece), and among the clay minerals (Figure 34). Microporosity constitutes most of the porosity below the hydrocarbon-bearing zones in several of the sandstones. Microporous intervals have high water saturations due to irreducible water (water held by capillary pressure).

## Fracture Porosity

Vertical fractures are numerous in the Creacraft core from the Athens field, but only a few vertical fractures occur in the Kebert core from the Geneva field. A lesser number of horizontal fractures are also present in both cores. The vertical fractures have an average length of 18 to 40 cm (7 to 16 in.) and an average width of 0.5 to 1 mm. The vertical fractures in the Creacraft core intersect in three directions to create wedge-shaped blocks of sandstone (Figure 35). Fractures cross both grain and cement boundaries, indicating that they formed after most of the diagenetic events discussed so far. They are often filled with hematite, indicating that this late stage diagenetic mineral followed the fracturing event. The horizontal fractures tend to parallel stylolite seams, and appear to be tensional fractures derived from the unloading of the sandstone parallel to the direction of maximum stress at the time the core was removed from the subsurface (Nelson, 1981).

Porosity associated with the vertical fractures does occur, but it is negligible due to extensive healing by epigenetic minerals. The following epigenetic minerals precipitated on the vertical fracture surfaces (in sequential order): (1) goethite and hematite; (2) calcite; and (3) anhydrite and gypsum. The goethite is present as an aggradation of minute, radial crystals which cover the fracture surfaces. Some of the goethite has altered to hematite. Milky white calcite crystals encrust the goethite crystals as overlapping rhombs, and fibrous gypsum and anhydrite crystals overlap the goethite and calcite, filling the fractures. Goethite lines the vertical fractures only in the red sandstones. In the gray sandstones, calcite, anhydrite, and gypsum line the vertical fractures (Figure 35).

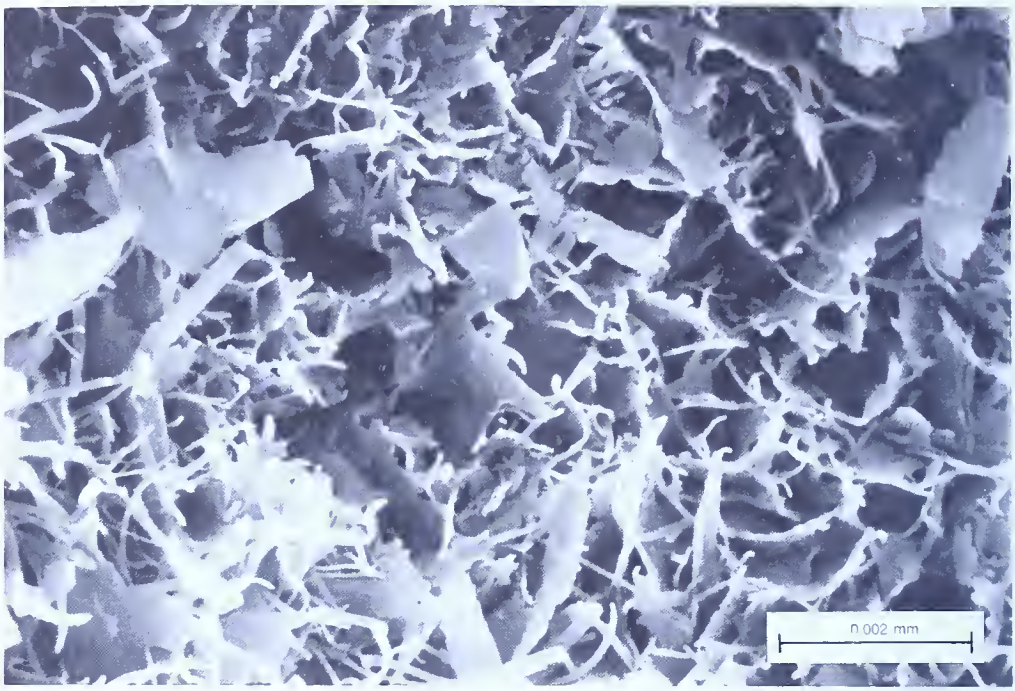


Figure 34. Microporosity associated with authigenic illite.

## Discussion

The distribution of secondary pore types is illustrated in Figure 37. In the Creacraft core from the Athens field, secondary intergranular and moldic porosity are the dominant void types. These are accompanied by lesser amounts of relict primary, micro-, intraconstituent, and fracture porosity. In the Kebert core from the Geneva field, fabric-selective interlaminar porosity is the principal void type. Subordinate amounts of moldic porosity occur, and all of the other types are present in insignificant amounts.

The development of secondary sandstone porosity is the result of the chemical interaction between the rock constituents and mobile pore fluids (Schmidt and McDonald, 1979; Al-Shaieb and Shelton, 1981). Carbonic acid is thought to be the principal reagent responsible for the dissolution of carbonate minerals, feldspars, and lithic fragments (McBride, 1977; Schmidt and McDonald, 1979). Schmidt and McDonald (1979) consider the decarbonization of organic matter during thermal maturation in hydrocarbon source beds to be the process that generates the carbonic acid. This fluid accompanies the initial subsurface waters that migrate out of the source beds and through the adjacent strata ahead of the hydrocarbons. The development of secondary sandstone porosity thus is connected with the principal phases of hydrocarbon generation in sedimentary basins (Al-Shaieb and Shelton, 1981).

The recovery efficiency in reservoir sandstones is controlled by the *pore-to-pore-throat size ratio*, the *pore-to-pore-throat coordination*, the arrange-

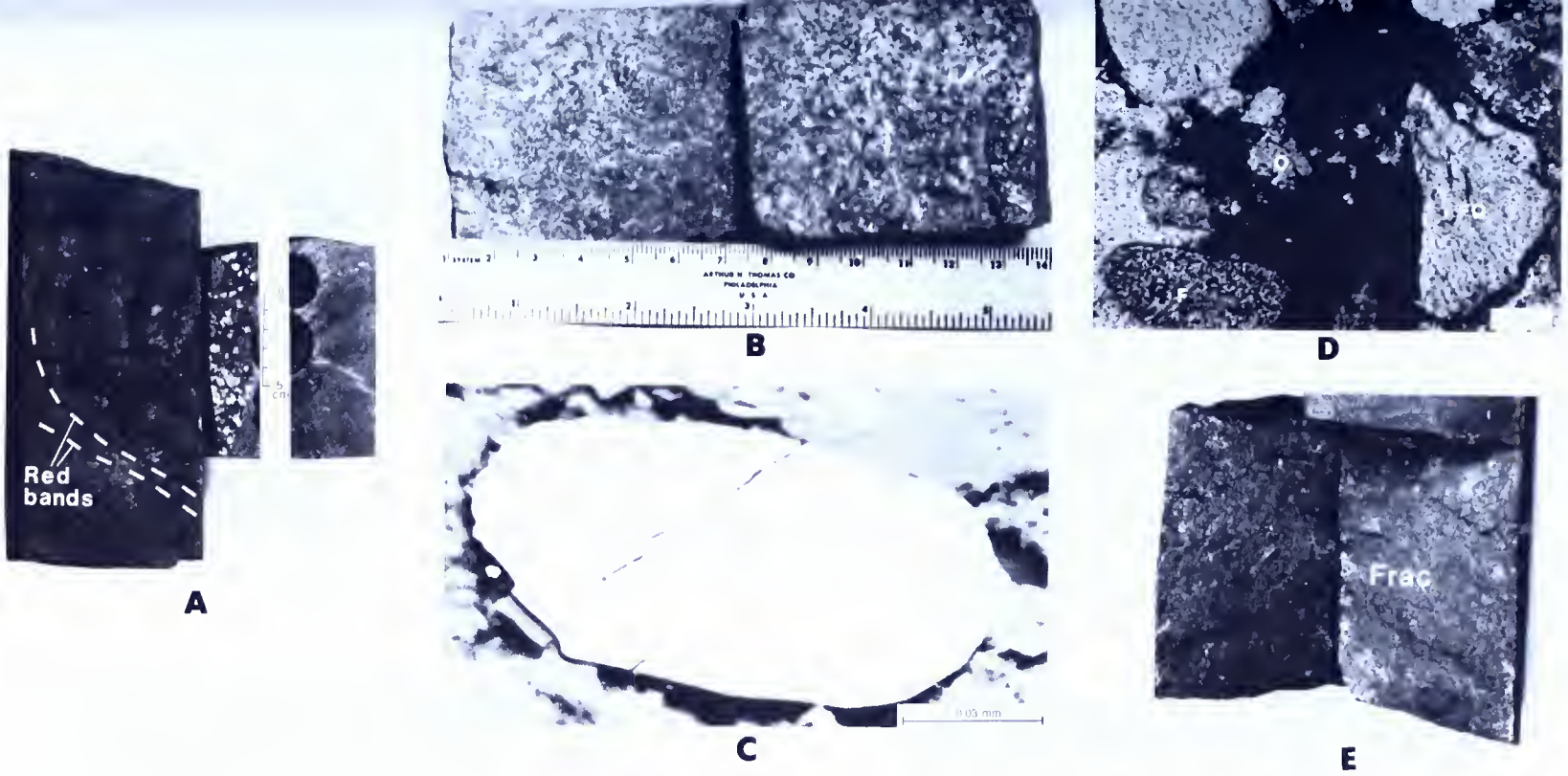


Figure 35. Fractures and epigenetic minerals in the Medina Group reservoir sandstones.

A. Vertical fractures in the Grimsby Sandstone (facies 2) from the Creacraft core. In the sample on the left, the red bands which extend out from a healed fracture represent the movement of oxidizing fluids through the sandstone. On the right, an exposed fracture surface shows the sequence of epigenetic minerals that line the fractures—goethite, calcite, and anhydrite.

B. Fracture surface in the Whirlpool Sandstone from the Creacraft core. The fracture surface is lined with calcite and anhydrite.

C. Fractured authigenic pyrite.

D. Hematite-filled vertical fracture pore. Note the rotated feldspar (F) grain, the sheared quartz overgrowth (O), and the fractured quartz grain (FQ).

E. Vertical fracture (Frac), filled with hematite, crosses grain and cement boundaries.

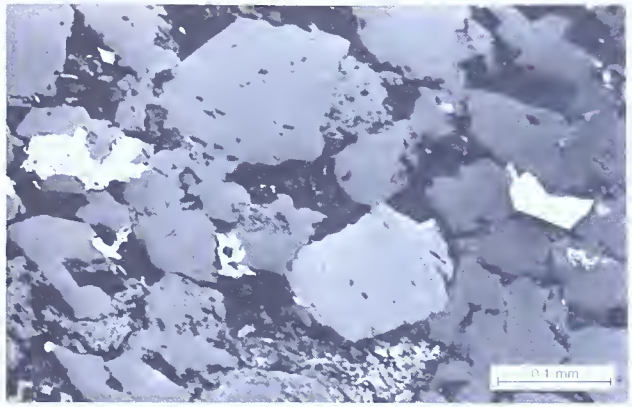


A

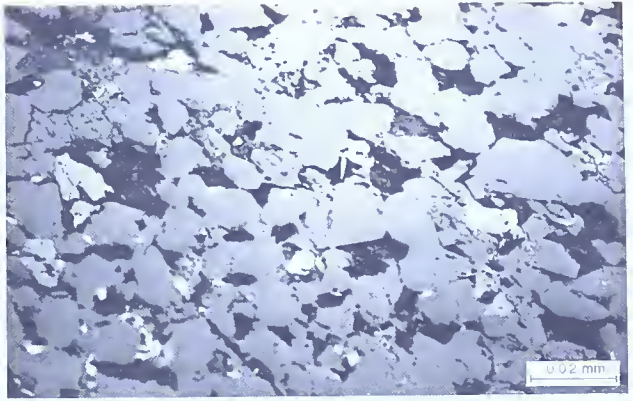


B

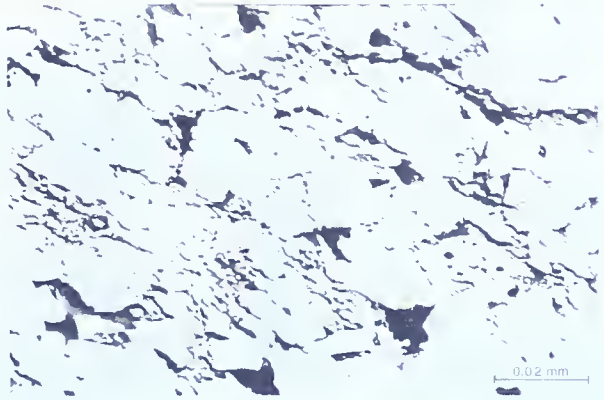


C

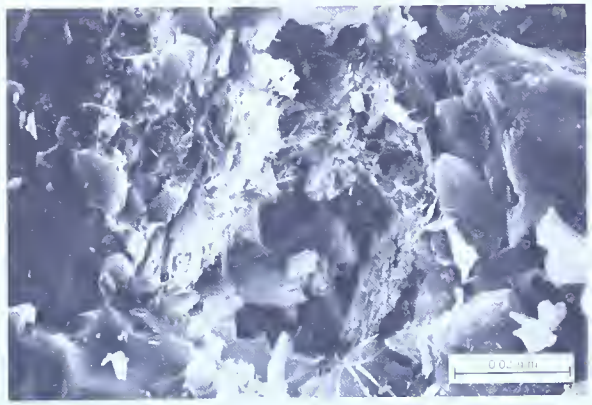

D

Figure 36. Pore geometry in the Medina sandstones. The four backscatter SEM photomicrographs illustrate the heterogeneous pore texture of the fluvial (A) and littoral (B) Grimsby sandstones, and the upper (C) and lower (D) Whirlpool sandstones in the Creacraft core. Note the mainly isolated pores, and their lack of significant interconnection. Also note the extremely restricted pore throats. Small intraconstituent pores are also present.

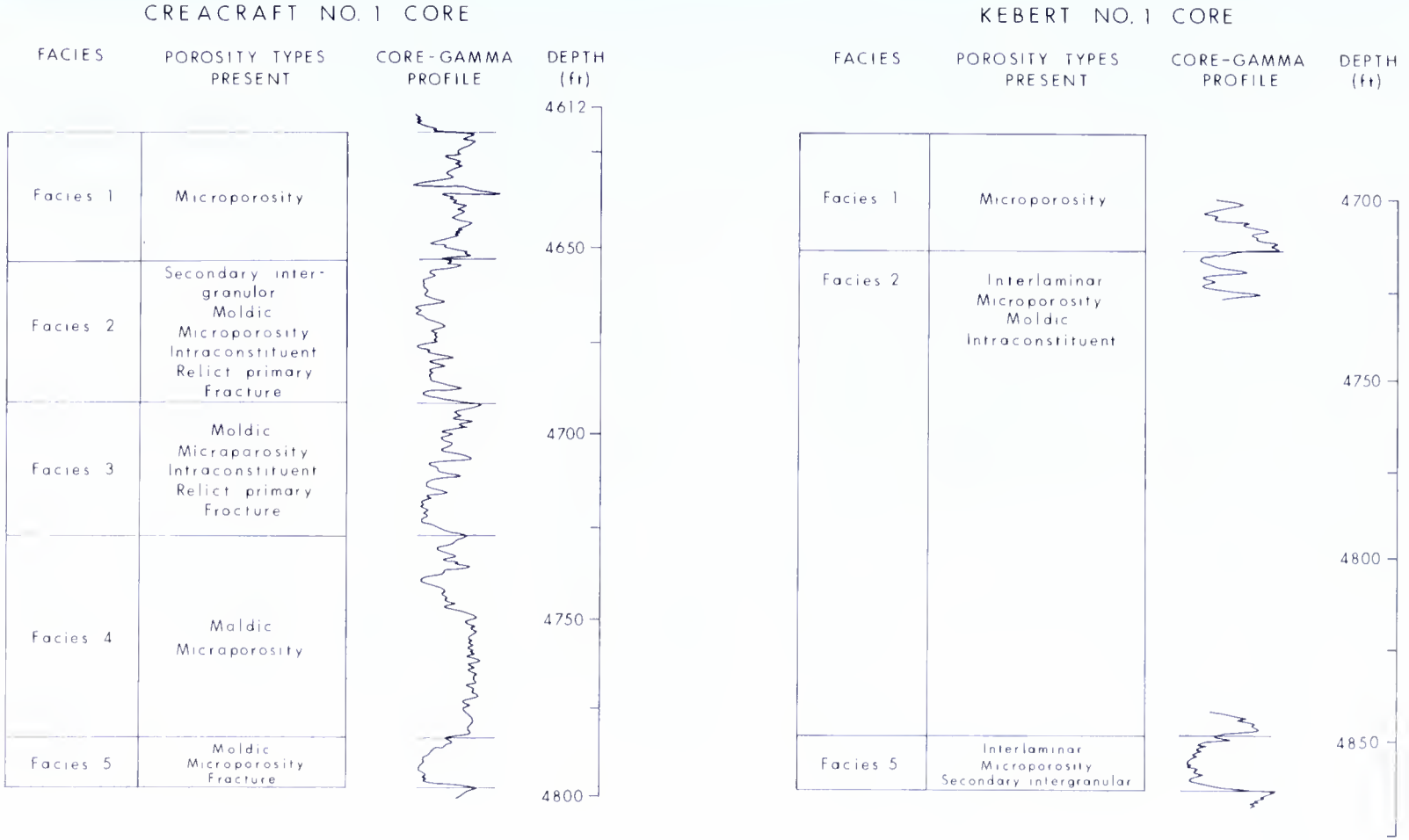


Figure 37. Distribution of secondary pore types in the Creacraft and Kebert Developers cores.

ment of pores and throats of differing sizes, and the surface roughness of the pores (Wardlaw and Cassan, 1978). In the Medina Group sandstones described above, the pore-to-pore-throat size contrast is very high. Few pore throats connect with each pore; therefore, coordination, a measure of the pore system's connectivity, is very low. The pore system consists of moldic and oversized intergranular pores that are isolated within a matrix of very low lamellar and relict primary voids and minor intraconstituent pores and micropores. The pore walls display significant surface roughness. The recovery efficiency of such sandstones is typically less than 15 percent (Wardlaw and Cassan, 1978), and massive hydraulically induced fractures are necessary for commercial production.

### PARAGENETIC SEQUENCE

Evidence from thin-section and SEM analyses suggests that a complete diagenetic sequence in the study area involves the following sequential stages:

Stage 1: deposition of the sediment (grains plus depositional matrix)
Stage 2: early stage precipitation of feldspar overgrowths and nodular anhydrite cements
Stage 3: clay-mineral authigenesis
Stage 4: calcite and siderite cementation
Stage 5: compaction and pressure solution
Stage 6: silica cementation
Stage 7: dolomitization
Stage 8: secondary porosity development
Stage 9: titanium-mineral authigenesis and hematite cementation

The sequential order proposed above is based on the initiation of each diagenetic stage. Several of the stages overlapped, and many of the diagenetic reactions occurred concomitantly. Broadly defined early and late diagenetic stages can be grouped together on the basis of the physicochemical conditions necessary for their occurrence. The proposed paragenetic history of postdepositional events observed in the Medina Group is shown in Figure 38.

## RESERVOIR EVALUATION

### GENERAL STATEMENT

Wireline geophysical logs are the principal source of subsurface data in the Athens and Geneva fields. Various geophysical logs have been utilized to evaluate the formations in the two fields, including gamma-ray, neutron, density, induction, and sonic logs (Figure 39). Of these, the gamma-ray, compensated density and sidewall neutron, and induction electrical logs are

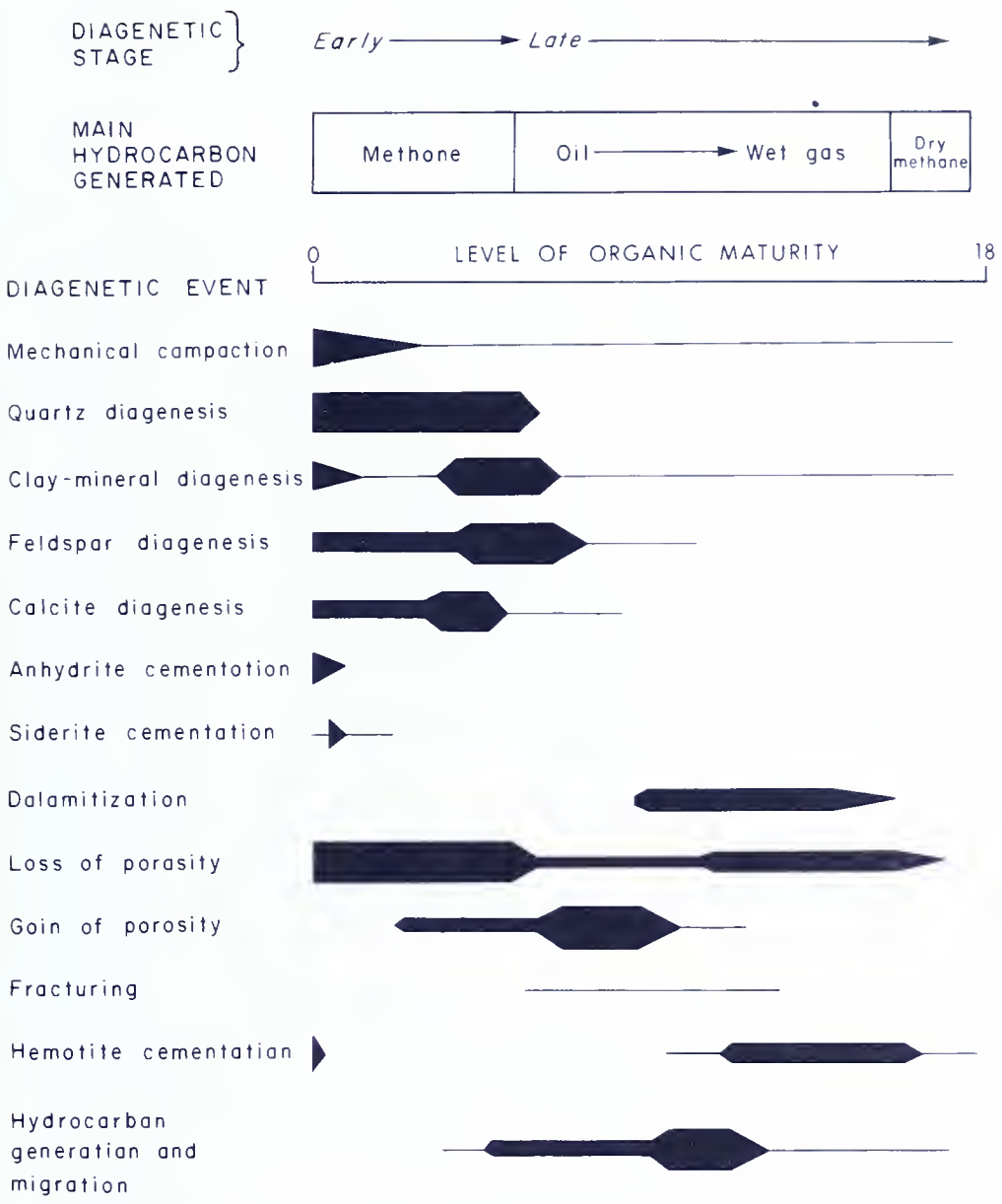


**Figure 38. Paragenetic history of postdepositional events observed in the Creacraft and Kebert Developers cores.**

most commonly utilized for reservoir evaluation in the study area. Supplemental subsurface data are provided by gas logs, which indicate the drilling penetration rate, lithology, and, most importantly, the kinds of hydrocarbon gases encountered in the borehole (Figure 5).

The various authigenic and detrital minerals that compose the Medina reservoir sandstones have significant effects on the petrophysical properties of the reservoir rocks as measured by logging instruments. The authigenic cements, particularly hematite and dolomite, affect the bulk density and

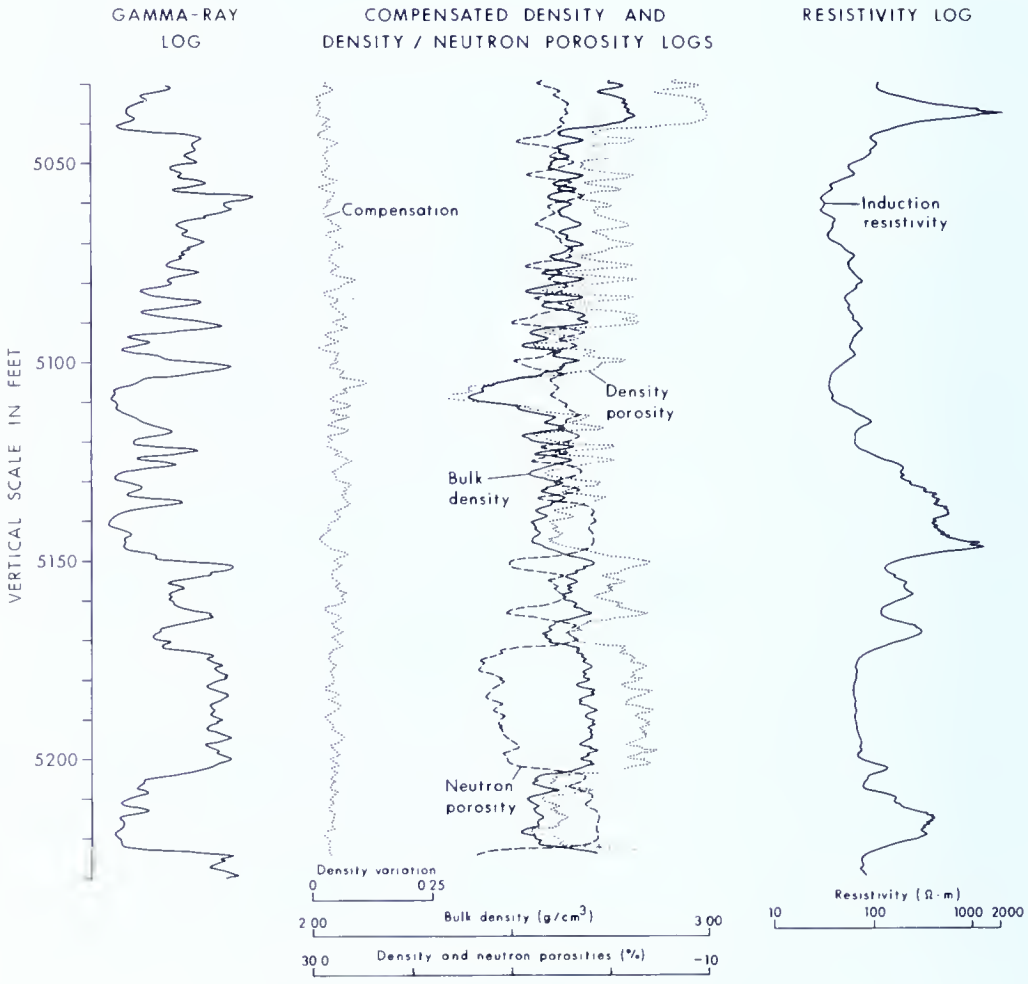


Figure 39. Geophysical-log suite from the

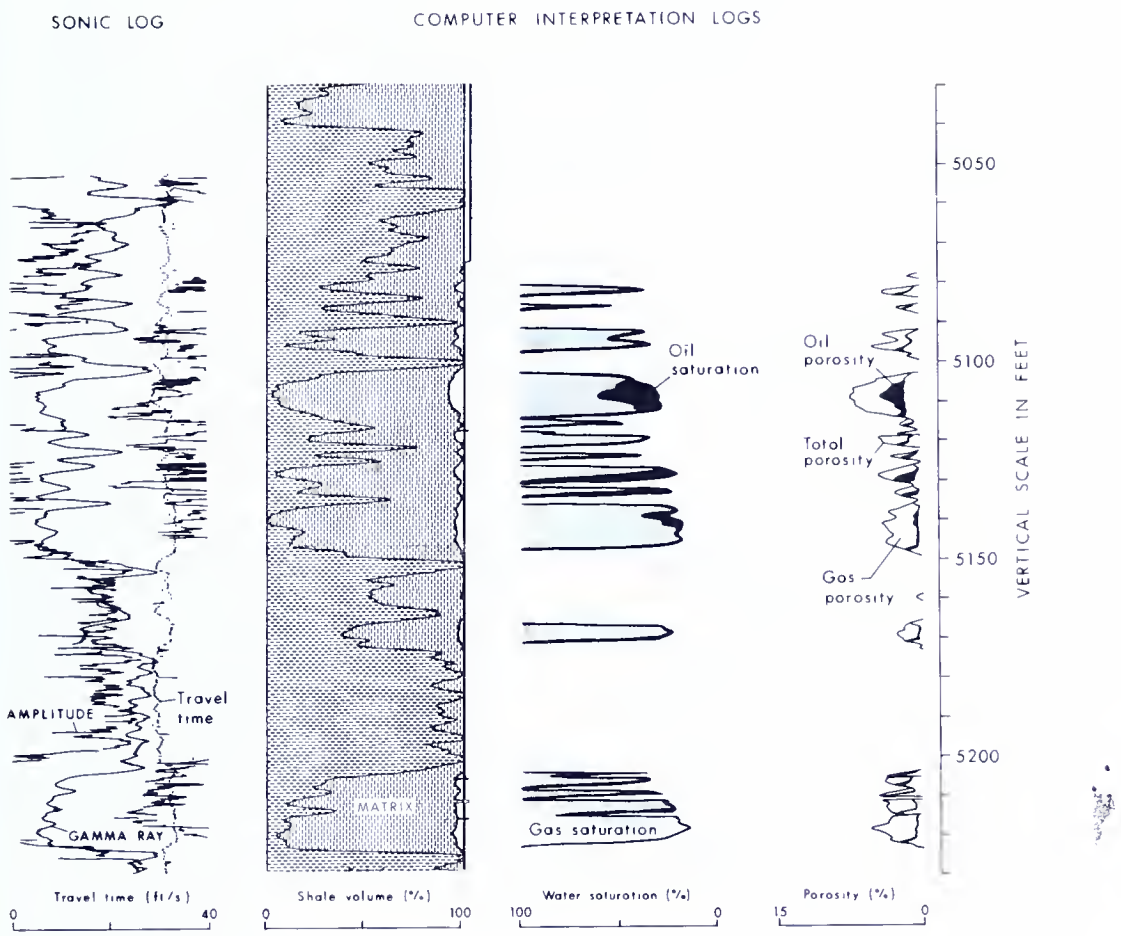


Robert L. Dallas No. 1 well in the Athens field.

sonic velocity. Authigenic clay minerals affect the gamma-ray response, the density and neutron response, and the calculated water-saturation values as measured by electrical logs. The recognition and characterization of specific diagenetically altered intervals on geophysical logs is difficult because the response of the wireline logs to the diagenetic assemblages is very subtle. Using geophysical logs, it is possible to correctly identify the end members within the different diagenetic facies of the Medina Group, through the application of the cross-plot techniques developed by Wescott (1983). The discrimination of diagenetic end members through the use of wireline logs, combined with careful descriptions of the well-cutting samples, permits the sufficiently accurate identification of diagenetic facies in a particular well. Reservoir evaluation, as well as stimulation techniques, can then be tailored to suit the character of a particular sandstone interval.

## Bulk Density

The density log measures the bulk density of a formation using Compton Scattering of gamma rays (Hilchie, 1978). Gamma rays emitted into a formation collide with electrons in the rock and energy is absorbed. As the electron density of the formation increases, the counting rate of the detector decreases. Electron density is related to bulk density, and therefore the response of the density tool is a measure of the bulk density of the rock. The bulk density of the formation is a function of the matrix (grain) density, the porosity, and the density of the fluid occupying the pores. It follows that porosity calculations from the bulk-density measurement depend upon a knowledge of the fluid density and the matrix density. Because the density measurement in the borehole is at the atomic level, compaction and complex pore geometry within the Medina sandstones have no effect on the measured density value. In low-porosity reservoirs such as the Medina in the Athens and Geneva fields, it is usually assumed that invasion is deep enough (3 to 6 inches, or 7.6 to 15.2 cm) that the density measurement is not significantly affected by the presence of hydrocarbons, which have lower densities than the contained waters (Hilchie, 1978)[1]. Fluid densities of 1.0 to 1.1 are used. Consequently, the porosity is derived from the measured deviation from the known matrix density.

The true density and the log (electron) density of quartz is 2.65 $g/cm^3$ (grams per cubic centimeter). This value is typically used as the matrix density value in density-porosity calculations for sandstone reservoirs. It is obvious that such an arbitrarily assigned matrix value is not appropriate for

[1]Kukal and others (1983) have demonstrated that this common assumption is not substantiated by the data derived from Medina core samples and from other tight gas sands in North America. Tight Medina sands actually have shallow invasion, and the invasion profile is variable. Density-derived porosity values are systematically higher than core analysis values. The implication is that the density tool is detecting gas close to the borehole. Furthermore, variable fluid densities mean that a calculation of flushed-zone saturation is necessary for accurate density porosities.

the Medina reservoirs in the Athens and Geneva fields because of their complex assemblage of diagenetic minerals. This statement is supported by the grain density measurements obtained from the core analyses. In the Creacraft well, most of the grain density measurements in the silica-cemented sandstone intervals fall between 2.64 and 2.66 g/cm$^3$. Grain density values in the Creacraft core, however, are as high as 2.76 g/cm$^3$ in the partially hematite cemented fluvial sandstones of the Grimsby Sandstone. Inasmuch as the sandstones of this facies constitute the principal reservoirs in the Athens field, an assumed grain density of 2.65 g/cm$^3$ introduces a serious error into the density-porosity calculation. Analyses of the Creacraft core indicate permeabilities of less than 0.1 mD in 68 of the analyzed core plugs and permeabilities greater than 0.1 mD in 29 of the analyzed plugs. Figure 40 is a histogram showing that the pay interval includes all sandstones having fractional porosities down to 2.0 percent. Based on the core analyses, these values correspond to 95 feet (29 m) of pay. Density-log porosity calculations for this same interval indicate a net pay of only 72 feet (22 m). The presence of 3 to 9 percent authigenic hematite, with a true grain density of 5.26 g/cm$^3$ introduces a 24 percent error into the density-derived estimate of pay thickness.

In the Kebert core, laboratory measurements indicate that the grain densities range from 2.70 to 2.76 g/cm$^3$. The high values, relative to the expected density of clean sandstone, are due to the extensive amounts of anhydrite and dolomite cements in the reservoir rocks. It is significant to take note of the wide range in the compositions of the authigenic mineral components and the corresponding range in matrix densities (2.64 to 2.76 g/cm$^3$) of the Medina Group sandstones over the relatively short geographical distance between the Athens and Geneva fields (Figure 1). Additional core analyses and/or more sophisticated log-derived values from the calculated density of the aggregate mineral composition are necessary if accurate and optimum porosity values are to be obtained.

## Sonic Velocity

The sonic or acoustic log is another primary-porosity tool (Figure 39). It consists of a sound generator and either one or two receivers. The log records the time necessary for a sound wave to move laterally through a formation. The travel time of the sound is dependent on the lithology and porosity of the potential reservoir rock. Before the travel time can be converted to porosity, the velocity of the sound waves in the formation's matrix is needed.

In sandstones that have homogeneous or intergranular porosity, sonic-log-derived porosities can be calculated with good results. In the Medina Group sandstones in the Athens and Geneva fields, the porosity is very heterogeneous and is characterized by moldic and vuggy secondary voids. The acoustic travel time for sound waves in these sandstones is shorter than

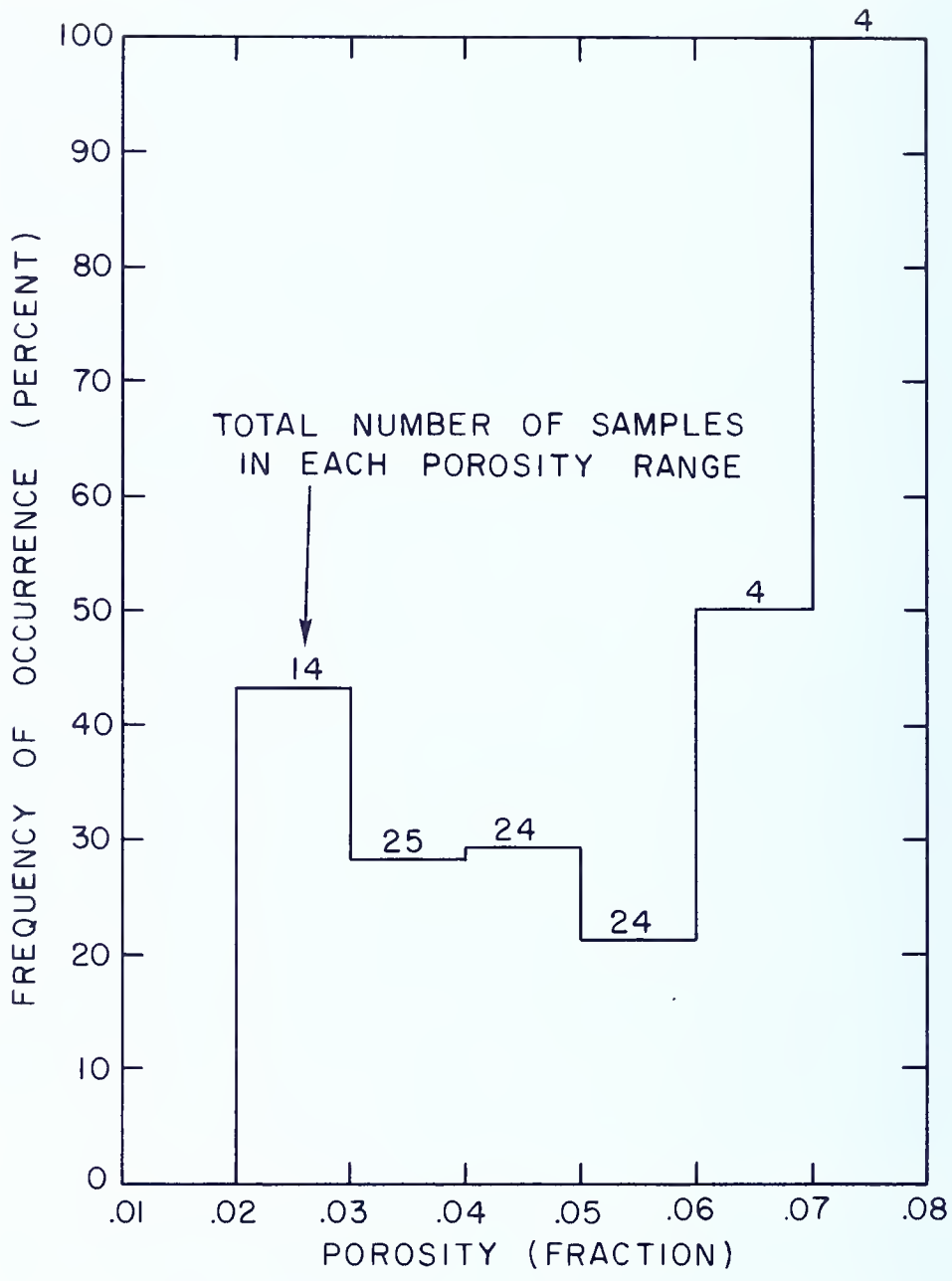


Figure 40. Permeability and porosity histogram for the Creacraft core, Athens field.

would be calculated for a given porosity. This is because the sonic log measures the fastest travel time through the sandstones. Because the pores are highly irregular and unevenly distributed, the compressional wave travels through the portions of the sandstone that have the least porosity. The actual porosity of the formation minus the calculated sonic-log porosity is a measure of the amount of secondary porosity developed in the Medina reservoirs.

## Gamma-Ray Response

The gamma-ray log is an indicator of the lithology or specifically the "shaliness" of a formation. Gamma rays emitted from the rock are detected in the borehole using a Geiger-Mueller counter or a scintillation instrument. The clay minerals of mudrocks and the authigenic and detrital clays within sandstones and siltstones have a relatively high concentration of natural radioactivity. The log is used for the correlation of the subsurface formations and for the determination of the volume of shale or clay minerals present in the formation.

The 70 percent clean sand baseline has generally been considered as the optimum economic cutoff for mapping Medina pay intervals and trends in northwestern Pennsylvania (Kelley, 1966; Kelley and McGlade, 1969; Piotrowski, 1981; Pees, 1983a). In practice, most operators have utilized a 55 to 65 percent cutoff in exploring for and developing Medina sandstone reservoirs. During the late 1970's and early 1980's, rising gas prices provided operators with the incentive to explore for and produce from Medina reservoirs that only a few years ago were considered uneconomic. Massive hydraulic-fracturing techniques have been used successfully to boost production from shaly, low-porosity Medina sandstones. An adequate number of wells have now been completed in the "dirty" Medina intervals to permit the comparison of productive clean reservoirs, developed in northwesternmost Pennsylvania, and productive shaly reservoirs, developed in the Athens and Geneva fields. This comparison is shown in Figure 41. The correlation of thick, clean porous sandstones with higher initial potentials in the Kastle and Pierce pools of the Conneaut field appears statistically valid. The trend is reversed, however, in the Athens and Geneva fields. High initial potentials correlate with the "dirty" or shaly intervals, whereas thick, clean sandstones are tight and nonproductive. This inversion of expected sandstone quality trends in the Athens and Geneva fields is a direct result of the diagenetic history of the reservoirs. Quartz arenites have high percentages of authigenic quartz and dolomite cements and are generally tight, low-porosity, low-permeability rocks with a clean (> 70 percent) gamma-ray deflection. Quartz wackes and arkosic wackes have good microporosity but are impermeable. These are characterized by a highly radioactive gamma-ray signature. Rocks classified as sublitharenites and subarkoses have good

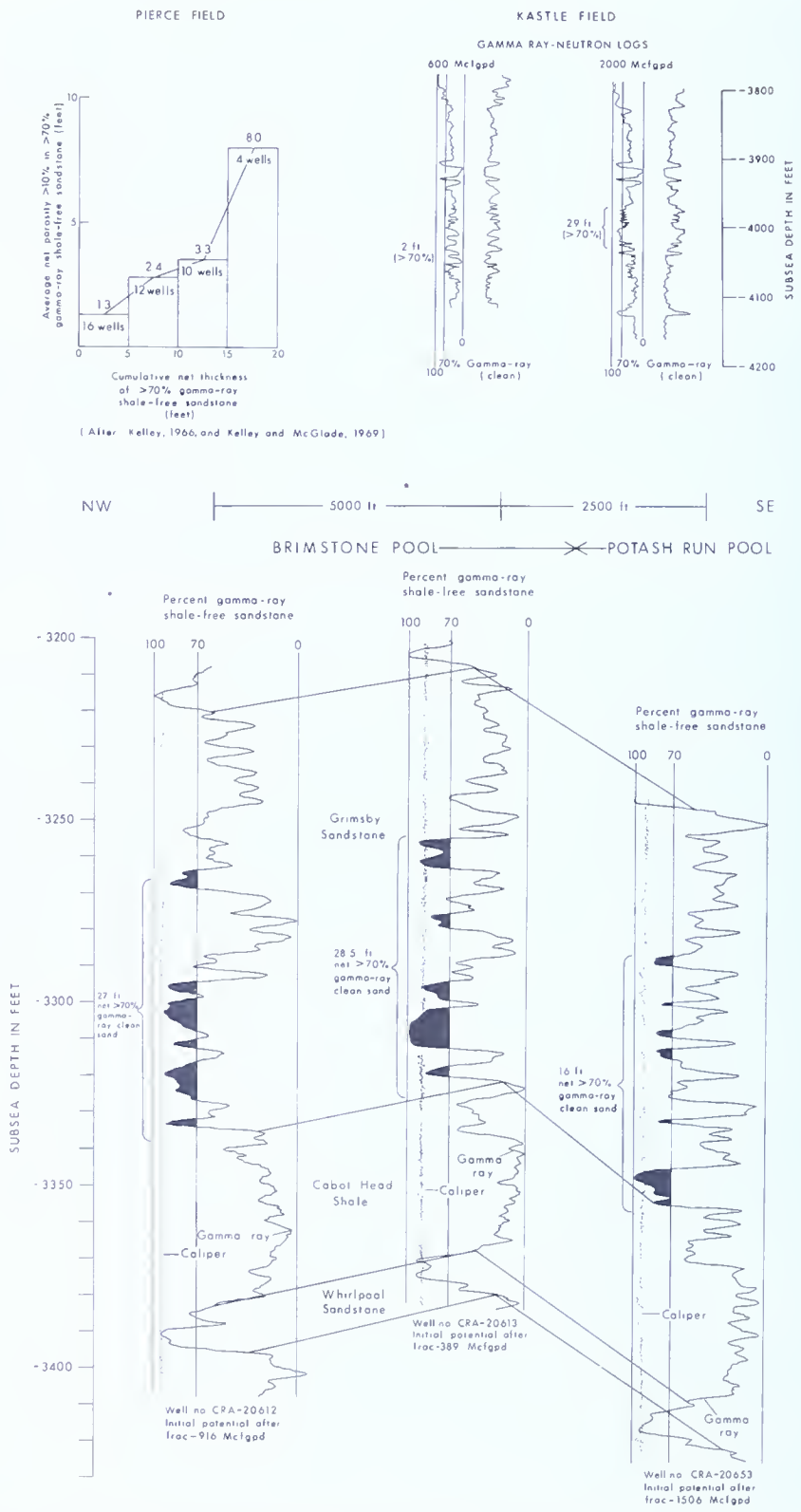


Figure 41. Comparison of Medina shale-free sandstone, porosity, and gas production trends in northwestern Pennsylvania.

secondary porosity due to the dissolution of lithic rock fragments, feldspars, and authigenic cements. These sandstones also have a relatively shaly gamma-ray signature due to the radioactivity of the lithic grains, potassium feldspars and their neoformed clay alteration products, and authigenic pore-lining and pore-filling clays.

Authigenic and detrital clay minerals, which are responsible for the shaly gamma-ray response of the productive Medina sandstones in the Athens and Geneva fields, are dispersed throughout the pay interval. Pay intervals within sandstones containing such structural clays typically produce down to the 40 percent sand cutoff (Hilchie, 1978). The Kebert well is a case-in-point. The core analyses of the Kebert core plugs indicate 20 feet (6.1 m) of sandstone in the top of the core and 16 feet (4.9 m) of sandstone in the Whirlpool. The histogram in Figure 42 suggests a very low average permeability. Pay based upon the core analyses equals 36 feet (11 m). Based upon the gamma-ray log of the correlative intervals and using the cleanest Medina sandstones as the 100 percent sand baseline and the average gamma deflection of the lower Cabot Head Shale as the 100 percent shale baseline, 27 feet (8.2 m) of pay is indicated when a 60 percent cutoff is used. A 40 percent cutoff, however, indicates 35 feet (10.7 m) of pay, a figure that agrees with the core analyses results.

The 40 percent sand baseline can be applied in the study area with one additional caution in mind. The 100 percent shale baseline shifts in the Medina Group. The shaly sediments associated with facies 1 and 2 sandstones are hematitic and less radioactive than the illitic/chloritic mudstones of the other intervals. Sample control and density measurements should be utilized to recognize the facies and select appropriate shale baselines during well evaluation (see Figure 43).

## Gas Detection with the Density and Neutron Log

In well-log evaluation, hydrocarbon-bearing zones are often indicated by the crossover that occurs on the density and neutron curves when these logs are run simultaneously on compatible porosity scales. Gas causes an apparent decrease in the density (or apparent increase in the porosity), whereas on the neutron log gas is recognized as an apparent decrease in porosity. In a shaly formation, the gas effect or crossover is often cancelled because the clay minerals affect the density and neutron logs in exactly the opposite way. Figure 43 shows the neutron and density logs from the Creacraft well. The crossover or gas-effect intervals are shaded. Notice that, where crossover occurs, the density and neutron logs mirror each other in the cleaner sandstones but not in the shaly sandstones. This indicates differential investigation depths for the two tools, the neutron log measuring deeper into the formation than the density log (Hilchie, 1978, p. 10–16). This effect is further complicated by the fact that iron minerals cause an increase in neutron porosity measurement. A standard gas correction in these zones would

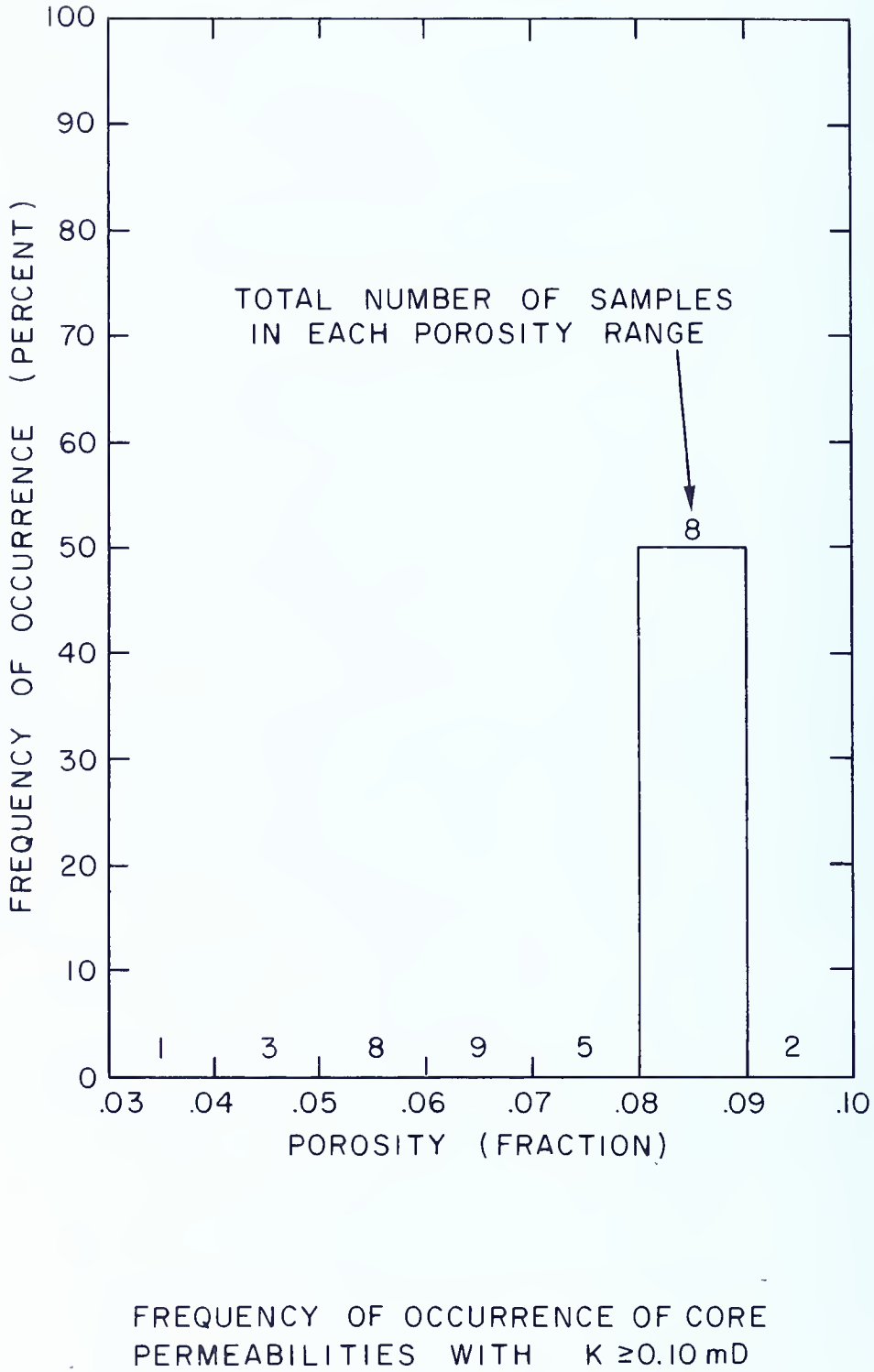


Figure 42. Permeability and porosity histogram for the Kebert Developers No. 1 core, Geneva field.

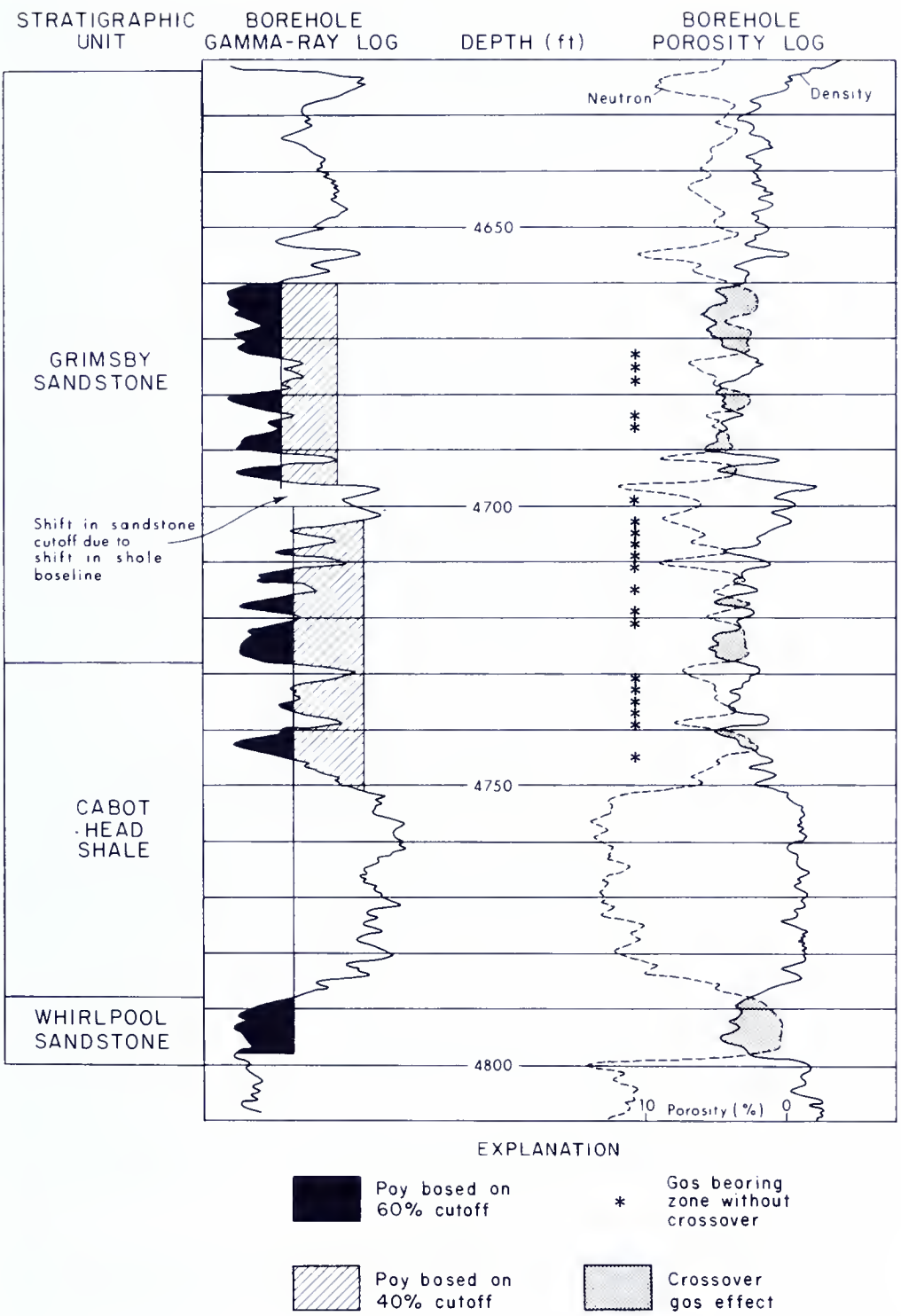


Figure 43. Gas effect on the neutron and density porosity logs in the Creacraft core.

lower the estimated porosities to values below the economic cutoff. Therefore, the density log should be used to estimate porosity, and the neutron should be ignored, except to recognize the hydrocarbon-bearing interval.

Analyses of the Creacraft core showed that most of the sandstone section is gas bearing and potentially productive. Figure 43 shows that crossover does not occur over this entire interval. In fact, crossover does not occur within the most porous zones of the Grimsby. In these intervals, the shaliness of the formation is due to diagenetic and detrital clay minerals, and the density and neutron logs do not cross although gas is still present. Because the gamma-ray curve reflects the total amount of clay present, and the neutron-density response is a function of the clay content, a plot of the gamma-ray observations versus the separation between the neutron and density log values should be a straight line (Hilchie, 1978). The presence of gas decreases neutron porosity and increases density porosity. Gas points fall off the straight-line plot to the lower right. These gas-bearing points or intervals are indicated by the asterisks in Figure 43. The combined thickness of the crossover intervals and the shaly gas-bearing intervals indicated by the asterisks agree with the thickness of the gas-bearing zone as indicated by the core analyses. Porosity and water saturation in the shaly intervals should be determined by the interpretation method of Fertl and Hammack (1971).

## Water Saturation

A comparison of the core-derived and log-derived water saturations in the Creacraft well shows that the log-calculated water saturations at low porosities are far too high (Figure 44). In low-porosity shaly sandstones, possible causes of the erroneous water saturation are variable values for the cementation exponent ($m$) and solid conductivity (Rosepiler, 1981). Both of these values play a role in the high log-calculated water saturations observed in the Creacraft well.

When only log data are available, $m$ typically is assumed to equal 2.15 (Hilchie, 1978). Core data suggest that an $m$ value of 1.46 is more appropriate for the Medina sandstones in the study area (Charles Grapes and John Flower, personal communication, 1983). An examination of the logging-data headings from logs available from the study area show that an $m$ value of 2.15 is routinely used. Geologists working in the field should keep this discrepancy in mind when beginning borehole-log evaluation of Medina wells.

Authigenic clays within the pore systems of the Medina sandstones affect both the physico- and electrochemistry of the reservoir rock. The mode of occurrence and crystal habit of the neoformed clays result in an extremely high ratio of surface area to volume (Davies, 1979, Table 9, Figure 22). Almon (1979) demonstrated that the large surface area and high cation-exchange capacity of clays results in an electrostatic double layer, called the Goury or Stern Layer, which forms near the clay surface. This is of major

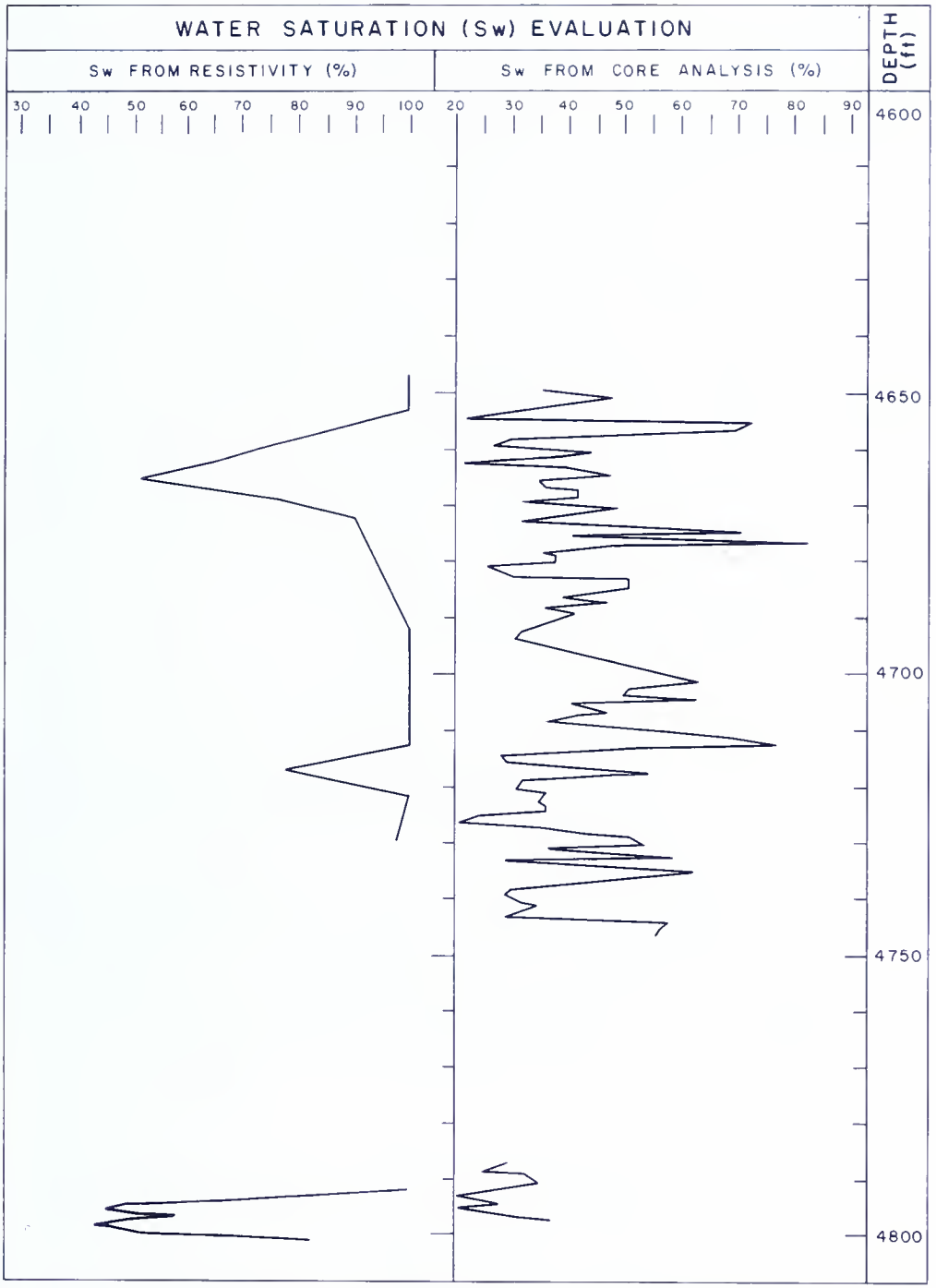


Figure 44. Core-derived and log-derived water saturations in the Creacraft well, Athens field.

significance in log evaluation because the electrical properties of the bound layer may differ from those of the bulk formation water, and consequently, reservoir resistivity as measured by electrical logs is decreased. This is particularly true of induction logs (Wescott, 1983).

The significance of water saturations in the Medina sandstones is unclear. Because of the flow characteristics of these tight formations, the relative importance of water saturation may be less than in more porous and permeable clastic reservoirs. Actual water saturations in the sandstones of the Creacraft core range from 22.2 percent to 73.0 percent, and the average water saturation is 40 percent. The irreducible water saturation is relatively large, a fact that is not surprising inasmuch as irreducible water saturation is controlled by the proportion of very small pores present in a reservoir. The highest irreducible water saturations are associated with the microporosity of the authigenic clay minerals. Because of the high irreducible water saturations, the reservoir sandstones have very long gas-to-water transition zones, and a gas/water contact is difficult to define. Critical water saturation is also high. Production data are consistent with these observations. Water production from the Creacraft well is minimal. For example, in 1981 the well was on line for 290 days and produced 19,474 Mcf of gas and only 261 barrels of water. For the month that it was on line in 1982, the Creacraft well produced 1,000 Mcf of gas and 9 barrels of water.

Kukal and others (1983, p. 19) have suggested an alternate approach to water-resistivity analysis of a formation:

> Sometimes the invasion characteristics of tight sands can be used to the advantage of the log analyst. If a formation is totally uninvaded, the density/neutron determined "invaded zone" saturation ($S_{xo}$) is actually $S_w$. This $R_t$-independent $S_w$ can then be combined with $R_t$ and porosity in conventional saturation equations to calculate $R_w$. Although this new $R_w$ technique has not been well documented, it has been discussed in general, and has been applied with success in geologic analysis and formation evaluation of tight sand sequences.

# EXPLORATION AND EXPLOITATION SIGNIFICANCE OF THE DEPOSITIONAL AND DIAGENETIC HISTORIES OF THE MEDINA GROUP SANDSTONES

## GRIMSBY SANDSTONE—FLUVIAL FACIES

In the Athens field, rapid vertical and lateral changes in the Grimsby Sandstone help explain one of the early problems with development of the reservoir, that is, the erratic distribution of more porous sandstones. The most porous sandstones are those of the braided fluvial channels (facies 2). The fluvial sandstones attain a net thickness of up to 60 feet (18 m) and form a northwest-trending unit across the field area. The channel geometry is straight to slightly sinuous, and the isolith map (Figure 11) shows that the reservoirs form a broad, continuous belt across the field area. The area of reservoir sand development consists of multilateral channel fills. In braided channels, bed accretion dominates the sediment infill so that the Medina channel fill is mainly sandstone. The cross-sectional geometry of the fluvial

sandstones (Figure 20) reveals a high width-to-depth ratio, which indicates deposition on basal scour surfaces of low to moderate relief. Multilateral channel fills volumetrically exceeded the muddy overbank deposits. All of these features suggest that the sandstones, as originally deposited, contained very few barriers to fluid flow and would have made relatively poor stratigraphic traps. These internal flow characteristics, however, played a major role in the later diagenetic modification of the reservoirs.

The amount of secondary porosity developed in the reservoir sandstones was controlled by two factors: (1) the amount of fluid moving through the reservoir prior to hydrocarbon accumulation; and (2) the amount of labile constituents present in the sandstones that could be dissolved to create secondary voids as the fluids passed through. Horizontal permeability parallels the direction of inclination in strata; the steeper the dips of the foresets, the weaker the horizontal vector of permeability (Pettijohn and others, 1972, p. 525). Therefore, in the fluvial Medina reservoirs, porosities are highest (6.0 to 7.3 percent) in the medium-grained sublitharenites that are trough cross-stratified. Internal foreset dips are not very steep; thus fluid flows were not hindered significantly. Dissolution of the sideritic lithic grains resulted in large (0.2 to 1.5 mm) secondary voids. Where basal lags of lithic grains are concentrated at the bases of trough cross-stratified fining-upward sequences, many of the constituent rock fragments were in grain-to-grain contact, and the dissolution of adjacent components resulted in the development of oversized intergranular voids. Intermediate porosities (4.0 to 6.0 percent) occur within the trough and low-angle cross-stratified subarkoses and quartz arenites. Moldic secondary porosity is the dominant void type and formed through the dissolution of feldspar and calcite that replaced feldspar.

The lowest effective porosities (2.1 to 4.0 percent) occur within the tabular cross-stratified subarkoses, and in sublitharenites where the trough cross-stratified sets have internal foresets with steep dips. The porosity in these intervals is also due to the dissolution of feldspar and lithic grains. Fluid movement into these sandstones was less effective in producing secondary porosity because of the less efficient flow characteristics of these bedding types.

Porosities are ineffective in the ripple cross-laminated, flaser- and lenticular-bedded intervals. The fine grain size and abundant laminations combine to cause low permeability, making these structures barriers to flow. Permeabilities in the fluvial sandstones range from 0.2 to less than 0.1 mD and follow the porosity trends, relative to the stratification.

## GRIMSBY SANDSTONE—LITTORAL FACIES

Littoral sandstones in the Athens field are not as porous as the fluvial sandstones, but they do contribute to production. Porosities in the littoral sandstones range from 1.6 to 5.8 percent. Relationships among lateral sand-

stone bodies in this facies are complex. Barrier-bar deposits can be traced for only short distances because they are interrupted regularly by tidal-inlet fill sequences (Figure 20). Littoral deposits in the Athens field attain a maximum thickness of 40 feet (12.2 m) and form a linear sand trend which parallels the depositional strike. Tidal-inlet fill sequences occur as multistory channel fills which are slightly subordinate to the barrier and back-barrier deposits in which they are encased. The channel fills are composed of a variety of fining-upward sequences which consist of sandstone, siltstone, and mudstone. Both bed and bank accretion deposits are preserved in the sediment infill. The tidal-channel infill deposits form thicker pods within the linear trend of the barrier-bar deposits. Where the bars are preserved, they exist as thick, uniform bodies of clean sandstone.

The reservoir quality of the littoral sandstones in the Athens field is controlled, as in the fluvial sandstone, by the internal flow characteristics of the original sediment. The initial porosities and permeabilities of the sandstones were very high; porosities were probably on the order of 41 to 43 percent and permeabilities ranged from 29,000 to 119,000 mD (Beard and Weyl, 1973). Planar and low-angle cross-stratified sandstones of the basal channel fills and upper shoreface would have conducted the highest fluid flows. Flows would have been somewhat lower in the tabular cross-stratified beds of the inlet fills due to the steep inclination of the internal foresets. Flows would have been lowest in the rippled sandstones and sands that had numerous reactivation surfaces. The clean quartzose sands of the high-energy littoral deposits had an abundant number of sites for the nucleation of quartz overgrowths. Calcite cements also precipitated early. The sandstones were thus cemented very tightly early in their burial history. The remaining permeability of the sandstones, although reduced, was still related to the original fabric and bedding of the rock. Fluids capable of dissolving labile constituents flowed preferentially through the planar and low-angle cross-stratified sandstones. The development of secondary porosity was hindered by the lower percentage of chemically unstable constituents and cement in these mineralogically mature and tightly silica cemented sandstones. Porosity is primarily moldic and secondary intergranular. Moldic pores formed through the dissolution of feldspars and mud chips. Secondary intergranular porosity developed through dissolution of calcite cement.

Littoral sandstones of the Grimsby Sandstone in the Geneva field have porosities that range from 5.1 to 9.0 percent. The porosity is essentially fabric-selective interlaminar. The interlaminar pores are extremely choked and extensively filled with authigenic illite, and porosities are ineffective below 8.0 percent (Figure 42). The original sandstones were sufficiently permeable to conduct moderate amounts of silica-bearing waters from which quartz overgrowths precipitated. Through-flow volumes were not nearly as large, however, as those reported for the littoral deposits from the Athens field. This was due to the more restricted flow characteristics of the

tabular cross-stratified and ripple cross-laminated sands, characterized by steep internal foreset dips, fine grain size, and numerous laminations. Cementation in these sandstones was dominated by reactions within the increasingly stagnant pore fluids which became connate with time.

Anhydrite and calcite cements precipitated. Where anhydrite precipitated, further diagenetic reactions essentially ceased. Where calcite precipitated, dolomite later formed during deep burial. Although littoral sand bodies in the Geneva field form continuous, linear bar-shaped sandstone bodies, they make poor reservoirs because migrating fluids capable of dissolving labile constituents only flowed with difficulty through these sandstones. The slow rates of flow through relatively more permeable laminae resulted in secondary porosity development followed by the neoformation of authigenic clay. Flow rates were not rapid enough to conduct the increasing amounts of dissolved ions out of the newly formed secondary voids before critical saturations were reached and diagenetic clays began to precipitate.

## CABOT HEAD AND WHIRLPOOL SANDSTONES—SUBLITTORAL FACIES

Sublittoral facies of the Cabot Head and Whirlpool sandstones in both fields are similar in character to the littoral Grimsby sandstones. In the Cabot Head sandstones in the Athens field, moldic secondary pores formed at the top of the coarsening-upward sequence through the partial dissolution of mud chips and glauconite grains. In the Whirlpool sandstones in the Athens field, porosity is very low and restricted to small moldic pores that formed through feldspar dissolution. In the Geneva field, the fabric-selective interlaminar porosity of the Whirlpool is identical to that of the Grimsby.

## ACCUMULATION AND ENTRAPMENT OF NATURAL GAS

In the Athens and Geneva fields, the absence of a water drive (depletion-type reservoirs; see Tables 1 and 2) permits the assumption that the reservoirs are sealed below the gas columns (Wilson, 1977). The sandstones do not pinch out updip. Updip reservoir limits appear to be defined by a loss of gas-filled porosity; that is, updip Medina sandstones produce small amounts of water and no gas. The gas-water interface is thus tilted as a result of the present-day regional southeasterly dip. Weeks (1958) pointed out that the interfaces between hydrocarbons and water tend to maintain their attitude even when later tectonic adjustments tilt the interfaces. Tilted hydrocarbon-water contacts are thought to be paleohydrodynamic phenomena (Wilson, 1977).

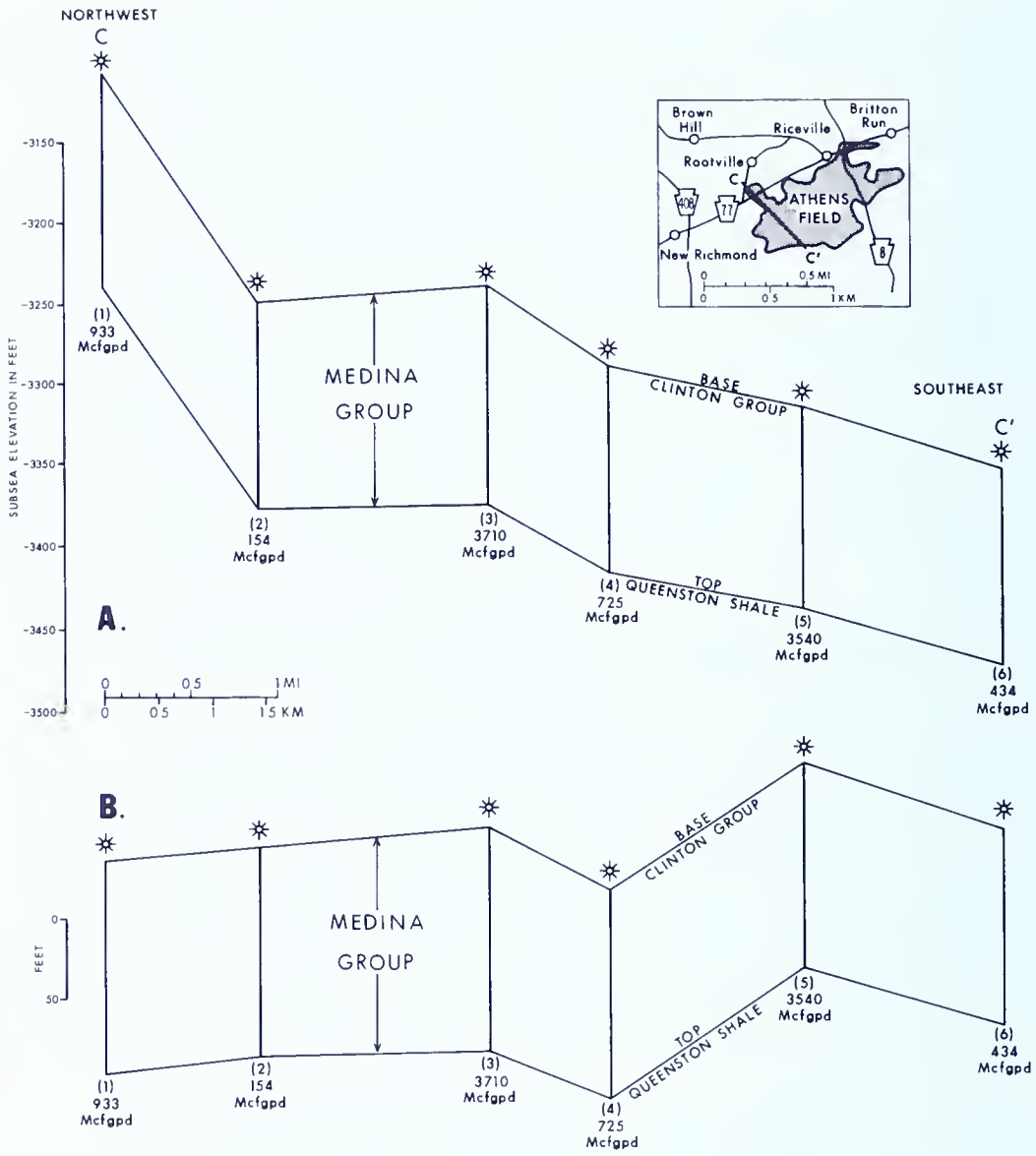


Figure 45. Present-day (A) and pre-tilt (B) structural cross sections of the Medina Group in the Athens field. Inset map shows the location of the structure section C-C'.

The gas accumulations in the Athens and Geneva fields are associated with structural noses (Figure 1). The association of structural noses and Medina gas production has been noticed by other investigators (Kelley, 1966; Kelley and McGlade, 1969). Kelley and McGlade (1969) demonstrated that structural nosing of Medina strata in the Pierce pool, Conneaut field, in Erie County results from a late southeasterly tilting of low-relief paleostructures on the northwestern flank of the Appalachian basin. Figure 45 illustrates that this is also the case in the Athens field. Note that the largest

initial open flows are associated with the wells that were drilled on the highest parts of the paleostructures. *In this report, it was shown that much of the secondary porosity in the Medina sandstones was subsequently plugged by late diagenetic cements, principally hematite and clays.* If gas was entrapped in the paleohighs before cementation and destruction of the secondary voids, the pores may have been preserved inasmuch as hydrocarbon emplacement inhibits further diagenesis (Heald, 1982). Cementation would have progressed in the water-bearing portion of the sandstone. Thus the gas accumulation would have been sealed in by diagenesis. Later uplift and development of a regional southeasterly dip obscured the earlier structures. During uplift, the gas could not escape updip through *tertiary migration* because of the diagenetic sealing of the hydrocarbons by cements which precipitated below the gas-water contact before tilt-out. Regional uplift and development of a southeasterly dip in this region occurred during the Late Paleozoic to Mesozoic (Tillman and Barnes, 1983). The generation and migration of hydrocarbons must have occurred before this time. Figure 46 shows the burial history of the Medina Group in the study area using compacted stratigraphic thicknesses of the strata. Diagenetic events are also indicated. The curve suggests that hydrocarbon generation and migration occurred just before tilt-out of the strata.

## POTENTIAL RESERVOIR PROBLEMS

The various diagenetic minerals identified in the Medina Group sandstones have a major influence on reservoir quality (Davies, 1979). *The low permeabilities of the reservoirs are due to the extensive amount of cementation that the sandstones have experienced. Authigenic clays substantially have reduced whatever effective permeabilities remained after cementation. Water saturation is particularly sensitive to the relative abundance of authigenic clays (Wilson and Pittman, 1977). The introduction of drilling and stimulation fluids can have a significant effect on these clays and results in either enhanced reservoir quality or reservoir damage.*

For a typical Medina sandstone reservoir examined in this study, the pores are lined with iron-rich chlorite, mixed-layer chlorite/illite, and illite. Minor amounts of corrensite may be present. Pore fills and replacement products composed of iron-rich chlorite, illite, and corrensite are present. Locally, the pores are filled with hematite, calcian dolomite, and anhydrite. Minor amounts of calcite are present. *The Medina sandstones have two principal engineering problems: (1) acid sensitivity (chlorite, hematite, and dolomite); and (2) migration of fines (illite). The possibility of a minor swelling-clay problem exists in zones that contain the corrensite and illite/chlorite mixed-layer clays.*

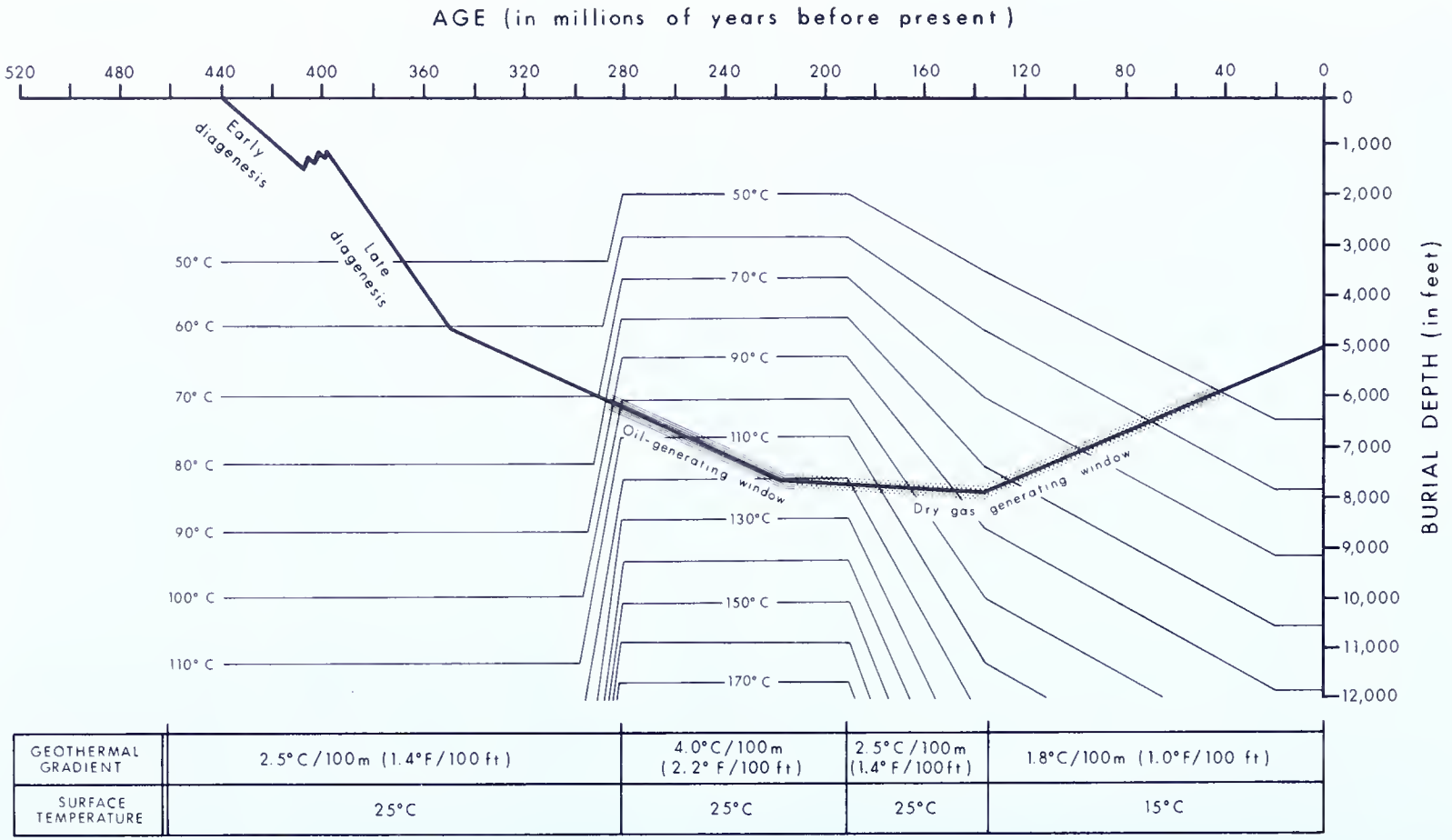


Figure 46. Burial history of the Medina Group in the vicinity of the Athens and Geneva fields.

## CHLORITE

The authigenic chlorite in the Medina Group sandstones contains high amounts of iron, and is extremely sensitive to acid and to oxygenated waters. *The chlorite dissolves readily in dilute HCl (hydrochloric acid), and the iron that is released during dissolution will reprecipitate as a gelatinous ferric hydroxide when the acid is spent (Davies, 1979). The ferric hydroxide occurs as large crystals which are bigger than the pore throats and cannot pass through them.*

## ILLITE

There are two problems associated with authigenic illite. *Illite occurs in the Medina sandstones as long, hairy laths. These laths reduce the permeability of the sandstones considerably. In the presence of fresh water, the illite fibers will clump together and further reduce permeability. They may also break off during production and migrate to the pore throats, where they act as a flow-blocking "valve." Illite also creates large volumes of microporosity. This micropore network binds waters to the host grains, which results in high, irreducible water saturations.*

## MIXED–LAYER CLAYS

This category includes the mixed-layer chlorite/illite and corrensite clays that are present in the sandstones. *These clays combine the reservoir problems described above for illite and chlorite: (1) the clays are extremely water sensitive; (2) the clays are acid sensitive; (3) the clay linings may break and migrate during swelling; and (4) the clay structure can cause the pore system to have a very high ratio of surface area to volume.* The latter yields high irreducible and critical water saturations, which can allow a well to produce water-free gas in the presence of high water saturations. If this fact is not considered, *potentially commercial wells may be plugged and abandoned without adequate testing because the log-derived water saturations were considered too high and volumetric reserves appeared too low.*

## COMPLETION RECOMMENDATIONS

Hall (1981) summarized the typical hydraulic fracturing procedure for Medina Group wells in northwestern Pennsylvania:

| *Procedure* | *Materials* |
|---|---|
| 1. Break down formation and open all perforations. | Use 500 gallons of 15 percent HCl with 1 gallon of inhibitor. Perforation balls should be used to open all perforations. |
| 2. Pump pad at 30 to 40 bpm (barrels per minute). | Use 50 to 165 barrels of gelled water with approximately 130 scf (standard cubic feet) of nitrogen per barrel of water. |
| 3. Pump proppant at 30 to 40 bpm. | Use 500 to 1,200 barrels of gelled water containing 1–1/2 to 3 pounds per gallon of sand and approximately 130 scf nitrogen per barrel of water. |
| 4. Pump flush at 30 to 40 bpm. | Use 75 to 100 barrels of water without additives. |
| 5. Shut-in then flow back to tanks. | |

The quantity of fluid used varies with the operator, well location, depth and spacing, and with the thickness and quality of the pay zone (Hall, 1981).

This study indicates that the Medina sandstones are acid sensitive. The routine use of acid breakdown (15 percent HCl) probably should be avoided in these sandstones. Iron-control additives are utilized, but weaker acids (5 to 7.5 percent HCl) together with the appropriate *iron-* and calcium-*chelating* agents are more likely to prevent formation damage due to incorrect acidization, provided the acid is removed from the well before it is spent (Davies, 1979).

The formation is water sensitive. Swelling problems can be avoided through the use of a 3 percent potassium chloride solution or an oil-based solution in fracturing fluids. The problem of migrating fines can be avoided through the use of a commercial clay-stabilizing agent early in the well completion program.

Dolomite cements in the Geneva field are high in calcium. The use of HF (hydrofluoric acid) should be avoided. Indiscriminate use of HF may result in the precipitation of insoluble calcium fluoride around the well bore.

## SUMMARY, CONCLUSIONS, AND RECOMMENDATIONS

The results of this investigation suggest the following conclusions concerning the origin and nature of the Medina Group reservoir sandstones in the Athens and Geneva fields:

1. Medina Group sandstones of the study area were deposited in a variety of shelf, paralic, and deltaic environments.

2. Sandstones of the Grimsby Sandstone can be divided into three facies. Facies 1 sandstones are composed of argillaceous, hematitic to sideritic, very fine to fine-grained nonreservoir sandstones (quartz and arkosic wackes), which were deposited as tidal-flat, tidal-creek, and lagoonal sediments. Facies 2 sandstones consist of medium-grained subarkoses and sublitharenites, and minor quartz arenite, which were deposited in braided fluvial channels. Fluvial sands were sometimes reworked by littoral processes. Facies 3 quartz arenites and sublitharenites represent littoral deposits that were cut by the fluvial channels.

3. Sandstones within the Cabot Head Shale (facies 4 sandstones) originated as offshore bars that were worked by a combination of tidal and storm-generated currents.

4. The Whirlpool Sandstone (facies 5) originated as a sublittoral sheet sandstone.

5. Braided fluvial sandstones are composed of elongate, multilateral sand bodies which trend perpendicular to depositional strike. They form excellent reservoirs in the study area.

6. Littoral and sublittoral sand bodies vary in geometry. Littoral deposits of the Grimsby in the Athens field formed primarily as tidal deltas and inlet fills. They form discontinuous to slightly continuous pods. Littoral deposits of Grimsby Sandstone in the Geneva field form more laterally continuous bar-type sand bodies. Sublittoral sandstones within the Cabot Head Shale form narrow, long and continuous sandstone bodies that trend perpendicular to depositional strike. Sublittoral sandstones of the Whirlpool Sandstone are characterized by a widespread sheet geometry. Littoral and sublittoral sandstones in the study area are fair to poor reservoirs.

7. Porosity in these sandstones is primarily of secondary dissolution origin. Individual pores range from large, irregularly shaped voids that are interconnected through very small pore throats to moldic pores of mean grain size dimensions that are isolated and not interconnected.

8. Locations of the highest porosity sandstones are controlled by both the original depositional environment and diagenesis. Both of these geological factors must be considered in exploitation programs.

9. Structure plays a subtle role in the geology of the Athens and Geneva fields. Gas accumulation occurred in structural noses which represent mild paleohighs. Mineral-water diagenetic reactions continued below the gas-water contact and effectively sealed the hydrocarbons in. This prevented the escape of the gases through tertiary migration during regional uplift and development of southeasterly dip during the Late Paleozoic to Mesozoic.

10. Geophysical-log signatures of the Medina Group sandstones are affected by the detrital and diagenetic mineralogy of the sandstone reservoirs. The gas effect on neutron-density cross plots is cancelled in the shaly intervals, and log-derived water saturation values are often excessively high due to the conductivity of the authigenic clays. The log interpretation scheme of Hilchie (1978), based on the Fertl and Hammack (1971) model, is recommended. Shaly pay zones can be identified by constructing plots of density-neutron porosity separation versus gamma-ray units. Because of the flow characteristics of these tight sands, the importance of water saturation is diminished as compared to more porous and permeable sandstone reservoirs.

11. The Medina sandstones of the study area are readily susceptible to formation damage, especially through indiscriminate use of fresh water, and hydrochloric and hydrofluoric acids. Completion efforts must be designed to be compatible with the diagenetic mineral assemblages that line the sandstone pores.

More combined petrographic and petrophysical studies, such as this one, are needed in Pennsylvania. Several recent investigations into the petrology of the Medina sandstones in other areas (Frech and Burford, 1982; Pratt, 1979) suggest that the kinds of diagenetic changes described in this report are of a regional nature. Studies of other Silurian-Devonian clastic reservoirs in the central Appalachians are beginning to reveal the widespread sig-

nificance of diagenetic modifications in hydrocarbon reservoirs (Wescott, 1982; Smosna, 1983; Sanders, 1982; Bruner and Heald, 1982). Investigations by industry have shown that the storage capacity of oil reservoirs in portions of the Bradford field is due to secondary porosity which developed through feldspar dissolution (Dixon, 1974). Laughrey and Harper (in press) recently compared the geological and engineering characteristics of the Upper Devonian and Lower Silurian tight formations in Pennsylvania. They noted that all of the available data suggest that these reservoirs "comprise a variety of quartzose, lithic, and feldspathic arenites whose diagenetic histories included formation of authigenic clays, cementation, dolomitization, solution of cements and grains (resulting in secondary porosity development), and recementation." The results of all of these studies point to the need for a total reevaluation of our approach to oil and gas exploration and exploitation in the area. Further petrographic studies of Pennsylvania's reservoirs combined with studies of the generation and migration of hydrocarbons in the basin could lead to more effective exploration, development, and optimum recovery of reserves in the Commonwealth.

## REFERENCES

Al-Shaieb, Z., and Shelton, J. W. (1981), *Migration of hydrocarbons and secondary porosity in sandstones*, American Association of Petroleum Geologists Bulletin, v. 65, p. 2433–2436.

Allen, J. R. L. (1965), *Fining upwards cycles in alluvial successions*, Geological Journal, v. 4, p. 229–246.

Almon, W. R. (1979), *A geologic appreciation of shaly sands*, Society of Professional Well Log Analysts, Annual Logging Symposium, 20th, Transactions, p. WW 1–14.

Ashley, G. H., and Robinson, J. F. (1922), *The oil and gas fields of Pennsylvania*, Pennsylvania Geological Survey, 4th ser., Mineral Resource Report 1, 79 p.

Beard, D. C., and Weyl, P. K. (1973), *Influence of texture on porosity and permeability of unconsolidated sand*, American Association of Petroleum Geologists Bulletin, v. 57, p. 349–369.

Berg, R. R. (1975), *Depositional environment of Upper Cretaceous Sussex sandstone, House Creek field, Wyoming*, American Association of Petroleum Geologists Bulletin, v. 59, p. 2099–2110.

Berner, R. A. (1981), *A new geochemical classification of sedimentary environments*, Journal of Sedimentary Petrology, v. 51, p. 359–365.

Berry, W. B. N., and Boucot, A. J. (1970), *Correlation of the North American Silurian rocks*, Geological Society of America Special Paper 102, 289 p.

Blatt, H. (1979), *Diagenetic processes in sandstones*, in Scholle, P. A., and Schluger, P. R., eds., *Aspects of diagenesis*, Society of Economic Paleontologists and Mineralogists Special Publication 26, p. 141–157.

Brett, C. E. (1982), *Stratigraphy and facies relationships of Silurian (Wenlockian) Rochester Shale: layer cake geology reinterpreted [abs.]*, American Association of Petroleum Geologists Bulletin, v. 66, p. 1165.

Bruner, K. R., and Heald, M. T. (1982), Petrology and diagenesis of the gas-bearing Tuscarora Sandstone, Kanawha County, West Virginia, in *The Thirteenth Annual Appalachian Petroleum Geology Symposium—Appalachian reservoirs and targets*, Morgantown, W. Va., 1982, West Virginia Geological and Economic Survey Circular 26, p. 10–11.

Campbell, C. V. (1971), *Depositional model—Upper Cretaceous Gallup beach shoreline, Ship Rock area, northwestern New Mexico*, Journal of Sedimentary Petrology, v. 41, p. 395–409.

Cate, A. S. (1961), *Stratigraphic studies of the Silurian rocks of Pennsylvania—Part 1. Stratigraphic cross sections of Lower Devonian and Silurian rocks in western Pennsylvania and adjacent areas*, Pennsylvania Geological Survey, 4th ser., Special Bulletin 10, 3 p.

Coleman, J. M. (1976), *Deltas: processes of deposition and models for exploration*, Champaign, Illinois, Continuing Education Publication Company, Inc., 102 p.

Coleman, J. M., and Prior, D. B. (1982), *Deltaic environments*, in Scholle, P. A., and Spearing, D. R., eds., *Sandstone depositional environments*, American Association of Petroleum Geologists Memoir 31, p. 139–178.

Collinson, J. D. (1978), *Alluvial sediments*, in Reading, H. G., ed., *Sedimentary environments and facies*, New York, Elsevier, p. 15–59.

Copley, D. L. (1980), *Upgrading Medina gas well production in western New York*, World Oil, v. 190, no. 5, p. 97–106.

Cotter, Edward (1982), *Tuscarora Formation in Pennsylvania*, Society of Economic Paleontologists and Mineralogists, Eastern Section, Field Trip Guidebook, 1982, 105 p.

_____ (1983), *Shelf, paralic, and fluvial environments and eustatic sea-level fluctuations in the origin of the Tuscarora Formation (Lower Silurian) of central Pennsylvania*, Journal of Sedimentary Petrology, v. 53, p. 25–49.

Curray, J. R., Emmel, F. J., and Crampton, P. J. S. (1969), *Holocene history of a strandplain, lagoonal coast, Nayarit, Mexico*, in Castanares, A. A., and Phleger, F. B., eds., *Coastal lagoons*, Symposium, Univ. Nacional Automoma, Mexico, p. 63–100.

Davies, D. K., and Ethridge, F. G. (1975), *Sandstone composition and depositional environment*, American Association of Petroleum Geologists Bulletin, v. 59, p. 239–264.

Davies, D. K. (1979), *Quality of sandstone reservoirs*, Lubbock, Texas, D. K. Davies, Inc., 51 p.

Dickinson, W. R., and Suczek, C. A. (1979), *Plate tectonics and sandstone compositions*, American Association of Petroleum Geologists Bulletin, v. 63, p. 2164–2182.

Dixon, W. H. (1974), *Reservoir geology of the Sage Farm Bradford oil field*, American Association of Petroleum Geologists Bulletin, Eastern Section, Field Trip Guidebook, p. 111–1 through 111–22.

Fertl, W. H., and Hammack, G. W. (1971), *A comparative look at water saturation computations in shaly pay sands*, Society of Professional Well Log Analysts Symposium, 1971.

Fisher, D. W. (1954), *Stratigraphy of Medinan Group, New York and Ontario*, American Association of Petroleum Geologists Bulletin, v. 38, p. 1979–1996.

Folk, R. L. (1960), *Petrography and origin of the Tuscarora, Rose Hill, and Keefer Formations, Lower and Middle Silurian of eastern West Virginia*, Journal of Sedimentary Petrology, v. 30, p. 1–58.

_____ (1968), *Petrology of sedimentary rocks*, Austin, Texas, Hemphill's, 170 p.

Frech, K. R., and Burford, A. E. (1982), *Aspects of porosity development in a tight sandstone, "Clinton" of eastern Ohio [abs.]*, American Association of Petroleum Geologists Bulletin, v. 66, p. 1168.

Friedman, G. M., and Sanders, J. E. (1978), *Principles of sedimentology*, New York, John Wiley and Sons, 792 p.

Hall, D. (1981), *Hydraulic fracturing of the Medina Sandstone in northwestern Pennsylvania*, in *Application for recommendation that certain portions of the Medina Sandstone be designated as a tight formation pursuant to the regulations of the FERC*, p. 658–659.

Harms, J. C., Southard, J. B., and Walker, R. G. (1982), *Structures and sequences in clastic rocks*, Society of Economic Paleontologists and Mineralogists Short Course 9, 249.

Harper, J. A., compiler (1981), *Oil and gas developments in Pennsylvania in 1980 with ten year review and forecast*, Pennsylvania Geological Survey, 4th ser., Progress Report 194, 97 p.

Harper, J. A., compiler (1982), *Oil and gas developments in Pennsylvania in 1981*, Pennsylvania Geological Survey, 4th ser., Progress Report 195, 116 p.

_____, compiler (1983), *Oil and gas developments in Pennsylvania in 1982*, Pennsylvania Geological Survey, 4th ser., Progress Report 196, 119 p.

Harris, A. G. (1979), *Conodont color alteration, an organo-mineral metamorphic index, and its application to Appalachian basin geology*, in Scholle, P. A., and Schluger, P. R., eds., *Aspects of diagenesis*, Society of Economic Paleontologists and Mineralogists Special Publication 26, p. 3–16.

Hayes, M. O. (1976), *Transitional-coastal depositional environments*, in Hayes, M. O., and Kana, T. W., eds., *Terrigenous clastic depositional environments*, American Association of Petroleum Geologists Bulletin Field Course, University of South Carolina, Coastal Research Division, Technical Report 11-CRD, p. 132–1111.

Hayes, J. B. (1979), *Sandstone diagenesis—the hole truth*, in Scholle, P. A., and Schluger, P. R., eds., *Aspects of diagenesis*, Society of Economic Paleontologists and Mineralogists Special Publication 26, p. 127–139.

Heald, M. T. (1982), *Effects of diagenetic changes in sandstone reservoirs*, in *The Thirteenth Annual Appalachian Petroleum Geology Symposium—Appalachian reservoirs and targets*, Morgantown, W. Va., 1982, West Virginia Geological and Economic Survey Circular 26, p. 32–33.

Heroux, Yvon, Chagnon, André, and Bertrand, Rudolf (1979), *Compilation and correlation of major thermal maturation indicators*, American Association of Petroleum Geologists Bulletin, v. 63, p. 2128–2144.

Heyman, Louis (1977), *Tully (Middle Devonian) to Queenston (Upper Ordovician) correlations in the subsurface of western Pennsylvania*, Pennsylvania Geological Survey, 4th ser., Mineral Resource Report 73, 16 p.

Hilchie, D. W. (1978), *Applied openhole log interpretation for geologists and engineers*, Golden, Colorado, D. W. Hilchie, Inc., 270 p.

Hobson, J. P., Jr., Fowler, M. L., and Beaumont, E. A. (1982), *Depositional and statistical exploration models, Upper Cretaceous offshore sandstone complex, Sussex Member, House Creek Field, Wyoming*, American Association of Petroleum Geologists Bulletin, v. 66, p. 689–707.

Hunt, J. M. (1979), *Petroleum geochemistry and geology*, San Francisco, W. H. Freeman and Company, 615 p.

Hurst, A., and Irwin, H. (1982), *Geological modelling of clay diagenesis in sandstones*, Clay Minerals, vol. 17, no. 1, p. 5–22.

Johnson, H. D. (1978), *Shallow siliciclastic seas*, in Reading, H. G., ed., *Sedimentary environments and facies*, New York, Elsevier, p. 207–258.

Johnson, D. P. (1982), *Sedimentary facies of an arid zone delta: Gascoyne Delta, western Australia*, Journal of Sedimentary Petrology, v. 52, p. 547–563.

Johnson, M. E. (1980), *Paleoecological structure in Early Silurian platform seas of the North American midcontinent*, Palaeogeography, Palaeoclimatology, Palaeoecology, v. 30, n. 1–2, p. 191–215.

Kelley, D. R. (1966), *The Kastle Medina gas field, Crawford County*, in Lytle, W. S., and others, *Oil and gas developments in Pennsylvania in 1965*, Pennsylvania Geological Survey, 4th ser., Progress Report 172, p. 30–44.

Kelley, D. R., and McGlade, W. G. (1969), *Medina and Oriskany production along the shore of Lake Erie, Pierce Field, Erie County, Pennsylvania*, Pennsylvania Geological Survey, 4th ser., Mineral Resource Report 60, 38 p.

Klein, G. DeV. (1977), *Clastic tidal facies*, Champaign, Illinois, Continuing Education Publication Company, Inc., 149 p.

Knight, W. V. (1969), *Historical and economic geology of Lower Silurian Clinton sandstone of northeastern Ohio*, American Association of Petroleum Geologists Bulletin, v. 53, p. 1421–1452.

Krinsley, D. H. (in preparation), *Petrographic examination of sedimentary rocks in the SEM using backscattered electron detectors.*

Krinsley, D. H., Donahue, J., and Laughrey, C. D. (in preparation), *Application of backscattered electron microscopy in sandstone reservoir characterization.*

Krinsley, D. H., Pye, K., and Kearsley, A. T. (1983), *Application of backscattered electron microscopy in shale petrology*, Geological Magazine, v. 120, no. 2, p. 109–208.

Kukal, G. C., Biddison, C. L., Hill, R. E., and others (1983), *Critical problems hindering accurate log interpretation of tight gas sand reservoirs*, in *Proceedings of the Society of Petroleum Engineers/Department of Energy Joint Symposium on Low Permeability Gas Reservoirs*, Denver, Colorado, 1983, p. 181–190.

Laughrey, C. D., and Donahue, J. (1982), *Diagenetic trends within the Tuscarora-Medina sequence in the northern Appalachians*, in proceedings of the Appalachian Basin Industrial Association, fall meeting, Blacksburg, Virginia, Proceedings, unpaginated [13 p.].

Laughrey, C. D., and Harper, J. A. (in press), *Comparisons of Upper Devonian and Lower Silurian "tight" formations in Pennsylvania: geological and engineering characteristics*, to be published in an American Association of Petroleum Geologists Memoir on North American tight gas sands.

Lytle, W. S., Heyman, Louis, Kelley, D. R., and Wagner, W. R. (1971), *Future petroleum potential of western and central Pennsylvania*, in Cram, I. H., ed., *Future petroleum provinces of the United States—their geology and potential*, American Association of Petroleum Geologists Memoir 15, v. 2, p. 1232–1242.

Martini, I. P. (1971), *Regional analysis of sedimentology of Medina Formation (Silurian), Ontario and New York*, American Association of Petroleum Geologists Bulletin, v. 55, p. 1249–1261.

Maurath, G., and Eckstein, Y. (1981), *Heat flow and heat production in northwestern Pennsylvania*, in *Geothermal energy, the international success story*, Transactions, Geothermal Resources Council, v. 5, p. 103–106.

McBride, E. F. (1977), *Secondary porosity—importance in sandstone reservoirs in Texas*, Transactions, Gulf Coast Association of Geological Societies, v. 27, p. 121–122.

Metzger, S. L. (1982), *Subsurface paleoenvironmental analysis of gas-producing Medina Group (Lower Silurian), Chautauqua County, New York [abs.]*, American Association of Petroleum Geologists Bulletin, v. 66, p. 606.

Miall, A. D. (1977), *A review of the braided river depositional environment*, Earth Science Review, v. 13, p. 1–62.

Mou, D. C., and Brenner, R. L. (1982), *Control of reservoir properties of Tensleep Sandstone by depositional and diagenetic facies: Lost Soldier field, Wyoming*, Journal of Sedimentary Petrology, v. 52, p. 367–381.

Multer, H. G. (1963), *Geology of the Silurian producing zones in the Moreland oil pool, Wayne County, northeastern Ohio*, Ohio Division of Geological Survey Report of Investigations 46, 48 p.

Nelson, R. A. (1981), *Significance of fracture sets associated with stylolite zones*, American Association of Petroleum Geologists Bulletin, v. 65, p. 2417–2425.

Overbey, W. K., and Henniger, B. R. (1971), *History, development, and geology of oil fields in Hocking and Perry Counties, Ohio*, American Association of Petroleum Geologists Bulletin, v. 55, p. 183–203.

Pees, S. T. (1983a), *Model area describes NW Pennsylvania's Medina play*, Oil and Gas Journal, v. 81, no. 21, p. 55–60.

_____ (1983b), *Remote sensing can aid finding efforts*, Northeast Oil Reporter, v. 3, no. 6, p. 33–36.

Pettijohn, F. J., Potter, P. E., and Siever, R. (1972), *Sand and sandstones*, New York, Springer-Verlag, 618 p.

Piotrowski, R. G. (1981), *Geology and natural gas production of the Lower Silurian Medina Group and equivalent rock units in Pennsylvania*, Pennsylvania Geological Survey, 4th ser., Mineral Resource Report 82, 21 p.

Pittman, E. D. (1972), *Diagenesis of quartz in sandstones as revealed by scanning electron microscopy*, Journal of Sedimentary Petrology, v. 42, p. 507–519.

_____ (1979), *Porosity, diagenesis and productive capability of sandstone reservoirs*, in Scholle, P. A., and Schluger, P. R., eds., *Aspects of diagenesis*, Society of Economic Paleontologists and Mineralogists Special Publication 26, p. 3–16.

Potter, P. E. (1967), *Sand bodies and sedimentary environments: a review*, American Association of Petroleum Geologists Bulletin, v. 51, p. 337–365.

Pratt, S. (1979), *Clay mineral authigenesis in the Medina Group sandstones*, unpublished M.S. thesis, State University of New York at Binghamton.

Radke, B. M., and Mathis, R. L. (1980), *On the formation and occurrence of saddle dolomite*, Journal of Sedimentary Petrology, v. 50, p. 1149–1168.

Reading, H. G., editor (1978), *Sedimentary environments and facies*, New York, Elsevier, 557 p.

Reineck, H. E., and Singh, I. B. (1973), *Depositional sedimentary environments*, New York, Springer-Verlag, 439 p.

Reinson, G. E. (in press), *Longitudinal and transverse bedforms on a large tidal delta, Gulf of St. Lawrence, Canada*, Marine Geology.

Rodgers, M. R. (1981), *Geological and geochemical investigations along the northwestern extension of the Tyrone-Mt. Union lineament in the Plateau province of northwestern Pennsylvania*, Unpublished M.S. thesis, University of Pittsburgh, 178 p.

Rosepiler, M. J. (1981), *Calculation and significance of water saturations in low porosity shaly gas sands*, Oil and Gas Journal, v. 79, no. 28, p. 180–187.

Sanders, A. W. (1982), *Oriskany matrix porosity in southwest-central Pennsylvania*, in *The Thirteenth Annual Appalachian Petroleum Geology Symposium—Appalachian reservoirs and targets*, Morgantown, W. Va., 1982, West Virginia Geological and Economic Survey Circular 26, p. 50.

Schmidt, V., and McDonald, D. A. (1979), *Texture and recognition of secondary porosity in sandstones*, in Scholle, P. A., and Schluger, P. R., eds., *Aspects of diagenesis*, Society of Economic Paleontologists and Mineralogists Special Publication 26, p. 209–225.

Seilacher, Adolf (1978), *Use of trace fossil assemblages for recognizing depositional environments*, in Basan, P. B., ed., *Trace fossil concepts*, Society of Economic Paleontologists and Mineralogists Short Course 5, p. 185–201.

Selley, R. C. (1981), *Concepts and methods of subsurface facies analysis*, American Association of Petroleum Geologists Educational Course Notes, Ser. 9, 86 p.

Shinn, E. A. (1983), *Birdseyes, fenestrae, shrinkage pores, and loferites: a reevaluation*, Journal of Sedimentary Petrology, v. 53, p. 619–628.

Siever, R. (1983), *Burial history and diagenetic reaction kinetics*, American Association of Petroleum Geologists Bulletin, v. 67, p 684–691.

Sisler, J. D., Ashley, G. H., Moyer, F. T., and Hickok, W. O., IV (1933), *Contributions to the oil and gas geology of western Pennsylvania*, Pennsylvania Geological Survey, 4th ser., Mineral Resource Report 19, 94 p.

Smosna, R. (1983), *Diagenetic history of the Silurian Keefer Sandstone in West Virginia and Kentucky*, Journal of Sedimentary Petrology, v. 53, p. 1319–1329.

Swift, D. J. P., Parker, G., Lanfredi, N. W., and others (1978), *Shoreface-connected sand ridges on American and European shelves; a comparison*, Estuarine Coastal Marine Science, v. 7, no. 3, p. 257–273.

Tillman, N. (1982), *Fractured reservoirs and targets of the Appalachian basin and thrust belt [abs.]*, in *The Thirteenth Annual Appalachian Petroleum Geology Symposium—Appalachian reservoirs and targets*, Morgantown, W. Va., 1982, West Virginia Geological and Economic Survey Circular 26, p. 54–57.

Tillman, J. E., and Barnes, H. L. (1983), *Deciphering fracturing and fluid migration histories in northern Appalachian basin*, American Association of Petroleum Geologists Bulletin, v. 67, p. 692–705.

Tissot, B. P., and Welte, D. H. (1978), *Petroleum formation and occurrence—A new approach to oil and gas exploration*, New York, Springer-Verlag, 538 p.

Walker, T. R. (1967), *Formation of red beds in modern and ancient deserts*, Geological Society of America Bulletin, v. 78, p. 353–368.

Waples, E. W. (1980), *Time and temperature in petroleum formation: application of Lopatin's method to petroleum exploration*, American Association of Petroleum Geologists Bulletin, v. 64, p. 916–926.

Wardlaw, N. C., and Cassan, J. P. (1978), *Estimation of recovery efficiency by visual observation of pore systems in reservoir rocks*, Bulletin of Canadian Petroleum Geology, v. 26, p. 572–585.

Weaver, C. C., and Beck, K. C. (1971), *Clay-water diagenesis during burial: How mud becomes gneiss*, Geological Society of America Special Paper 134, 96 p.

Weeks, L. G. (1958), *Habitat of oil and some factors that control it*, in Weeks, L. G., ed., *Habitat of oil*, American Association of Petroleum Geologists, p. 1–61.

Wescott, W. A. (1982), *Nature of porosity in Tuscarora sandstone (Lower Silurian) in the Appalachian basin*, Oil and Gas Journal, v. 80, no. 34, p. 159–173.

_____ (1983), *Diagenesis of Cotton Valley sandstone (Upper Jurassic), East Texas: implications for tight gas formation pay recognition*, American Association of Petroleum Geologists Bulletin, v. 67, p. 1002–1013.

Wheeler, R. L. (1980), *Cross-strike structural discontinuities, possible exploration tool for natural gas in Appalachian Overthrust Belt*, American Association of Petroleum Geologists Bulletin, v. 64, p. 2166–2178.

Wilson, H. H. (1977), *"Frozen-in" hydrocarbon accumulations or diagenetic traps—exploration targets*, American Association of Petroleum Geologists Bulletin, v. 61, p. 483–491.

Wilson, M. D., and Pittman, E. D. (1977), *Authigenic clays in sandstones: recognition and influence on reservoir properties and paleoenvironmental analysis*, Journal of Sedimentary Petrology, v. 47, p. 3–31.

Wilson, M. D. (1982), *Origins of clays controlling permeability in tight gas sands*, Journal of Petroleum Technology, Dec. 1982, p. 2871–2876.

Yeakel, L. S., Jr. (1962), *Tuscarora, Juniata, and Bald Eagle paleocurrents and paleogeography in the central Appalachians*, Geological Society of America Bulletin, v. 73, p. 1515–1540.

Ziegler, A. M., Hansen, K. S., Johnson, M. E., and others (1977), *Silurian continental distributions, paleogeography, climatology, and biogeography*, Tectonophysics, v. 40, p. 13–51.

# GLOSSARY

*Arenite.* A sandstone having less than 15 percent matrix (Pettijohn and others, 1972).

*Authigenic mineral.* "A mineral that has grown in place subsequent to the formation of the sediment or rock of which it constitutes a part" (Friedman and Sanders, 1978).

*Climbing ripples.* Ripple marks composed of slightly curved laminae lying one above the other, convex upward.

*Fabric selective.* The fabric of a sedimentary rock refers to the orientation and packing of the grains and to the nature of the boundaries between those grains. In many instances, the packing and orientation of grains in one sediment bed or laminae are more conducive to fluid flow than

the fabric characteristics of adjacent beds and laminae. When fluid flows preferentially through one fabric type relative to another in a sandstone, that flow is said to be fabric selective.

*Flaser bedding.* Stratification consisting of alternating rippled sandstone and mudstone drapes in which the minor lithology, mudstone, forms discontinuous layers.

*Fracture porosity.* Porosity in a rock that is due solely to secondary tectonic fracturing of the rock.

*Interlaminar porosity.* A type of secondary intergranular porosity in which thin, tight (impermeable) laminae are interbedded with thin, porous laminae (Wescott, 1982).

*Intraconstituent secondary porosity.* Porosity formed through dissolution within the constituent grains of a sandstone.

*Iron chelating.* Chelating agents are chemical species capable of donating several electron pairs to a central metal ion for attachment at a particular site in a geometric structure. Chelation is the process by which the agent and a metal ion bond. Sodium salts such as EDTA (ethylenediaminetetraacetic acid) are useful in controlling iron precipitation from solution. Iron (II) in the presence of EDTA is converted to $[Fe(EDTA)]^{2-}$ and the concentration of $Fe^{2+}$ is held small enough that iron will not precipitate, even as hydroxide if a base is later added to the water.

*Lenticular bedding.* Bedding that is lens shaped.

*Magmatic-arc and suture-belt provenances.* Magmatic-arc provenances are those in which sedimentary detritus is eroded from orogens that form where a plate of oceanic lithosphere collides with, and is subducted beneath, another oceanic or continental plate. Suture-belt provenances are those in which sedimentary detritus is eroded from orogens that form where continental margins are juxtaposed.

*Microporosity.* Porosity in which the pores have pore-aperture radii of less than 0.5 micron.

*Moldic secondary pores.* Pores formed through the dissolution of soluble sedimentary grains. The pores are isolated and generally retain the shape of the original grain.

*Oxygen scavenger.* An iron-control additive for fluids used in hydrofracturing wells. The iron-control additive helps to remove free oxygen and reduce ferric acid that may be contacted to ferrous iron. This improves the compatibility of the hydrofracturing fluid and formation fluid and helps in the avoidance of well damage.

*Poikilotopic.* A textural term denoting a fabric in sedimentary rocks in which smaller grains or crystals occur within a larger crystal of another mineral; for example, sand grains in a single cement crystal of calcite.

*Pore-to-pore-throat coordination.* A measure of the number of pore throats that connect with each pore.

*Pore-to-pore-throat ratio.* The ratio of the diameter of a pore to the diameter of the pore throats.

*Quartz arenites.* Sandstones composed of 95 percent or more detrital quartz grains and containing less than 15 percent matrix.

*Reactivation surfaces.* Internal discontinuities in the pattern and attitude of foreset laminae within stratified sandstones.

*Relict primary porosity.* Remaining primary intergranular voids in a sandstone that has undergone extensive diagenetic reduction in porosity.

*Secondary intergranular porosity.* Intergranular porosity that develops through the dissolution of sedimentary grains and authigenic cement.

*Subarkose.* A sandstone containing 5 to 25 percent unstable components, of which feldspar exceeds rock particles.

*Sublitharenite.* A sandstone containing 5 to 25 percent rock fragments, 0 to 10 percent feldspar, and 65 to 95 percent quartz. The rock contains less than 15 percent matrix.

*Synaerial shrinkage cracks.* Shrinkage cracks that form subaqueously through synaeresis in fine-grained sediments. Synaeresis is the spontaneous liberation of liquid accompanied by the shrinkage of a gel. Synaerial shrinkage cracks are sometimes mistaken for mudcracks, which form subaerially through desiccation.

*Syntaxial.* Pertaining to overgrowths that are in optical continuity with their host grain.

*Tertiary migration.* The movement of an oil or gas accumulation out of or to a different part of the reservoir rock.

*Wackes.* Sandstones containing 15 percent or more argillaceous matrix materials (Pettijohn and others, 1972).

*Water sensitive.* Pertaining to the swelling behavior of particular clay minerals in a reservoir rock when stimulation fluids are introduced into the formation. Variable amounts of water enter between unit layers, causing them to expand. Smectites are the most water-sensitive clays, and the degree of water sensitivity is generally dependent on the amount of sodium in the ion-exchange sites. Illite is a hydrated silicate that does not expand or swell in the presence of fresh water. Illite fibers, however, tend to clump together and reduce permeability in the presence of fresh water, and are, in this sense, water sensitive.

*Wavy bedding.* Continuous layers of rippled sand alternating with mud.

# APPENDICES

## APPENDIX 1. LIST OF WELLS, GEOPHYSICAL-LOG CALCULATIONS,[1] AND INITIAL OPEN FLOWS, ATHENS AND GENEVA FIELDS, CRAWFORD COUNTY, PENNSYLVANIA

*Wells Completed in the Athens Field*

| Permit number | Completion date | Average effective porosity (%) | | Net feet of effective porosity | | Water saturation (%) | | Initial potential (Mcf) |
|---|---|---|---|---|---|---|---|---|
| | | Grimsby | Whirlpool | Grimsby | Whirlpool | Grimsby | Whirlpool | |
| CRA-20462 | 12-06-74 | — | — | — | — | — | — | — |
| CRA-20559 | 12-23-78 | 6.95 | 4.60 | 36 | 10 | 43.57 | 27.83 | 7,839 |
| CRA-20560 | 1-10-79 | — | — | — | — | — | — | 3,000 |
| CRA-20566 | 1-22-79 | — | — | — | — | — | — | 830 |
| CRA-20561 | 1-30-79 | 5.57 | 4.44 | 43 | 7 | 51.11 | 49.86 | 7,898 |
| CRA-20565 | 3-01-79 | 5.82 | 5.06 | 57 | 14 | 41.31 | 36.14 | 5,700 |
| CRA-20667 | 3-18-79 | 4.81 | 4.20 | 25 | 5 | 43.97 | 35.56 | 540 |
| CRA-20574 | 3-27-79 | 6.90 | 6.25 | 37 | 12 | 75.29 | 38.33 | 240 |
| CRA-20572 | 4-05-79 | 5.38 | 4.63 | 39 | 8 | 36.54 | 67.86 | 173 |
| CRA-20564 | 4-12-79 | 6.04 | 5.86 | 51 | 11 | 31.88 | 31.92 | 398 |
| CRA-20573 | 4-13-79 | 5.20 | 4.60 | 34 | 10 | 65.90 | 62.00 | 211 |
| CRA-20575 | 4-26-79 | — | — | — | — | — | — | 2,800 |
| CRA-20576 | 5-05-79 | — | — | — | — | — | — | 6,023 |
| CRA-20579 | 5-13-79 | — | — | — | — | — | — | 398 |
| CRA-20578 | 5-20-79 | — | — | — | — | — | — | 3,780 |
| CRA-20580 | 5-27-79 | — | — | — | — | — | — | 3,180 |
| CRA-20582 | 6-09-79 | 5.60 | 4.60 | 28 | 2 | 48.60 | 32.20 | 3,364 |
| CRA-20583 | 6-19-79 | 4.90 | 4.40 | 33 | 3 | 44.00 | 20.90 | 905 |
| CRA-20589 | 7-11-79 | 5.36 | 4.30 | 39 | 5 | 37.60 | 26.10 | 1,271 |
| CRA-20581 | 7-19-79 | 6.64 | 6.35 | 32 | 8 | 39.53 | 32.75 | 651 |
| CRA-20591 | 7-27-79 | 5.00 | 5.23 | 28 | 10 | 40.66 | 36.83 | 1,165 |

| | | | | | | | | |
|---|---|---|---|---|---|---|---|---|
| CRA-20592 | 8-03-79 | 5.00 | 4.30 | 33 | 4 | 43.90 | 33.50 | 1,095 |
| CRA-20595 | 8-10-79 | 6.22 | 4.75 | 62 | 8 | 36.48 | 46.25 | 137 |
| CRA-20596 | 8-17-79 | 5.00 | 4.60 | 15 | 5 | 44.90 | 30.00 | 154 |
| CRA-20594 | 8-24-79 | — | — | — | — | — | — | 1,544 |
| CRA-20597 | 9-01-79 | 6.10 | 4.40 | 42 | 2 | 57.20 | 95.00 | 710 |
| CRA-20600 | 9-11-79 | 6.60 | 5.98 | 63 | 11 | 31.60 | 26.21 | 198 |
| CRA-20610 | 9-18-79 | 5.52 | 4.78 | 60 | 11 | 35.28 | 30.87 | 1,218 |
| CRA-20613 | 9-26-79 | 5.64 | 4.73 | 42 | 9 | 42.13 | 30.89 | 389 |
| CRA-20614 | 10-03-79 | 4.98 | 5.04 | 33 | 6 | 46.84 | 40.84 | 149 |
| CRA-20612 | 10-11-79 | 6.76 | 7.47 | 73 | 10 | 35.24 | 23.11 | 916 |
| CRA-20611 | 10-17-79 | 5.12 | 4.41 | 19 | 7 | 53.92 | 40.98 | 3,380 |
| CRA-20648 | 10-26-79 | — | — | — | — | — | — | 704 |
| CRA-20651 | 11-02-79 | 6.50 | 5.60 | 50 | 10 | — | — | 365 |
| CRA-20653 | 11-10-79 | 5.66 | 4.45 | 26 | 4 | 40.66 | 25.66 | 1,506 |
| CRA-20656 | 11-18-79 | 7.30 | 6.30 | 33 | 9 | | | 2,450 |
| CRA-20652 | 11-29-79 | 7.26 | 7.11 | 67 | 10 | 24.80 | 22.46 | 1,260 |
| CRA-20659 | 12-14-79 | — | — | — | — | — | — | 264 |
| CRA-20663 | 1-25-80 | 6.03 | 4.67 | 83 | 6 | 33.74 | 27.39 | 654 |
| CRA-20662 | 2-03-80 | 5.60 | 5.54 | 54 | 10 | 59.30 | 48.40 | 1,013 |
| CRA-20664 | 2-11-80 | 5.55 | 4.28 | 55 | 4 | 36.18 | 67.71 | 1,629 |
| CRA-20665 | 2-29-80 | 4.47 | — | 27 | — | 90.67 | — | 1,343 |
| CRA-20668 | 3-11-80 | 6.87 | 6.53 | 53 | 12 | 25.67 | 20.12 | 2,245 |
| CRA-20670 | 3-19-80 | 4.80 | 4.00 | 44 | 4 | 39.00 | 48.50 | 324 |
| CRA-20669 | 3-26-80 | 5.53 | — | 33 | — | 51.40 | — | 194 |
| CRA-20673 | 4-15-80 | 5.06 | 4.75 | 16 | 3 | 40.25 | 39.00 | 280 |
| CRA-20667 | 4-23-80 | 5.10 | — | 50 | — | 43.45 | — | 1,218 |
| CRA-20666 | 4-30-80 | 6.34 | — | 10 | — | 50.00 | — | 1,178 |
| CRA-20672 | 5-07-80 | 4.74 | 4.50 | 35 | 8 | — | — | 926 |
| CRA-20677 | 5-14-80 | 4.32 | — | 4 | — | 62.86 | — | 926 |
| CRA-20676 | 5-20-80 | 5.33 | 5.61 | 54 | 7 | 38.78 | 39.71 | 434 |
| CRA-20681 | 5-30-80 | — | — | — | — | — | — | 316 |
| CRA-20683 | 6-06-80 | — | — | — | — | — | — | 966 |
| CRA-20682 | 6-09-80 | 4.72 | 4.35 | 13 | 5 | 61.64 | 51.59 | 265 |

[1] Geophysical data are not given for wells from which logs were not available.

*Wells Completed in the Athens Field (Continued)*

| Permit number | Completion date | Average effective porosity (%) | | Net feet of effective porosity | | Water saturation (%) | | Initial potential (Mcf) |
|---|---|---|---|---|---|---|---|---|
| | | Grimsby | Whirlpool | Grimsby | Whirlpool | Grimsby | Whirlpool | |
| CRA-20686 | 6-13-80 | 4.70 | 4.60 | 66 | 3 | — | — | 3,540 |
| CRA-20678 | 6-16-80 | 6.13 | 4.71 | 18 | 2 | 57.81 | 40.50 | 3,710 |
| CRA-20684 | 6-19-80 | 5.43 | — | 21 | — | 49.50 | — | 1,178 |
| CRA-20680 | 6-25-80 | — | — | — | — | — | — | 725 |
| CRA-20679 | 6-26-80 | 5.64 | — | 1 | — | 50.91 | — | 1,629 |
| CRA-20703 | 7-02-80 | 5.79 | 4.45 | 42 | 8 | 50.10 | 64.40 | 1,547 |
| CRA-20705 | 7-03-80 | 4.69 | 4.15 | 28 | 4 | 60.50 | 60.50 | 805 |
| CRA-20706 | 7-11-80 | — | — | — | — | — | — | 4,870 |
| CRA-20734 | 7-13-80 | 7.03 | 5.50 | 26 | 10 | 34.15 | 37.80 | 725 |
| CRA-20702 | 7-19-80 | 6.00 | — | 7 | — | 61.86 | — | 1,218 |
| CRA-20733 | 7-21-80 | 5.53 | — | 40 | — | 44.56 | — | 1,013 |
| CRA-20731 | 7-26-80 | 7.40 | 5.80 | 58 | 8 | 29.00 | 24.00 | 1,424 |
| CRA-20732 | 7-27-80 | 5.58 | 4.11 | 51 | 15 | 32.06 | 28.00 | 845 |
| CRA-20729 | 8-02-80 | 5.41 | 4.30 | 46 | 10 | 44.74 | 52.00 | 412 |
| CRA-20735 | 8-03-80 | 7.00 | 4.50 | 38 | 8 | 43.94 | 52.50 | 1,739 |
| CRA-20743 | 8-08-80 | 7.68 | 5.69 | 92 | 16 | 37.24 | 35.50 | 933 |
| CRA-20787 | 8-16-80 | 6.70 | 6.00 | 18 | 16 | — | — | 311 |
| CRA-20716 | 8-24-80 | — | — | — | — | — | — | 337 |
| CRA-20797 | 8-31-80 | 8.53 | 8.60 | 38 | 10 | 38.53 | 23.00 | 381 |
| CRA-20717 | 9-09-80 | 5.60 | 4.00 | 10 | 2 | 52.75 | 74.00 | 113 |
| CRA-20715 | 9-16-80 | 5.28 | — | 24 | — | 63.63 | — | 894 |
| CRA-20704 | 9-24-80 | 4.92 | 4.10 | 11 | 5 | 42.50 | 37.00 | 1,639 |
| CRA-20785 | 10-01-80 | 7.11 | — | 28 | — | 40.21 | — | 2,144 |
| CRA-20888 | 10-09-80 | 4.46 | — | 3 | — | 57.20 | — | 31 |
| CRA-20822 | 10-17-80 | 5.83 | 4.70 | 40 | 10 | 46.45 | 50.20 | 127 |
| CRA-29786 | 11-01-80 | 5.36 | 4.90 | 20 | 2 | 33.06 | 17.44 | 5,069 |
| CRA-20884 | 11-16-80 | — | — | — | — | — | — | — |
| CRA-20682 | 12-05-80 | — | — | — | — | — | — | — |

| | | | | | | | | |
|---|---|---|---|---|---|---|---|---|
| CRA-20978 | 1-28-81 | 5.80 | 5.20 | 26 | 7 | 46.00 | 29.00 | 531 |
| CRA-21097 | 2-05-81 | 7.20 | 5.40 | 38 | 11 | 58.00 | 68.40 | 189 |
| CRA-21099 | 2-12-81 | 7.30 | 5.50 | 60 | 4 | 38.20 | 27.50 | 6,200 |
| CRA-21101 | 2-18-81 | 6.30 | 5.90 | 70 | 13 | 36.00 | 29.00 | 1,132 |
| CRA-21102 | 2-19-81 | 5.90 | 5.10 | 42 | 8 | 43.00 | 43.00 | 959 |
| CRA-21104 | 2-25-81 | 5.80 | 4.60 | 25 | 4 | 34.00 | 30.00 | |
| CRA-21109 | 2-26-81 | 5.20 | 6.20 | 47 | 10 | 45.00 | 27.00 | 933 |
| CRA-21140 | 3-03-81 | 8.20 | 7.39 | 38 | 17 | 23.04 | 16.36 | 7,583 |
| CRA-21137 | 3-16-81 | 6.00 | 6.20 | 48 | 8 | 45.00 | 50.00 | 155 |
| CRA-21138 | 4-03-81 | 5.70 | 5.70 | 46 | 11 | 31.00 | 22.00 | 440 |
| CRA-21133 | 4-11-81 | 6.52 | 5.59 | 54 | 14 | 37.80 | 23.98 | 713 |
| CRA-21144 | 4-20-81 | 5.92 | 5.49 | 50 | 11 | 42.42 | 27.07 | 1,739 |
| CRA-21142 | 4-27-81 | 7.05 | 6.43 | 53 | 8 | 55.67 | 40.11 | 746 |
| CRA-21143 | 4-27-81 | 6.83 | 5.35 | 35 | 9 | 34.04 | 22.27 | 866 |
| CRA-21139 | 5-03-81 | 6.57 | — | 42 | — | 35.62 | — | 179 |
| CRA-21132 | 5-07-81 | 5.90 | 5.70 | 42 | 13 | 43.00 | 46.00 | 402 |
| CRA-21145 | 5-13-81 | 6.40 | 5.80 | 42 | 16 | 54.00 | 35.00 | 1,550 |
| CRA-21136 | 5-18-81 | 5.80 | 5.40 | 53 | 12 | 54.00 | 36.00 | 4,421 |
| CRA-21135 | 5-25-81 | 5.10 | 4.90 | 36 | 10 | 66.00 | 37.00 | 198 |
| CRA-21215 | 6-01-81 | 5.77 | 7.62 | 52 | 10 | 36.52 | 16.81 | 0 |
| CRA-21223 | 6-07-81 | 5.49 | 6.04 | 52 | 10 | 36.64 | 23.14 | 253 |
| CRA-21224 | 6-14-81 | 7.09 | 7.08 | 70 | 15 | 44.01 | 33.41 | 4,950 |
| CRA-21252 | 6-23-81 | 5.84 | 4.50 | 37 | 4 | — | — | 603 |
| CRA-21291 | 8-10-81 | 6.41 | 6.22 | 43 | 6 | 37.58 | 21.95 | 984 |
| CRA-21353 | 8-17-81 | 6.00 | 6.55 | 49 | 14 | 21.19 | 13.94 | 823 |
| CRA-21352 | 8-23-81 | 6.38 | 4.00 | 44 | 4 | 53.50 | 56.00 | 1,067 |
| CRA-21347 | 8-29-81 | 5.72 | 5.14 | 48 | 9 | 49.32 | 28.13 | 660 |
| CRA-21383 | 9-06-81 | 7.80 | 8.40 | 30 | 11 | 42.00 | 19.00 | 5,776 |
| CRA-21392 | 9-14-81 | 6.73 | 4.76 | 53 | 7 | 38.37 | 28.02 | 4,759 |
| CRA-21351 | 9-21-81 | 5.89 | — | 37 | — | 42.91 | — | 4,953 |
| CRA-21445 | 10-11-81 | 6.26 | 5.20 | 58 | 10 | 30.48 | 29.40 | 2,058 |
| CRA-21405 | 10-15-81 | — | — | — | — | — | — | 1,307 |
| CRA-21446 | 10-17-81 | 5.81 | 4.48 | 31 | 1 | 37.18 | 27.75 | 959 |
| CRA-21444 | 12-18-81 | 9.00 | 8.20 | 46 | 14 | 34.00 | 29.00 | 1,122 |
| CRA-21553 | 3-02-82 | 6.67 | 6.82 | 82 | 14 | 28.63 | 22.36 | 1,200 |

### Wells Completed in the Athens Field (Continued)

| Permit number | Completion date | Average effective porosity (%) Grimsby | Average effective porosity (%) Whirlpool | Net feet of effective porosity Grimsby | Net feet of effective porosity Whirlpool | Water saturation (%) Grimsby | Water saturation (%) Whirlpool | Initial potential (Mcf) |
|---|---|---|---|---|---|---|---|---|
| CRA-21575 | 3-04-82 | — | — | — | — | — | — | — |
| CRA-21667 | 5-23-82 | 7.47 | 10.09 | 33 | 11 | 27.58 | 23.49 | 696 |
| CRA-21632 | 6-01-82 | — | — | — | — | — | — | 465 |
| CRA-21707 | 6-01-82 | — | — | — | — | — | — | — |
| CRA-21723 | 6-09-82 | 6.16 | 6.66 | 51 | 15 | 32.78 | 31.62 | 947 |
| CRA-21677 | 6-16-82 | 5.56 | 5.80 | 20 | 10 | 32.29 | 32.95 | 866 |
| CRA-21728 | 6-23-82 | 6.08 | 5.50 | 38 | 10 | 27.01 | 33.04 | 235 |
| CRA-21724 | 6-28-82 | 6.50 | 6.21 | 59 | 14 | 30.77 | 29.94 | 3,033 |
| CRA-21777 | 7-24-82 | 6.87 | 5.17 | 72 | 9 | 27.38 | 26.43 | 2,054 |
| CRA-21788 | 8-09-82 | 5.82 | 5.66 | 70 | 10 | 34.90 | 32.80 | 696 |
| CRA-21744 | 8-16-82 | 6.00 | 4.50 | 47 | 8 | 44.00 | 20.00 | 1,892 |

### Wells Completed in the Geneva Field

| Permit number | Completion date | Average density porosity (%) Grimsby and Whirlpool | Net feet of effective porosity Grimsby and Whirlpool | Water saturation (%) | Initial potential (Mcf) |
|---|---|---|---|---|---|
| CRA-20433 | 2-10-74 | 8.1 | 24 | 33 | 353 |
| CRA-20453 | 3-10-74 | 7.3 | 24 | 31 | 765 |
| CRA-20482 | 10-23-75 | 7.7 | 48 | 27 | Junked hole |
| CRA-20483 | 10-24-75 | 5.4 | 32 | 43 | 250 |
| CRA-20435 | 11-07-75 | 7.3 | 32 | 30 | 1433 |
| CRA-20438 | 11-07-75 | 6.6 | 26 | 42 | 2078 |
| CRA-20430 | 11-07-75 | 5.8 | 28 | 43 | 1229 |
| CRA-20437 | 12-13-75 | 7.6 | 32 | 30 | 1421 |

# APPENDIX 2. ANALYSES OF TWO CORES, CRAWFORD COUNTY, PENNSYLVANIA

*Wainoco Oil and Gas Company, Creacraft No. 1 Well, Athens Field, Crawford County, Pennsylvania*

| Sample number | Depth (feet) | Permeability (mD) | Porosity (%) | Fluid saturation Oil (%) | Fluid saturation Water (%) | Grain density ($g/cm^3$) |
|---|---|---|---|---|---|---|
| | 4614.0–4649.0 | Shale—core not submitted for analysis | | | | |
| 1 | 4649.0–4650.0 | <0.1 | 2.2 | 0.0 | 36.4 | 2.65 |
| 2 | 4650.0–4651.0 | <0.1 | 4.5 | 0.0 | 46.7 | 2.65 |
| | 4651.0–4654.0 | Shale—core not submitted for analysis | | | | |
| 3 | 4654.0–4655.0 | <0.1 | 5.4 | 0.0 | 22.2 | 2.66 |
| 4 | 4655.0–4656.0 | <0.1 | 3.7 | 0.0 | 73.0 | 2.66 |
| 5 | 4656.0–4657.0 | <0.1 | 2.1 | 0.0 | 61.9 | 2.65 |
| 6 | 4657.0–4658.0 | <0.1 | 3.3 | 0.0 | 36.4 | 2.65 |
| 7 | 4658.0–4659.0 | <0.1 | 4.9 | 0.0 | 28.6 | 2.65 |
| 8 | 4659.0–4660.0 | <0.1 | 5.2 | 0.0 | 26.9 | 2.65 |
| 9 | 4660.0–4661.0 | 0.2 | 4.2 | 0.0 | 43.6 | 2.65 |
| 10 | 4661.0–4662.0 | 0.2 | 4.1 | 0.0 | 36.6 | 2.67 |
| 11 | 4662.0–4663.0 | 0.2 | 4.5 | 0.0 | 22.2 | 2.65 |
| 12 | 4663.0–4664.0 | <0.1 | 5.0 | 0.0 | 40.0 | 2.65 |
| 13 | 4664.0–4665.0 | <0.1 | 5.0 | 0.0 | 48.0 | 2.65 |
| 14 | 4665.0–4666.0 | <0.1 | 5.7 | 0.0 | 35.1 | 2.65 |
| 15 | 4666.0–4667.0 | <0.1 | 4.4 | 0.0 | 36.4 | 2.65 |
| 16 | 4667.0–4668.0 | <0.1 | 5.2 | 0.0 | 42.3 | 2.65 |
| 17 | 4668.0–4669.0 | <0.1 | 5.2 | 0.0 | 42.3 | 2.66 |
| 18 | 4669.0–4670.0 | 0.2 | 4.9 | 0.0 | 32.6 | 2.66 |
| 19 | 4670.0–4671.0 | 117.0 | 3.5 | 0.0 | 48.6 | 2.66 |
| 20 | 4671.0–4672.0 | 0.2 | 3.8 | 0.0 | 42.1 | 2.65 |
| 21 | 4672.0–4673.0 | 0.2 | 3.7 | 0.0 | 32.4 | 2.65 |
| | 4673.0–4674.0 | Core too broken for analysis | | | | |
| 22 | 4674.0–4675.0 | 0.2 | 2.1 | 0.0 | 71.4 | 2.76 |

*Wainoco Oil and Gas Company, Creacraft No. 1 Well, Athens Field, Crawford County, Pennsylvania (Continued)*

| Sample number | Depth (feet) | Permeability (mD) | Porosity (%) | Fluid saturation Oil (%) | Fluid saturation Water (%) | Grain density ($g/cm^3$) |
|---|---|---|---|---|---|---|
| 23 | 4675.0–4676.0 | 0.2 | 4.4 | 0.0 | 40.9 | 2.65 |
| 24 | 4676.0–4677.0 | <0.1 | 4.0 | 0.0 | 82.5 | 2.65 |
| 25 | 4677.0–4678.0 | 0.2 | 5.6 | 0.0 | 48.2 | 2.68 |
| 26 | 4678.0–4679.0 | 0.2 | 5.0 | 0.0 | 36.0 | 2.67 |
| 27 | 4679.0–4680.0 | 0.2 | 6.4 | 0.0 | 37.5 | 2.66 |
| 28 | 4680.0–4681.0 | 0.2 | 5.3 | 0.0 | 37.7 | 2.66 |
| 29 | 4681.0–4682.0 | <0.1 | 3.8 | 0.0 | 26.3 | 2.65 |
| 30 | 4682.0–4683.0 | 0.2 | 5.3 | 0.0 | 30.2 | 2.66 |
| 31 | 4683.0–4684.0 | 0.2 | 7.1 | 0.0 | 50.7 | 2.67 |
| 32 | 4684.0–4685.0 | 0.2 | 7.1 | 0.0 | 50.7 | 2.67 |
| 33 | 4685.0–4686.0 | 0.2 | 7.2 | 0.0 | 38.9 | 2.67 |
| 34 | 4686.0–4687.0 | <0.1 | 6.0 | 0.0 | 46.7 | 2.66 |
| 35 | 4687.0–4688.0 | 0.2 | 7.3 | 0.0 | 35.6 | 2.67 |
| 36 | 4688.0–4689.0 | <0.1 | 5.4 | 0.0 | 40.7 | 2.65 |
| | 4689.0–4690.0 | Shale—core not submitted for analysis | | | | |
| 37 | 4690.0–4691.0 | <0.1 | 4.0 | 0.0 | 35.0 | 2.65 |
| 38 | 4691.0–4692.0 | 0.2 | 6.2 | 0.0 | 32.3 | 2.66 |
| 39 | 4692.0–4693.0 | <0.1 | 4.5 | 0.0 | 31.1 | 2.66 |
| 40 | 4693.0–4694.0 | <0.1 | 3.4 | 0.0 | 35.3 | 2.64 |
| | 4694.0–4701.0 | Shale—core not submitted for analysis | | | | |
| 41 | 4701.0–4702.0 | <0.1 | 1.6 | 0.0 | 62.5 | 2.65 |
| 42 | 4702.0–4703.0 | <0.1 | 5.5 | 0.0 | 56.4 | 2.66 |
| 43 | 4703.0–4704.0 | <0.1 | 4.2 | 0.0 | 54.8 | 2.66 |
| 44 | 4704.0–4705.0 | <0.1 | 4.9 | 0.0 | 63.3 | 2.66 |
| 45 | 4705.0–4706.0 | <0.1 | 5.3 | 0.0 | 41.5 | 2.66 |
| 46 | 4706.0–4707.0 | 0.2 | 4.7 | 0.0 | 46.8 | 2.65 |
| 47 | 4707.0–4708.0 | <0.1 | 4.9 | 0.0 | 40.8 | 2.65 |

| | | | | | | |
|---|---|---|---|---|---|---|
| 48 | 4708.0–4709.0 | <0.1 | 3.3 | 0.0 | 36.4 | 2.65 |
| 49 | 4709.0–4710.0 | <0.1 | 5.5 | 0.0 | 47.3 | 2.65 |
| 50 | 4710.0–4711.0 | <0.1 | 3.5 | 0.0 | 60.0 | 2.64 |
| 51 | 4711.0–4712.0 | 0.2 | 3.2 | 0.0 | 65.6 | 2.65 |
| 52 | 4712.0–4713.0 | <0.1 | 2.2 | 0.0 | 77.3 | 2.64 |
| 53 | 4713.0–4714.0 | <0.1 | 2.0 | 0.0 | 50.0 | 2.64 |
| 54 | 4714.0–4715.0 | <0.1 | 4.3 | 0.0 | 27.9 | 2.65 |
| 55 | 4715.0–4716.0 | <0.1 | 4.2 | 0.0 | 28.6 | 2.65 |
| 56 | 4716.0–4717.0 | <0.1 | 2.9 | 0.0 | 41.4 | 2.64 |
| 57 | 4717.0–4718.0 | <0.1 | 5.6 | 0.0 | 54.3 | 2.65 |
| 58 | 4718.0–4719.0 | <0.1 | 3.8 | 0.0 | 42.1 | 2.64 |
| 59 | 4719.0–4720.0 | 0.2 | 2.5 | 0.0 | 32.0 | 2.64 |
| 60 | 4720.0–4721.0 | <0.1 | 5.2 | 0.0 | 30.8 | 2.65 |
| 61 | 4721.0–4722.0 | <0.1 | 5.0 | 0.0 | 36.0 | 2.65 |
| 62 | 4722.0–4723.0 | <0.1 | 5.8 | 0.0 | 34.5 | 2.65 |
| 63 | 4723.0–4724.0 | <0.1 | 5.4 | 0.0 | 25.9 | 2.64 |
| 64 | 4724.0–4725.0 | <0.1 | 5.4 | 0.0 | 25.9 | 2.64 |
| 65 | 4725.0–4726.0 | <0.1 | 5.0 | 0.0 | 24.0 | 2.64 |
| 66 | 4726.0–4727.0 | <0.1 | 3.7 | 0.0 | 21.6 | 2.65 |
| 67 | 4727.0–4728.0 | 0.1 | 3.2 | 0.0 | 34.4 | 2.70 |
| 68 | 4728.0–4729.0 | <0.1 | 4.9 | 0.0 | 42.9 | 2.66 |
| 69 | 4729.0–4730.0 | <0.1 | 3.5 | 0.0 | 51.4 | 2.64 |
| 70 | 4730.0–4731.0 | <0.1 | 4.3 | 0.0 | 53.5 | 2.65 |
| 71 | 4731.0–4732.0 | <0.1 | 6.3 | 0.0 | 38.1 | 2.65 |
| 72 | 4732.0–4733.0 | <0.1 | 3.2 | 0.0 | 59.4 | 2.66 |
| 73 | 4733.0–4734.0 | <0.1 | 4.1 | 0.0 | 29.3 | 2.65 |
| 74 | 4734.0–4735.0 | <0.1 | 4.0 | 0.0 | 52.5 | 2.65 |
| 75 | 4735.0–4736.0 | 0.6 | 4.2 | 0.0 | 61.9 | 2.64 |
| 76 | 4736.0–4737.0 | 0.2 | 3.3 | 0.0 | 51.5 | 2.67 |
| 77 | 4737.0–4738.0 | <0.1 | 5.9 | 0.0 | 44.1 | 2.64 |
| 78 | 4738.0–4739.0 | 0.2 | 5.3 | 0.0 | 30.2 | 2.65 |
| 79 | 4739.0–4740.0 | <0.1 | 4.2 | 0.0 | 28.6 | 2.66 |
| 80 | 4740.0–4741.0 | <0.1 | 3.4 | 0.0 | 29.4 | 2.65 |
| 81 | 4741.0–4742.0 | <0.1 | 3.7 | 0.0 | 32.4 | 2.64 |

*Wainoco Oil and Gas Company, Creacraft No. 1 Well, Athens Field, Crawford County, Pennsylvania (Continued)*

| Sample number | Depth (feet) | Permeability (mD) | Porosity (%) | Fluid saturation Oil (%) | Fluid saturation Water (%) | Grain density (g/cm³) |
|---|---|---|---|---|---|---|
| 82 | 4742.0–4743.0 | <0.1 | 3.4 | 0.0 | 35.3 | 2.64 |
| | 4743.0–4744.0 | Shale—core not submitted for analysis | | | | |
| 83 | 4744.0–4745.0 | <0.1 | 3.5 | 0.0 | 28.6 | 2.64 |
| 84 | 4745.0–4746.0 | <0.1 | 3.3 | 0.0 | 57.6 | 2.64 |
| 85 | 4746.0–4747.0 | <0.1 | 3.0 | 0.0 | 56.7 | 2.66 |
| 86 | 4747.0–4748.0 | 0.4 | 2.7 | 0.0 | 55.5 | 2.66 |
| | 4748.0–4787.0 | Shale—core not submitted for analysis | | | | |
| 87 | 4787.0–4788.0 | 0.4 | 2.0 | 0.0 | 30.0 | 2.65 |
| 88 | 4788.0–4789.0 | <0.1 | 3.2 | 0.0 | 25.0 | 2.65 |
| 89 | 4789.0–4790.0 | <0.1 | 2.9 | 0.0 | 31.8 | 2.65 |
| | 4790.0–4791.0 | 0.2 | 2.9 | 0.0 | 34.5 | 2.64 |
| 91 | 4791.0–4792.0 | <0.1 | 2.6 | 0.0 | 30.0 | 2.65 |
| 92 | 4792.0–4793.0 | 0.4 | 2.5 | 0.0 | 24.0 | 2.65 |
| 93 | 4793.0–4794.0 | 0.1 | 3.0 | 0.0 | 20.0 | 2.64 |
| 94 | 4794.0–4795.0 | <0.1 | 2.9 | 0.0 | 27.6 | 2.64 |
| 95 | 4795.0–4796.0 | <0.1 | 3.0 | 0.0 | 20.0 | 2.65 |
| 96 | 4796.0–4797.0 | <0.1 | 4.3 | 0.0 | 30.4 | 2.64 |
| 97 | 4797.0–4797.6 | <0.1 | 1.6 | 0.0 | 37.5 | 2.66 |
| | 4797.6–4800.0 | Shale—core not submitted for analysis | | | | |

## *N-Ren Corporation, Kebert Developers No. 1 Well, Greenwood Pool, Crawford County, Pennsylvania*

| Sample number | Depth (feet) | Permeability to air (mD) | | Porosity (%) | Grain density (g/cm³) |
|---|---|---|---|---|---|
| | | 90° | Vertical | | |
| 1 | 4700.0–4701.0 | <0.1 | <0.1 | 5.3 | 2.72 |
| 2 | 4701.0–4702.0 | <0.1 | <0.1 | 6.7 | 2.72 |
| 3 | 4702.0–4703.0 | <0.1 | <0.1 | 7.6 | 2.72 |
| 4 | 4703.0–4704.0 | <0.1 | <0.1 | 7.0 | 2.70 |
| 5 | 4704.0–4705.0 | <0.1 | <0.1 | 8.6 | 2.73 |
| 6 | 4705.0–4706.0 | <0.1 | <0.1 | 8.9 | 2.73 |
| | 4706.0–4713.0 | Shale—core not submitted for analysis | | | |
| 7 | 4713.0–4714.0 | <0.1 | <0.1 | 5.1 | 2.71 |
| 8 | 4714.0–4715.0 | <0.1 | <0.1 | 8.0 | 2.76 |
| 9 | 4715.0–4716.0 | <0.1 | <0.1 | 9.0 | 2.74 |
| 10 | 4716.0–4717.0 | <0.1 | <0.1 | 7.4 | 2.72 |
| 11 | 4717.0–4718.0 | <0.1 | <0.1 | 6.9 | 2.71 |
| 12 | 4718.0–4719.0 | <0.1 | <0.1 | 7.1 | 2.71 |
| 13 | 4719.0–4720.0 | <0.1 | <0.1 | 6.6 | 2.70 |
| 14 | 4720.0–4721.0 | <0.1 | <0.1 | 6.7 | 2.71 |
| 15 | 4721.0–4722.0 | 0.2 | <0.1 | 8.3 | 2.76 |
| 16 | 4722.0–4723.0 | 0.2 | <0.1 | 8.5 | 2.73 |
| 17 | 4723.0–4724.0 | 0.6 | 0.4 | 8.8 | 2.75 |
| 18 | 4724.0–4725.0 | 0.2 | 0.2 | 8.1 | 2.71 |
| | 4725.0–4726.0 | Shale—core not submitted for analysis | | | |
| 19 | 4726.0–47.27.0 | <0.1 | <0.1 | 7.8 | 2.74 |
| 20 | 4727.0–4728.0 | <0.1 | <0.1 | 5.7 | 2.72 |
| | 4728.0–4842.0 | Core not submitted for analysis | | | |
| | 4842.0–4847.0 | Shale—core not submitted for analysis | | | |
| 21 | 4847.0–4848.0 | <0.1 | <0.1 | 4.6 | 2.72 |
| 22 | 4848.0–4849.0 | <0.1 | <0.1 | 3.8 | 2.72 |
| 23 | 4849.0–4850.0 | <0.1 | | 5.2 | 2.73 |

*N-Ren Corporation, Kebert Developers No. 1 Well, Greenwood Pool, Crawford County, Pennsylvania (Continued)*

| Sample number | Depth (feet) | Permeability to air (mD) 90° | Permeability to air (mD) Vertical | Porosity (%) | Grain density (g/cm³) |
|---|---|---|---|---|---|
| 24 | 4850.0–4851.0 | <0.1 | <0.1 | 4.3 | 2.71 |
| 25 | 4851.0–4852.0 | <0.1 | <0.1 | 8.2 | 2.75 |
| 26 | 4852.0–4853.0 | <0.1 | <0.1 | 6.5 | 2.72 |
| 27 | 4853.0–4854.0 | <0.1 | <0.1 | 5.6 | 2.72 |
| 28 | 4854.0–4855.0 | <0.1 | <0.1 | 8.6 | 2.75 |
| 29 | 4855.0–4856.0 | <0.1 | <0.1 | 4.9 | 2.71 |
| 30 | 4856.0–4857.0 | <0.1 | <0.1 | 6.8 | 2.76 |
| 31 | 4857.0–4858.0 | <0.1 | <0.1 | 5.9 | 2.74 |
| 32 | 4858.0–4859.0 | <0.1 | <0.1 | 8.2 | 2.71 |
| 33 | 4859.0–4860.0 | <0.1 | <0.1 | 5.6 | 2.73 |
| 34 | 4860.0–4861.0 | <0.1 | <0.1 | 8.7 | 2.74 |
| 35 | 4861.0–4862.0 | <0.1 | <0.1 | 6.5 | 2.75 |
| 36 | 4862.0–4863.0 | <0.1 | <0.1 | 5.1 | 2.74 |
| | 5863.0–4869.0 | Shale—core not submitted for analysis | | | |

ISBN: 0-8182-0054-5